

50989

0-315-03093-3



National Library of Canada

Bibliothèque nationale du Canada

CANADIAN THESES ON MICROFICHE

THÈSES CANADIENNES SUR MICROFICHE

STUART GLENN COUPLAND

NAME OF AUTHOR/NOM DE L'AUTEUR

TIME-DOMAIN ANALYSIS OF STEADY-STATE ELECTRORETINAL AND

TITLE OF THESIS/TITRE DE LA THÈSE

VISUAL EVOKED RESPONSE TO INTERMITTENT PHOTIC STIMULATION

SIMON FRASER UNIVERSITY, Burnaby, B.C. V5A 1S6

UNIVERSITY/UNIVERSITÉ

DEGREE FOR WHICH THESIS WAS PRESENTED/
GRADE POUR LEQUEL CETTE THÈSE FUT PRÉSENTÉE

Ph.D.

YEAR THIS DEGREE CONFERRED/ANNÉE D'OBTENTION DE CE GRADE

1979

NAME OF SUPERVISOR/NOM DU DIRECTEUR DE THÈSE

A. Leonard Diamond, Full Professor
Dept. of Psychology

Permission is hereby granted to the NATIONAL LIBRARY OF CANADA to microfilm this thesis and to lend or sell copies of the film.

L'autorisation est, par la présente, accordée à la BIBLIOTHÈQUE NATIONALE DU CANADA de microfilmer cette thèse et de prêter ou de vendre des exemplaires du film.

The author reserves other publication rights, and neither the thesis nor extensive extracts from it may be printed or otherwise reproduced without the author's written permission.

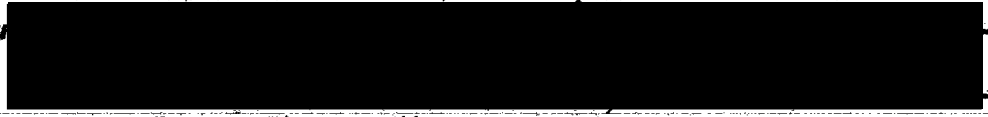
L'auteur se réserve les autres droits de publication; ni la thèse ni de longs extraits de celle-ci ne doivent être imprimés ou autrement reproduits sans l'autorisation écrite de l'auteur.

DATED/DATE

Feb. 18/79.

SIGNED/SIGNÉ

PERMANENT ADDRESS/RÉSIDENCE FI





National Library of Canada

Cataloguing Branch
Canadian Theses Division

Ottawa, Canada
K1A 0N4

Bibliothèque nationale du Canada

Direction du catalogage
Division des thèses canadiennes

NOTICE

The quality of this microfiche is heavily dependent upon the quality of the original thesis submitted for microfilming. Every effort has been made to ensure the highest quality of reproduction possible.

If pages are missing, contact the university which granted the degree.

Some pages may have indistinct print especially if the original pages were typed with a poor typewriter ribbon or if the university sent us a poor photocopy.

Previously copyrighted materials (journal articles, published tests, etc.) are not filmed.

Reproduction in full or in part of this film is governed by the Canadian Copyright Act, R.S.C. 1970, c. C-30. Please read the authorization forms which accompany this thesis.

**THIS DISSERTATION
HAS BEEN MICROFILMED
EXACTLY AS RECEIVED**

AVIS

La qualité de cette microfiche dépend grandement de la qualité de la thèse soumise au microfilmage. Nous avons tout fait pour assurer une qualité supérieure de reproduction.

S'il manque des pages, veuillez communiquer avec l'université qui a conféré le grade.

La qualité d'impression de certaines pages peut laisser à désirer, surtout si les pages originales ont été dactylographiées à l'aide d'un ruban usé ou si l'université nous a fait parvenir une photocopie de mauvaise qualité.

Les documents qui font déjà l'objet d'un droit d'auteur (articles de revue, examens publiés, etc.) ne sont pas microfilmés.

La reproduction, même partielle, de ce microfilm est soumise à la Loi canadienne sur le droit d'auteur, SRC 1970, c. C-30. Veuillez prendre connaissance des formulaires d'autorisation qui accompagnent cette thèse.

**LA THÈSE A ÉTÉ
MICROFILMÉE TELLE QUE
NOUS L'AVONS REÇUE**

TIME-DOMAIN ANALYSIS OF
STEADY-STATE ELECTRORETINAL AND VISUAL EVOKED RESPONSE
TO INTERMITTENT PHOTIC STIMULATION

by

Stuart Glenn Coupland
B.Sc., University of Alberta, Edmonton, 1969

A THESIS SUBMITTED IN PARTIAL FULFILLMENT
OF THE REQUIREMENTS FOR THE DEGREE OF
DOCTOR OF PHILOSOPHY

in the Department

of

Psychology



Stuart Glenn Coupland 1978

SIMON FRASER UNIVERSITY

December 1978

All rights reserved. This thesis may not be
reproduced in whole or in part, by photocopy
or other means, without permission of the author.

APPROVAL

Name: Stuart Glenn Coupland

Degree: Doctor of Philosophy

Title of Thesis: Time-Domain Analysis of Steady-state Electroretinal
and Visual Evoked Response to Intermittent Photic
Stimulation.

Examining Committee:

Chairman: Vito Modigliani

A. Leonard Diamond
Senior Supervisor

Raymond F. Koopman

Barry L. Boyerstein

Richard Fatechand
External Examiner
University of British Columbia
Vancouver, B.C.

Date Approved: 12/12/78

PARTIAL COPYRIGHT LICENSE

I hereby grant to Simon Fraser University the right to lend my thesis or dissertation (the title of which is shown below) to users of the Simon Fraser University Library, and to make partial or single copies only for such users or in response to a request from the library of any other university, or other educational institution, on its own behalf or for one of its users. I further agree that permission for multiple copying of this thesis for scholarly purposes may be granted by me or the Dean of Graduate Studies. It is understood that copying or publication of this thesis for financial gain shall not be allowed without my written permission.

Title of Thesis/Dissertation:

TIME-DOMAIN ANALYSIS OF STEADY-STATE ELECTRORETINAL
AND VISUAL EVOKED RESPONSE TO INTERMITTENT PHOTIC
STIMULATION

Author: _____

(signature)

Stuart Glenn Cowland

(name)

August 1, 1979.

(date)

ABSTRACT

Two electrophysiological indices of visual activity, the electroretinogram (ERG) and the visual evoked potential (VEP) were employed in an investigation of peripheral and central correlates of the visual flicker response in humans. Simultaneous ERG and VEP recordings were obtained from five alert human subjects in response to a brief incrementally flicker-modulated stimulus over a flicker frequency range of 4.75 to 25 Hz.. The resultant steady-state averaged-electroretinal and visual evoked potential activity was analysed using two time-domain analytic techniques.

Time-domain analysis of the averaged-ERG and VEP activity was conducted by two methods: a time-difference latency calculation (2-D LC) which derived steady-state EP latency from the average slope intercept of least squares linear regression lines fitted through EP peak reference points. The second technique (3-D LC) required observers to visually inspect three-dimensional perspective displays of electrophysiological data and psychophysically fit or place quasi-regression lines through surface feature regularities (peaks, pits, ravines, ridges), thereby predicting corresponding time-axis intercepts. The corresponding average time-axis intercept value of these quasi-regression lines in tridimensional space determined the steady-state latency.

Time-difference analysis indicated a flicker frequency-dependent latency shift in the VEP, with no frequency-dependent latency changes in the electroretinal steady-state response. The theoretical significance of these experimental findings in terms of a time-domain model of visual flicker signal processing suggests that observed latency shift appears to originate at some central site (above the primary ganglion layer) in the visual system. In addition, empirical support that both the 2-D LC and 3-D LC procedures derived a sufficiently equivalent quantification of steady-state electroretinal and visual evoked potential events was demonstrated.

DEDICATION

This thesis is dedicated both to my father, *Fred E. Coupland,
who first introduced me to the nature of visual perception
and to Margo J. Taylor, my significant other.

ACKNOWLEDGEMENTS

This is to acknowledge the contribution of those members of the S.F.U. academic community for their aid and cooperation in the production of this thesis. My warmest thanks to Len Diamond for his ever cheerful encouragement and the many hours spent in the lab. Thanks to Richard Fatechand for his guidance and advice on electroretinographic recording. My appreciation is extended to Ray Koopman for statistical advice and assistance. I also wish to thank Barry Beyerstein for proofreading of the initial drafts. I also want to thank Doug Seeley for his contribution with the 3-D graphics display and the use of the Evans & Sutherland Picture System. Thanks to Hal Weinberg for use of his PDP-12. There is also much appreciation to Howard F. Gabert for his design of the Stimulus Control Unit (SCU) and the FABO software.

I want to thank my good friends Paul Brickett, Dave Hallman, Carol Rourke, and Alan Quapick for their endurance as subjects and raters in this investigation. I really appreciated their assistance, encouragement and comraderie as fellow graduate students. Most of all I want to express my gratitude to Margo J. Taylor who was most supportive and encouraging throughout the entire project. Thanks Margo for being a subject, psychophysical rater, typist and a most patient listener all this time.

APPROVAL	ii
ABSTRACT	iii
DEDICATION	v
ACKNOWLEDGMENTS	vi
LIST OF TABLES	ix
LIST OF FIGURES	x
CHAPTER	
1 INTRODUCTION	1
The Linear Approach to Flicker: Fourier's Theorem	3
The Linear Model and Underlying Assumptions	5
Psychophysical Data	10
Electrophysiological Data I: The Electroretinogram (ERG)	12
Electrophysiological Data II: Fourier Analysis of Evoked Potentials	17
Other Methods Based on Fourier Analysis	25
Time-domain vs. Frequency-domain Analysis	32
2 METHOD	38
General Experimental Procedure	39
Study 1 and 2: ERG Electrode Recording Configuration	43
Study 1: A Comparison of Two Corneal Electroretinographic Recording Assemblies	47
Study 2: A Comparison of Corneal and Noncorneal Electroretinographic Recording Sites	53
Study 3: Selection of Test and Surround Field Luminances	57
Parametric Flicker Response Study	67
Overview of Perspective Latency Calculation	74
Picture Presentation and Preparation	75
Procedure for Perspective Latency Calculation	77
3 RESULTS	87
Time-difference Calculation	87
The Effect of Flicker rate: the 2-D LC	88
The Effect of Flicker rate: the 3-D LC	115
ANOVA of the 3-D LC Steady-state latency	118

4	DISCUSSION	126
	Consistency between 2-D LC and 3-D LC Calculations	126
	Discussion of Results from 3-D LC ANOVA	128
	Theoretical Significance of Experimental Results	129
	Conclusions	133
APPENDICES		
Q	SUBJECT CONSENT AND MEDICAL RELEASE FORMS	135
U	PEAK IDENTIFICATION ALGORITHM FOR 2-DLC	138
A	SUMMARY TABLES OF (E) AND (EE) VALUES FOR 2-D LC	141
P	E & S PICTURE SYSTEM USER'S MANUAL	146
I	2-D TIME-DIFFERENCE LATENCY ESTIMATES	153
C	ISI VALUES AND ASSOCIATED FLICKER FREQUENCY	159
K	3-D LC INTEROBSERVER AGREEMENT FOR C.R. DATA	161
	REFERENCES	178

LIST OF TABLES

TABLE		PAGE
I.	STEADY-STATE LATENCY DERIVED FROM THE AVERAGE X - INTERCEPT OF REGRESSION LINES DERIVED FROM THE 2-D LC PROCEDURE	89
II.	MEAN STANDARD ERROR AND VARIANCE OF STEADY- STATE LATENCY DERIVED FROM 3-D LC PROCEDURE	117
III.	ANOVA SUMMARY TABLES FOR 3-D LC DETERMINED STEADY-STATE LATENCY	120
IV.	3-D LC CALCULATED STEADY-STATE LATENCIES	124

LIST OF FIGURES

FIGURE		PAGE
1	A simple linear stimulus-EP system	7
2	Sinusoidally modulated stimulus	9
3	Squarewave modulated stimulus	20
4	Three stages of growth and decay of vibration displacement	27
5	Graphic description of time-difference latency calculation	35
6	Effect of mydriatic agent on VEP	41
7	Burian-Allen contact-lens electrode	45
8a	Averaged-ERG recorded from Burian-Allen contact-lens electrode	49
8b	Averaged-ERG recorded from hydrophilic contact-lens electrode	51
9	ERG from corneal and infracorbital placements	56
10	Stimulus viewing configuration	59
11a	ERG and VEP as a function of increasing flicker luminance at various levels of constant adapting luminance	64
11b	ERG and VEP to constant flicker luminance as a function of increasing adapting luminance	66
12a	3-D averaged-ERG for fast flicker series	80
12b	3-D averaged-ERG for fast flicker series with linear interpolation across diagonals	82
13a	3-D averaged-ERG for slow flicker series	84
13b	3-D averaged-ERG for slow flicker series with linear interpolation across diagonals	86
14a	VEP latencies for CR for slow flicker series	93

14b	ERG positive reference points for CR for slow flicker series	95
14c	ERG negative reference points for CR for slow flicker series	97
14d	VER positive reference points for CR for fast flicker series	99
14e	VER negative reference points for CR for fast flicker series	101
14f	ERG positive reference points for CR for fast flicker series	103
14g	ERG negative reference points for CR for fast flicker series	105
15a	VEP latency shift of positive component as a function of ISI range	108
15b	VEP latency shift of negative component as a function of ISI range	110
16a	ERG latency shift of positive component as a function of ISI range	112
16b	ERG latency shift of negative component as a function of ISI range	114

CHAPTER 1

INTRODUCTION

Visual flicker phenomena have been widely investigated since Sir d'Arcy's (1765) quantification of visual persistence. Some impression of the empirical richness of flicker response research is reflected by Landis' (1953) flicker bibliography containing over 1149 publication abstracts covering the period from 1754-1952. Landis' annotated bibliography is probably the most complete collection of visual flicker references ever assembled containing every citation on flicker phenomena from all major abstract journals (including Norwegian and Japanese translations) and every relevant reference cited by each of the investigators so listed. This mammoth effort was chiefly the result of the Columbia-Greystone Brain Research Project, which first revealed that critical flicker fusion (CFF) threshold was diminished after surgical intervention in the human frontal lobes. It was in an attempt to find some neurophysiological explanation of this observed sensory deficit that the compilation of all existing knowledge on visual flicker phenomena was conducted. It was Landis' hope that, "a bibliography such as this will unify in some part this chaos of knowledge." Unfortunately, a quarter of a century later there still exists no comprehensive theory of flicker which successfully encompasses all of the available

empirical evidence. More recently, Ginsburg (1968), one of Landis' former students, has collected almost 1300 flicker research citations covering the period from 1953-1967, clearly indicating the impact of flicker phenomena has had on sensory research. Ginsburg's bibliography while not annotated is indexed into 90 categories.

Both psychophysical and electrophysiological measures of the visual flicker response have been used in a wide variety of ways in the study of sensory coding processes and the underlying mechanisms of vision. From the combined neurophysiological, psychophysical and psychobiological research certain facts emerge, forming our present understanding of visual flicker response. A modern restatement of the classical flicker theory was proposed by Pieron (1964). Pieron's synthesis of psychophysical and electrophysiological research provides a thorough treatment of both the empirically-derived laws relating CFF to various stimulus parameters (including intensity, area, repetition frequency) in addition to the possible psychophysiological mechanisms purported to underlie the observed sensory processes of flicker and fusion. Although electrophysiological citations are somewhat sparse this review of psychophysical flicker literature is worth reading. Another excellent introduction to visual flicker research is Brown's

chapter in Graham's (1966) text on visual perception. At this point a brief historic review of the psychophysics of flicker is in order.

Visual flicker-fusion threshold was first measured by Plateau (1824) by adjusting the rotational velocity of black and white and colored sectored disks as they were viewed through a slit until fusion occurred. This initial quantification of the critical flicker-fusion (CFF) threshold marked the beginning of the systematic psychophysical investigation of flicker.

THE LINEAR APPROACH TO FLICKER: FOURIER'S THEOREM

Excellent treatments of Fourier analytic applications to visual flicker can be found in Kelly's (1974) chapter in the Handbook of Sensory Physiology or Sperling's (1964) introductory remarks at the Flicker Symposium held in Amsterdam in 1963. Since the mid-fifties Fourier analytic methods have enjoyed an increasingly prominent position not only as powerful analytic procedures but also in the construction of theoretical models of visual flicker perception; some models emphasizing psychophysical aspects of flicker response (DeLange, 1961; Kelly, 1974; Pieron, 1964), while other researchers concerned with neurophysiological implications have succeeded in measuring some of the bioelectric properties of visual flicker response (Spekreijse, Estevez and

Reits, 1977; Regan, 1977). While a comprehensive treatment of Fourier series and integral-transform techniques is beyond the focus of this dissertation, it should be pointed out that any periodic function which indefinitely repeats itself can be harmonically decomposed, and thus described, as a linear sum of elementary sinusoidal terms, called Fourier Components.

As Kelly (1974) and Sperling (1964) both conclude, one basic problem for the psychophysicist and sensory psychophysicist lies in the production of theoretical flicker models which can successfully predict the flicker response (output waveform) to a variety of stimulus (input) waveforms, including square waves, triangular waves, pulses, etc. Herein lies the advantage of a linear approach to flicker investigation - by collecting data using a set of basic sinusoidal input waveforms one can still predict the visual flicker response to any input waveform (triangular, square wave, ramp shaped) since it will be a linear combination of some set of basic sinewave components.

Fourier first developed the mathematical techniques which allow any infinitely recurring periodic function to be harmonically decomposed into a finite number of sinusoidal components. The first application of Fourier theorem in the sensory sciences was Ohm's (1843) psychoacoustic law (not to be confused with the electrical law of the same name) which

described tone perception in terms of harmonic decomposition of complex acoustic stimuli. A more detailed discussion of linearity assumptions and linear system properties now follows.

THE LINEAR MODEL AND UNDERLYING ASSUMPTIONS

Figure 1 illustrates a simple descriptive linear model of flicker perception. The stimulus (input) waveform is comprised of sinusoidal time-averaged luminance (L_0) (see Figure 2) The depth of modulation is defined as the ratio of modulation amplitude (mL_0) and the time-averaged luminance (L_0), usually expressed as percent modulation ($\%m$). The frequency of modulation (F) is expressed in cycles per second (or Hertz). The time-averaged luminance (L_0) defines the light adaptation level and remains independent of modulation depth ($\%m$) and modulation frequency (F). The response output waveform from the system is illustrated in the right half of Figure 1. A linear system is one in which the relationship between the input and output quantities can be described by linear equations. Another feature of the linear model is the principle of superposition which holds only when the total output corresponding to the sum of 2 simultaneous given inputs is equivalent to the sum each of the outputs measured separately. This property of superposition allows any complex input to be harmonically decomposed into Fourier components of known

Figure 1

A simple linear stimulus-EP system.

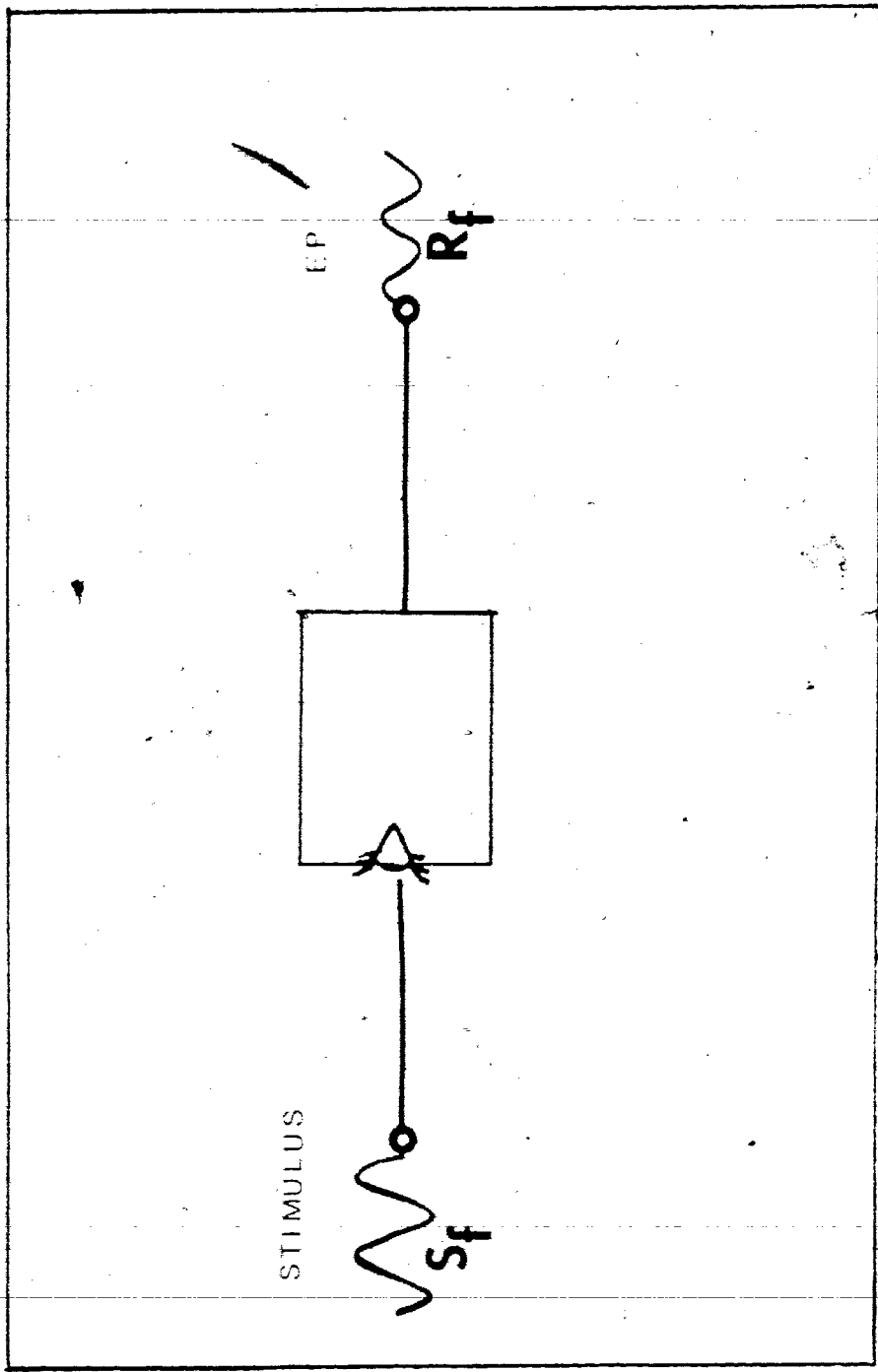


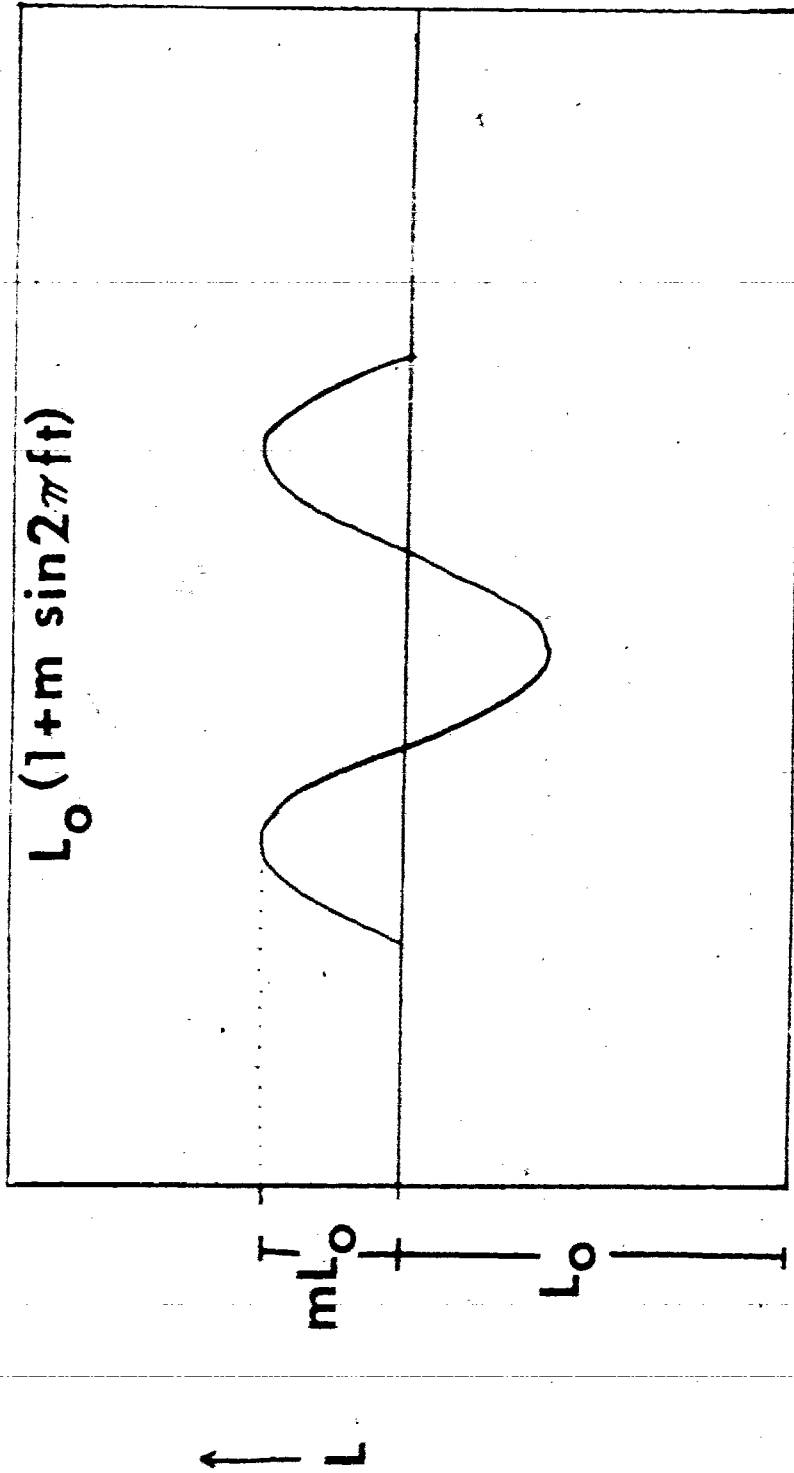
Figure 2

Sinusoidally modulated stimuli.

Ordinate: relative luminance units

Abscissa: time

Time-average luminance of modulated stimulus (L_0).



amplitude and phase characteristics. The visual system's sensitivity can be separately determined to flicker at each of these known frequencies, using the inverse of modulation depth for perceived flicker as the index of sensitivity. The corresponding response waveforms could be predicted from the linear combination (Fourier Synthesis) of the individual responses for each Fourier Component.

Psychophysical Data

The first reported use of the linear systems approach to the psychophysical description of flicker was Ives' (1922a, b) prediction of flicker threshold to high frequency nonsinusoidal stimulus waveforms derived from sinewave flicker thresholds at scotopic adaptation levels.

Ives' (1922a, b) theory of intermittent vision has relied upon his earlier work on visual diffusivity (Ives 1916, 1917). According to Ives, the interval between sensory reception and perception should be related inversely to the ease of conduction or diffusivity. Psychophysically he quantified this interval for different colors and intensities, and for rod and cone processes. Ives' theory of flicker perception was composed of three process steps; the first being a photochemical process. The second stage was a neural conduction process by diffusion of the substance

formed by the photochemical process. The third stage described the perception of flicker or intermittency as being dependent upon the rate of diffusion of this transmitted reaction. Ives' diffusion theory was criticized for theoretical inconsistencies by Cobb (1934a). Although Ives and Cobb both advocated the use of sinusoidal modulation, neither investigator conducted systematic parametric studies of sufficient length to clearly demonstrate its methodological utility to the scientific community. Certainly, the most significant advance towards the clarification of the totally confused state of psychophysical flicker theory came not from collaborative efforts of psychophysicologists but rather from the single-handed, pioneer experimentation of an electrical engineer, Hendrik deLange.

DeLange's contribution lies chiefly in his being the first investigator to rigorously apply the linear systems approach in the systematic psychophysical examination of flicker phenomena. From 1951-1958, conducting most of his experimentation in his home with a precise 2-channel Maxwellian optical system of his own design, DeLange determined temporal modulation transfer functions (or attenuation characteristics as he called them) at photopic adaptation levels over broad frequency ranges and to varying stimulus wavelengths. As a result of deLange's prodigious efforts in determining the nature of temporal MTF, at the 1963 Flicker Symposium it was decided to refer to these

attenuation characteristics as deLange curves (Henkes & van der Tweel, 1964) in memory of deLange's contribution to sensory psychophysiology. DeLange (1952, 1954) was able to demonstrate the Fourier equivalence of various nonsinusoidal stimulus waveforms and predict their high frequency flicker thresholds for given adaptation levels from the amplitude of the waveforms' fundamental (i.e., first Fourier) component. DeLange also proposed a reducibility hypothesis stating that the corresponding fundamental sine wave would have the same flicker fusion threshold as the complex waveform, both being psychophysically equivalent stimuli.

DeLange (1958) finally proposed an electronic analogue or model to account for the linear filter attenuation characteristics that he had observed. This model was composed of a number of cascading identical resistance-capacitance stages, each RC-stage would increase the overall attenuation characteristic especially at high temporal frequencies. DeLange's RC-stage model will be reviewed in greater detail in subsequent sections on neurophysiological modelling.

Electrophysiological Data I: The Electroretinogram (ERG)

The two electrophysiological indicators of visual activity, the electroretinogram (ERG) and the visual evoked potential (VEP)

have been exhaustively studied under conditions of intermittent stimulation. The ERG has received more intensive scrutiny under flicker conditions than the VEP; a situation that has been changing in the last decade. The first recording of the ERG in humans predates the EEG by some 50 years.

Dewar (1877) first described a method for recording the ERG in humans using a wick electrode immersed in a saline bath covering the eye. Although cumbersome and extremely crude this method produced reliable recordings of electroretinal activity. Using a galvanometer and an observer to record the potential at 2.5 second intervals (paced by a metronome) Dewar & M'Kendrick (1873a,b,c) successfully quantified electrophysiological activity to a variety of transient light sources. However, it was not until the introduction of the contact lens electrode by Riggs (1941) that human electroretinographic recordings became a routine clinical procedure.

Adrian (1945) was one of the first to investigate the relationship between visual psychophysical observations and concurrent electroretinal activity. Although Adrian did not perform a parametric investigation of each stimulus variable, he clearly demonstrated how retinal duplicity could be investigated through observation of corresponding changes in visual perception and electroretinal activity. Adrian concentrated upon the

isolation of photopic and scotopic components of the B-wave of the electroretinogram using flickering stimuli of various wavelengths and frequencies. Adrian reported that the scotopic B-wave was most clearly seen in response to slow flickering (<3hz) shorter wavelengths (450nm), whereas the photopic component B-wave was most visible in those recordings to faster flickering (>15hz) longer wavelength stimuli (\approx 650nm). This reported differential sensitivity of the ERG components to changing stimulus frequency became the standard methodology for selectively eliciting photopic or scotopic activity in later research (Bornschein & Schubert, 1953; Dodt, 1951b,c; Arrington & Biersdorf, 1956).

Although later studies confirmed Adrian's analysis in terms of component duplicity they also revealed that the flicker response was more complex than he had realized. The properties of the human ERG show characteristic changes with increasing stimulus frequency (Arrington, 1974). In the light adapted eye, at a repetition frequency of 4 Hz, the b-wave amplitude becomes stabilized at a level far below the transient (b-wave) response amplitude, exhibiting distinct scotopic components in the presence of photopic components (Arrington & Biersdorf, 1956). The b-wave amplitude reduction in the flicker-ERG was considered to be caused by light adaptation (Adrian, 1945). Arden et al. (1960) concluded that neural suppression effects contributed more

to b-wave amplitude reduction than photochemical effects. In the dark adapted eyes of decerebrate cats the amplitude of flickering wavelets (b-waves) were found to vary inversely with flicker frequency. By systematically varying the "on" and "off" periods of photic stimulation, Arden et al. (1960) found that frequency-dependent amplitude diminution depends upon the exponential decay during the dark interval of a suppressive process elicited by a flash and independent of the duration of the light period. As flicker frequency is increased the "off" effect and a-wave become more pronounced and the x-wave appears (Arden, Granit & Ponte, 1960). The flicker ERG becomes predominantly photopic at 20 Hz (Arrington & Biersdorf, 1956). Bornschein & Schubert (1953) reported amplitude and waveform changes occurring at higher flicker rates than those used by Adrian. At flicker rates between 20-30 Hz the electroretinal components begin to overlap and summate, augmenting peak to peak amplitude and producing a simple sinusoidal waveform. With increasing flicker rates above 30 cps, the electroretinal amplitude begins to attenuate until it subsides into the background activity.

Several attempts have been made to study the relationship between electroretinal activity and psychophysically-determined flicker threshold (CFP). Sachs (1929) first reported that subjective disappearance of flicker was accompanied by

disappearance of ripples in the ERG, concluding that ripple fusion coincides with sensory fusion. Cooper, Creed & Granit (1933) and Bernhard (1940) both reported electroretinal fusion preceding subjective (CFP) fusion. Cooper et al. (1933) believed that limitations in recording technique were partly responsible for a lower electroretinal fusion threshold. With the advent of signal averaging computers in the early 1960's averaged-ERG's of smaller amplitude ($\approx 1\mu V$) could be reliably recorded. Riggs et al. (1962) using signal averaging techniques were able to detect ERG response to flicker rates up to 110 Hz; whereas psychophysical CFP occurred around at 65 Hz leading them to conclude that the site of psychophysical fusion was beyond the site of the origin of the electroretinogram. This apparently poor correlation between electrophysical activity and flicker perception has been reported consistently (Van der Tweel, 1964; Regan, 1968, 1972).

DeVoe (1963, 1964) investigated the flicker-electroretinogram in intact wolf-spider's light adapted eyes by several methods appropriate to linear systems, such as Fourier Analysis, superposition and sine wave analysis. DeVoe (1964) demonstrated that 8% incremental flicker and sinusoidal response could be determined directly through Fourier Analysis of the stimulus and visual receptor response.

Electrophysiological Data II: Fourier Analysis of Evoked Potentials

Consequent to DeLange's (1958) success in applying linear systems theory to the psychophysical investigation of flicker response, sensory psychophysicists were quick to grasp the methodological significance of a sinusoidally modulated stimulus.

Traditionally, photic flicker was produced in one of two ways: through the periodic occlusion of the light pathway itself or through the presentation of repetitive brief-duration flashes. Both methods have their own heuristic utility in terms of the nature of the problem being investigated. Whenever the flicker parameter of interest was stimulus waveform, PCF (pulse-to cycle fraction) or "on" versus "off"-type response the epicotister was used since it can be designed to produce a multitude of light/dark ratios, and waveform shapes (square, sawtooth, trapezoidal or ramp-shaped). On the other hand, photic stimulation produced by electronic stroboscopes was much more intense and could be presented and precisely controlled for briefer durations, typically less than 50 usec. Unfortunately, serious methodological problems arise upon the presentation of repetitive flashes from electronic stroboscopic sources. Since the time-averaged luminance of these intermittent flash sources is proportional to repetition frequency the resulting degree of

light adaptation will vary with flicker rate. This is not the case with square-wave or sinusoidal modulated stimuli (see Fig. 2) since the time-averaged luminance (L_0) is independent of frequency (F) and modulation depth (M). While square-wave modulated sources as produced by superposition of incremental flicker (dL) upon a steady background luminance (L_b) have frequency and modulation depth independence in terms of time-averaged light adaptation (see Fig. 3) they still are not ideal sources for the study of linear systems, although Van der Tweel (1964) and others (DeVce, 1964; Troelstra & Schweitzer, 1964) have successfully used them. The basic problem with any non-sinusoidal intermittent source is that of harmonics present in the stimulus producing harmonically distorted responses. Any occurrence of harmonic distortion in the evoked response to nonsinusoidal stimulation need not necessarily be due to visual system nonlinearity but rather to the presence of harmonics in the source itself.

Van der Tweel (1964), using both incremental squarewave and sinusoidally modulated light sources, was one of the first to apply linear systems analysis to the investigation of the relation between psychophysics and the electrophysiology of flicker.

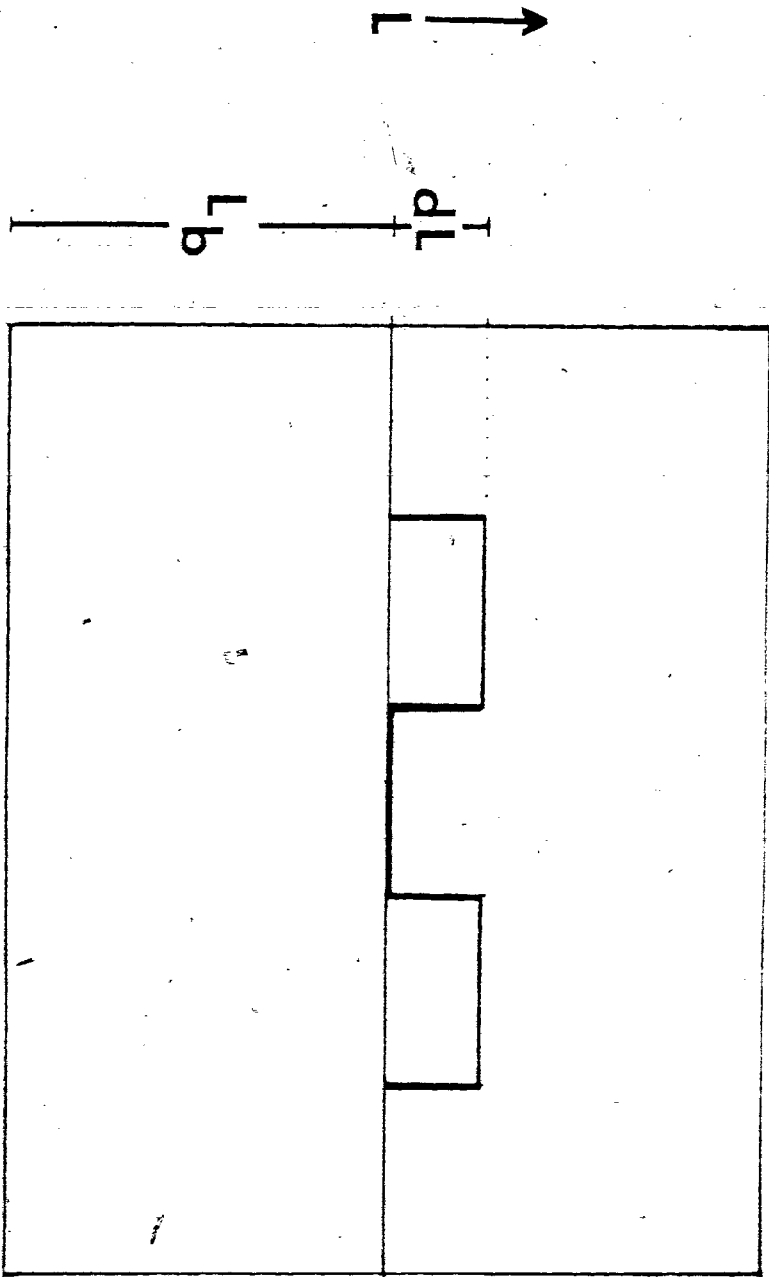
According to Fourier's theorem, any infinite periodic

Figure 3

A squarewave modulated stimulus.

Incremental flicker (dL) upon a steady

background luminance (L_b).



function can be mathematically decomposed into a set of elementary sinusoids (Fourier Components). Each Fourier Component accounts for a certain proportion of waveform content and the Fourier Component amplitude expresses this relative contribution. The lowest component frequency is usually that of the periodic phenomenon itself and is called the Fundamental Frequency. All other Fourier Components are some multiple of the Fundamental Frequency and are called harmonics. In addition to amplitude, each Fourier Component has some expression of the phase relation to the complex waveform from which it was derived. This expression of phase describes how far from some arbitrary zero point on the complex waveform each Fourier Component is shifted. Phase shift information has been used by Van der Tweel (1964) and others (Regar, 1968, 1972; Spekrijse, 1966) to calculate apparent latency of the cortical following response. These calculation procedures will be reviewed forthwith. In summary, Fourier Component is thus characterized by these two parameters; its relative amplitude and phase-shift.

The methodological advantage of sinusoidal modulation in linear systems analysis lies in the fact that the ERG or VEP resulting from sinusoidal stimulation of frequency (F) should differ from the input in amplitude and/or phase lag but should still be a sine wave of the same frequency (that is, $S_f = R_f$ in Fig. 1). This is the essential property of linearity, that a

sinusoidal stimulus elicits a sinusoidal response of the same frequency. By determining the amplitude and phase shift characteristics at a number of stimulation frequencies a complete knowledge of the visual flicker response would develop. Response predictions to nonsinusoidal stimuli could be developed by Fourier Analysis of the input waveform to determine its harmonic composition and resynthesizing of the component responses previously determined to pure (component) sinewaves (deVoe, 1964).

The sinusoidal stimulus can also be utilized to determine empirically the existence and degree of visual system nonlinearities. Using a sinusoidally modulated light as stimulus and recording the occipital VEP, Van der Tweel and Verduyn Lunel (1965) investigated nonlinearities in the human visual system. Using 20 subjects, Van der Tweel in 1964 and with Verduyn Lunel in 1965 studied the effect of modulation depth and dichoptic antiphase stimulation upon the visual evoked responses to sinusoidal modulation ranging from 5-60 Hz. Basically their results can be summarized as follows: With modulation frequencies around 5 Hz, using large low luminance fields, second harmonic amplitudes often were larger than those of the fundamental, persisting down to 5% modulation depths. Since sinewaves pass through a linear system without frequency distortions, any presence of harmonics which reliably persist at

low modulation depths confirms the presence of essential nonlinearity (Van der Tweel, 1964; Regan, 1972). Besides second harmonic distortion at 5 Hz, Van der Tweel (1964, 1965) reported equally large harmonics around 10 Hz as well. The relation between frequency response and spontaneous EEG activity (alpha) was further investigated with a sharply tuned frequency analyser revealing that modulation frequency and alpha amplitude were essentially independent. This finding was later confirmed by Regan (1966) who reported the amplitude and phase characteristics of the following response were independent of the occurrence of alpha activity even when such activity was some 15 times the amplitude of the ongoing following response. Van der Tweel concluded that the visual system behaved linearly for small modulation depths (<25%) at low intensity between 9-15 Hz. Within the stimulus frequency range van der Tweel estimated the latency of the cortical following response as 250-300 msec. Dichoptic stimulation confirmed earlier reports of additivity effects by Auerbach et al. (1960). Van der Tweel (1964), separately stimulating the two eyes, reported out of phase stimulation produced amplitude cancellation effects of the fundamental (but not the 2nd harmonic) component in the 9-15 Hz range. Perhaps the most outstanding finding of Van der Tweel and Verduyn Lunel (1965) was the striking lack of correspondence between these electrophysiological data and the existing psychophysical literature on visual flicker response and the

DeLange characteristic. Marked intersubject differences in the EEG-following response around 10 Hz were not found in subjective modulation thresholds. In addition, the predominance of second harmonics at low (<5 Hz) and high (>25 Hz) modulation frequencies were not reflected in psychophysical DeLange characteristics.

Other research comparing psychophysical observation and neural representation of flicker have also reported rather poor correspondence. Regan (1968) suggests that the amplitude saturation characteristic of the steady-state EP with increasing modulation depth reported by Van der Tweel & Lunel (1965) and Spekrijse (1966) is evidence of a functional branching in the visual information system. Regan's model of flicker response suggests that one branch of this fork relates to the neural representation of flicker and the generation of the VEP, a second branch relates to the mechanisms of flicker perception. The EP is only indirectly related to the perception of flicker or may be subject to contamination by mechanisms other than those of flicker perception. Regan (1968, 1972) concludes that poor correlations between VEP and flicker sensation could be accounted for in part by the incorrect choice of the neural correlate of flicker. The steady-state VEP measures of amplitude, phase and harmonic composition may be systematic signs rather than sensory codes (Uttal, 1972) or perhaps the neural correlates in question are not precisely time locked to the stimulus (Regan, 1968).

At this point further clarification is in order concerning the theoretical distinction between sensory codes and signs. Uttal (1972) defines a sensory code as a set of symbols and transformation rules which allow for the condensation of information into a form amenable to decoding by some interpretive CNS mechanism. In order for any neural correlate to attain the status of sensory code it must be demonstrated that the code is actually interpreted by some subsequent CNS mechanism. Any event-related signal which is not interpreted is considered to be a sign.

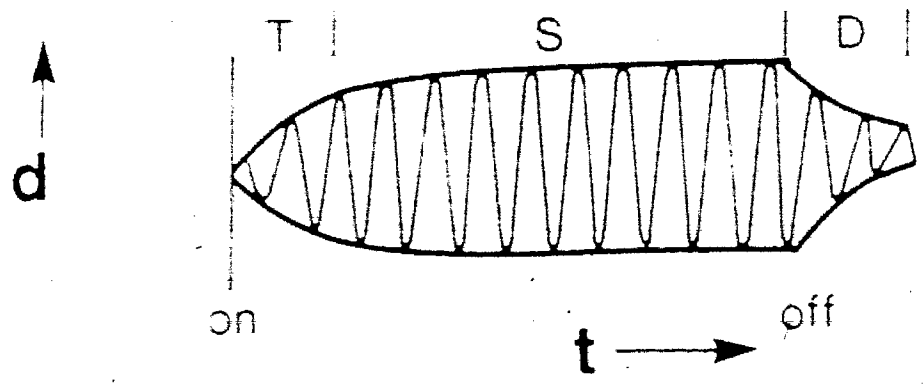
Other Methods Based on Fourier Analysis

When any physical system (such as a taut string) is subjected to an initial step or impulse input (e.g., the string is plucked or released) the system's response is transient in that it rapidly decreases in amplitude over time. If the same system is subjected to a continuous repetitive displacement (e.g., if the string is bowed), it quickly establishes a (steady state) periodic response for as long as the stimulus is applied (see Figure 4). Regan (1966) introduced the steady state model into EP research and suggested that steady state EPs might provide insights into sensory functioning not attainable through the use of transient evocative techniques.

Figure 4

The three stages of growth and decay of vibration displacement (d) by time (t): Initial transient phase (T), steady state (S) followed by decay (D). "On" and "off" mark the presence of stimulus force.

5



Regan (1966) described an apparatus designed to extract the amplitude and phase relation of the steady-state synchronous component of the EEG to a 100% sinusoidally modulated source. Briefly, Regan's frequency amplifier is capable of extracting from the EEG any frequency component which is phase locked to the stimulus. This is achieved by separately multiplying the raw EEG by $\sin(2\pi ft)$ and $\cos(2\pi ft)$ waveforms. Since Fourier Theory assumes the EEG following response is harmonically comprised of a set of elementary sinusoids, the phase of any of these frequency components other than the synchronous component will produce A.C. when multiplied by the sine and cosine waveforms. This A.C. is attenuated by low pass filtering. Only the synchronous (fundamental) component of the EEG-following will produce a D.C. output after multiplication. The mean D.C. outputs are used in the calculation of amplitude and phase characteristics of the synchronous or fundamental component. If the product of EEG amplitude times $\sin(2\pi ft) = A$ and if EEG amplitude times $\cos(2\pi ft) = B$ then: $P = \tan^{-1}(A/B)$ and $S = C\sqrt{A^2 + B^2}$ where P is the measure of phase shift of the fundamental component and S is the amplitude of the fundamental component obtained. C is a correction constant derived by calibration of the phase locked amplifier. Harmonic components can be similarly extracted by substituting the desired frequency multiple in the sine and cosine equations. Regan's (1968) phase locked amplifier

performed Fourier analysis limited to the fundamental (F) and second harmonic (2F) components, providing a running average of each component's amplitude and phase. More recently, Regan (1972, 1975b, 1977) and others (Regan & Cartwright, 1970; Cartwright & Regan, 1974) have developed more powerful, frequency component extraction methods based upon Fourier Analysis. The advantage of methods based on Fourier Analysis over signal averaging techniques will now be considered.

Using this Fourier analyser, Regan (1966) was able to calculate the attainment of steady-state stationarity (of amplitude and phase) as occurring after about 12-20 seconds from stimulus onset. Regan investigated the phase lag and amplitude changes as functions of modulation frequency. Fundamental component amplitude was found to peak at about 10 Hz as had been previously reported (Van der Tweel, 1964; Van der Tweel & Verduyn Lunel, 1965). Amplitude peaking was also found to be related to sudden phase shifts at 10 Hz. Phase shift measured in the linear region between 12 and 30 Hz derive calculated "apparent" latency of 38 msec, in clear disagreement to Van der Tweel's (1964) latency calculation of 300 msec in the 9-18 Hz range. Although differing stimulus luminance could account in part for this discrepancy in the steady-state "apparent" latency in the 10-30 Hz range Regan (1963) later reported closer agreement with Van der Tweel (1965) in latency calculation in frequencies from 32-58

cps derived again from the slope of phase versus modulation frequency. After correction for frequency-dependent amplitude changes Regan (1968) calculated the fundamental synchronous component's apparent latency to be 62 msec, which agrees well with Van der Tweel and Verduyn Lunel (1965) estimate of 60 msec for the frequency range of 35-68 Hz.

Regan (1972, 1977) has argued quite persuasively of the power of the application of frequency analysis techniques to the study of steady-state evoked potentials, proposing that Fourier analysers are more appropriately used with rapidly repetitive stimulation than straightforward signal averaging techniques (Regan (1977)). Regan (1977) contends that on-line Fourier Analysis is a convenient, more rapid technique for recording VEP latencies. Using a multiple stimulus method in which three or four slightly differing stimulus frequencies are simultaneously presented and recording the event-related EEG through a parallel bank of Fourier filters each tuned to one of the stimulus frequencies, Regan (1975) was able to estimate VEP latency from the resultant phase shift values in about 1/4 of the recording time it normally took to record each frequency separately. In situations where EP variability occurs over a time span of a few minutes this simultaneous-stimulation technique has considerable advantage over standard recording techniques (Cartwright & Regan, 1974; Regan & Cartwright, 1970). At this point it is worth

pausing and reflecting upon the old newspaper editor's advice to the young cub reporter, "there's no free lunch". Before the young psychophysiolgist runs out and acquires the nearest phase-locked amplifier, careful consideration should be given to the "real cost" of this increased speed and signal to noise enhancement of frequency analytic techniques. The cost of the five to tenfold increase in signal to noise enhancement in frequency analytic methods over signal averaging is traded off in terms of signal bandwidth. As Regan (1972, 1977) has cautioned this extremely narrow effective bandwidth of a Fourier analyser (0.001 Hz) can ultimately blind the experimenter to salient event-related signal components in the brain response. Since frequency analytic techniques only sample an extremely small portion of the EEG frequency spectrum they might not provide an adequate overall picture of the flicker-following response, and should not be expected to do so. Rather, frequency-domain analysis should be used in combination with appropriate time-domain analytic techniques to gain a more complete understanding of the visual flicker response. One objective of this thesis is to describe the appropriate application of time-domain analytic techniques to the study of electroretinal and occipital events in response to intermittent photic stimulation in humans.

TIME-DOMAIN VS. FREQUENCY-DOMAIN ANALYSIS

The phrase "time-domain analysis" was first introduced to EP research by Regan (1972) as a descriptive of transient event-related potentials in terms of component peak latency and amplitude. Regan (1977) argues that when a rapidly repetitive stimulus is used, the resultant averaged VEP may be uninterpretable by time-domain techniques, since transient VEP's will increasingly overlap as flicker frequency is increased. This overlapping of components will result in a VEP waveform, "in which no individual response cycle can be associated with a particular stimulus cycle." Regan (1972, p. 75). When this steady-state has become established, Regan (1977) contends it is more appropriate to describe the resultant VEP in terms of component frequency amplitude and phase, this Regan (1972) called "frequency-domain analysis". Frequency analytic techniques already reviewed have been used successfully to derive information on steady-state response, in terms of EEG synchronous component amplitude and calculation of "apparent latency" (Regan, 1968; Van der Tweel, 1964; Van der Tweel & Verduyn Lunel, 1965; Spekrijse, 1966). "Apparent latency" (t) is calculated from the phase angle difference P (in radians or degrees) by which the synchronous VEP component lags a sinusoidal stimulus. The assumptions necessary for this calculation are that the VEP is

sinusoidal in waveform. The sinewave stimulus must produce a waveform whose phase and amplitude remain constant from moment to moment. Finally, the stimulus-EP system must be linear, i.e., when stimulated by a sinusoidal input of frequency (FHz) the linear system responds with a sinusoidal output of frequency (FHz) whose output amplitude and phase are related to the sinusoidal input and described by a set of linear equations. Van der Tweel (1964) and others (Van der Tweel & Verduyn Lunel, 1965; Regan, 1966; Spekrijse, 1966) calculate the apparent latency (Regan's term) or transport time (Van der Tweel's term) according to the formula:

$$t = dp / 2\pi df$$

in which dp is the phase difference in radians for a frequency difference (df) in cycles per second. Apparent latency is directly estimable from the slope of the phase shift by frequency plots.

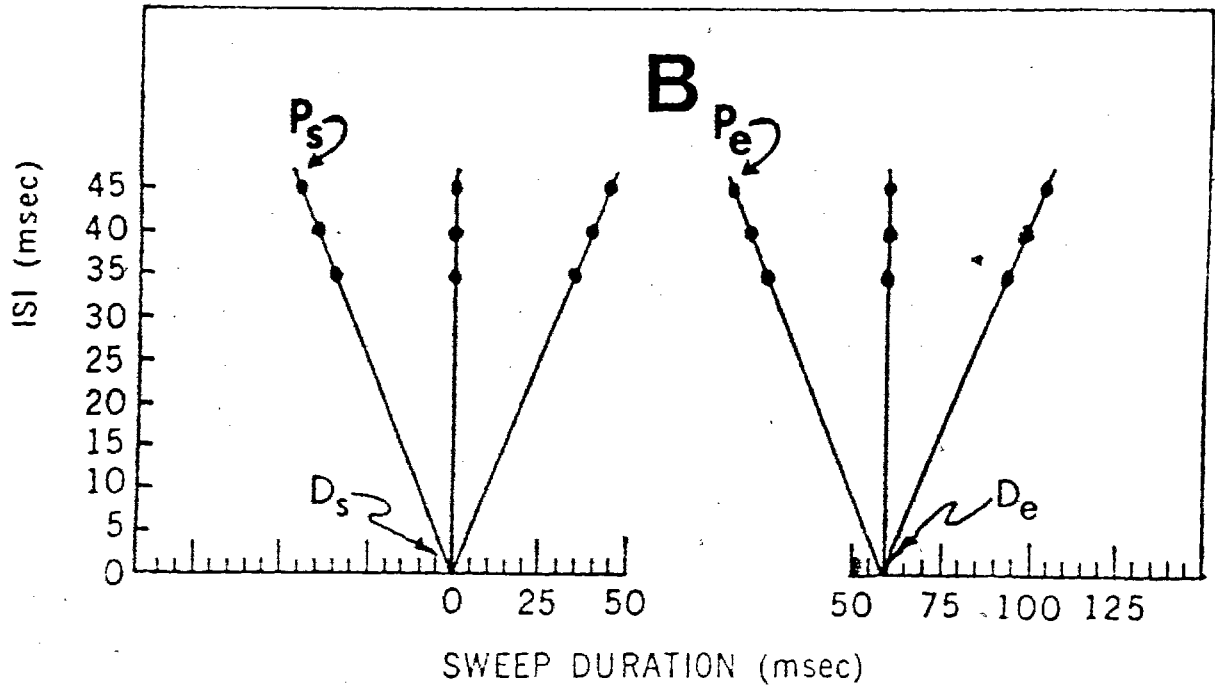
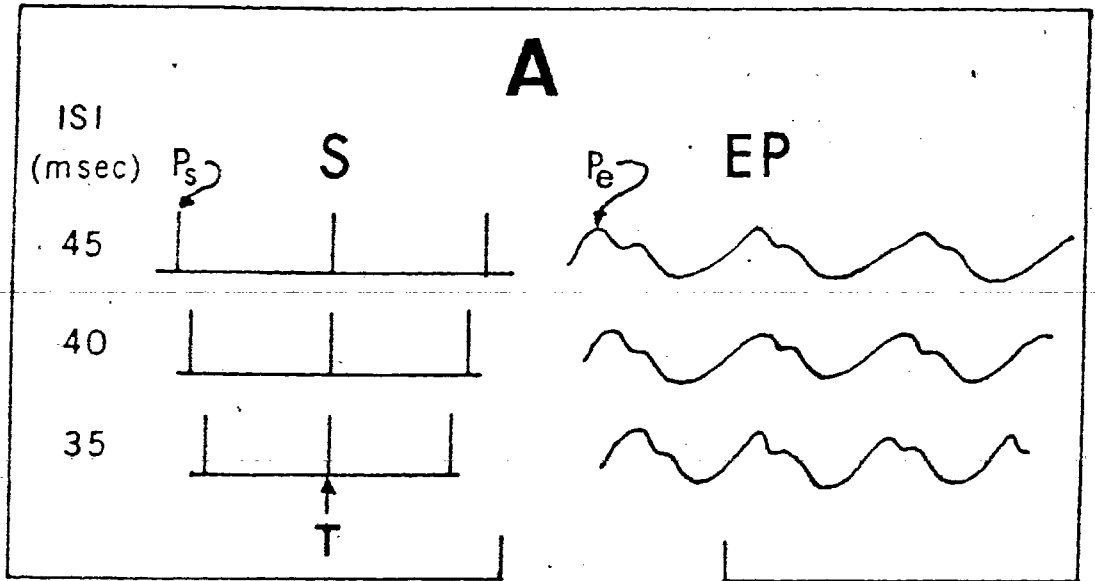
More recently Diamond (1977a, b) has described a time difference calculation of steady-state latency. Diamond's method calculates "true latency" from the time differences between stimulus and VEP peak reference points. Figure 5 graphically describes time-difference latency calculation, from a fictitious (for the purpose of explanation) a plot of stimulus and EP peak reference points. Here the stimulus (Fig. 5a) was a flash

Figures 5a and 5b

Graphic description of time-difference latency calculation.

(A) Artificial EP waveform to pulsed stimuli repeated at three interstimulus intervals (ISI). T indicates stimuli which trigger electronic averager at the zero value of its sweep duration. Ps and Pe are the stimulus and EP reference points chosen for the analysis. The sweep duration axis is broken and spread so stimuli and EP can be viewed apart.

(B) Plot of stimuli and EP peaks, Ps and Pe. Regression lines through points converge to two intercepts, Ds and De at ISI=0. Steady-state EP latency (t) = De - Ds.



produced by a stroboscope triggered by a squarewave pulse of 50 usec duration at various interstimulus intervals. The corresponding averaged EP of 150 msec duration is represented by an artificial EP waveform located to the right of the stimulus. T indicates the stimuli which trigger the signal averager at time-0 of its sweep duration. Ps and Pe are the stimulus and EP reference points chosen for the analysis. Fig. 5b illustrates the plot of stimulus and EP peak reference points. It can be seen that regression lines drawn through plotted stimulus and EP peak reference points converge to two intercepts Ds and De at ISI=0. EP latency (t) is calculated as the time-difference of De and Ds.

Diamond (1977b) contends that time-difference latency calculation can be applied to evoked potentials resulting from any repetitive stimulus waveform (squarewave, spike impulse, ramp shaped or sinusoidal) since, unlike the phase-difference calculation, there is no assumption of linearity in the stimulus-EP system. As mentioned previously, nonsinusoidal stimulation has not been widely used for phase-difference calculation because of the presence of harmonic frequency distortion, even though Spekrijse (1977) and others (van der Tweel, 1964; Regan, 1972; de Voe, 1964) have described linearizing methods to reduce the effect of stimulus-EP

nonlinearity. Diamond (1977b) suggests that the time-difference latency calculation is complementary to the phase-difference approach since it can not only be used to provide EP-latency calculation to repetitive nonsinusoidal stimulation but it can also be used to study specific time components of the steady state EP; whereas frequency-domain methods do not treat the EP in this manner.

The present study was an investigation of peripheral and central electrophysiological correlates of the visual flicker response in humans. Simultaneous electroretinal (ERG) and visual evoked potential (VEP) recordings were obtained in alert human subjects in response to a brief incrementally modulated light source over stimulus frequency range of 4-25 Hz. The resultant steady state averaged-ERG and visual evoked responses were analysed using two time-difference derivations of steady-state latency. It will be shown that both techniques provide substantially similar information regarding steady-state latency determination both at peripheral (retinal) and more central loci in the human visual system.

CHAPTER 2

METHOD

The outline of the method section will follow the chronological order in which these studies were planned and conducted. First is a description of the general experimental procedure and the stimulus-adaptation cycle outlining the events from the time the S enters the preparation room to have the electrodes applied till the S leaves the laboratory. Following this three pilot studies concerned with recording methodology and determination of experimental parameters will be discussed. The first two studies review the search for an adequate electroretinal recording configuration. The third pilot study concerns the experimental selection of test field and surround luminance and control of specific light adaptation effects. Following is a detailed description of the parametric incremental-flicker frequency study, including detailed discussion of the stimulus, electrode configuration, amplification and filtering, signal averaging, digitization and data storage. The method section will be completed by an inclusive description of the frequency and time domain analytic techniques used to derive respective amplitude and latency estimates of the electroretinal and cortical activity.

GENERAL EXPERIMENTAL PROCEDURE

A general procedure was followed for all experiments detailed below. The S enters the preparation room and after having obtained their informed consent (see consent and medical release forms in Appendix Q) electrodes were applied. A cycloplegic (1% cyclogyl) is instilled into the right eye to induce mydriasis. Earlier pilot research by the experimenter had demonstrated mydriatic induced amplitude augmentation of various steady state electroretinal and visual evoked potential components. Figure 6 illustrates this VEP amplitude augmentation effect of a cycloplegic agent which lasts for several hours. Steady state VEP activity was sampled for a 35 msec sweep duration and signal averaged over 512 sweeps. The upper traces represent the EP recorded over an ISI range (30-45 msec). The lower traces were recorded under identical experimental conditions 45 minutes after the instillation of 1% Cyclogyl. Resultant EPs appeared to be more sinusoidal in waveform and peak to peak amplitude was seen to increase at all ISI's. Corresponding steady state VEP latency calculated by time-difference procedure was seen to decrease from 66.2 to 58.3 msec. Arrington's (1964) classic study of short and long term flicker adaptation reported that mydriatic agents also remove the d.c. component of the ERG without significantly affecting the waveform. In addition, artifactual myogenic contamination due to

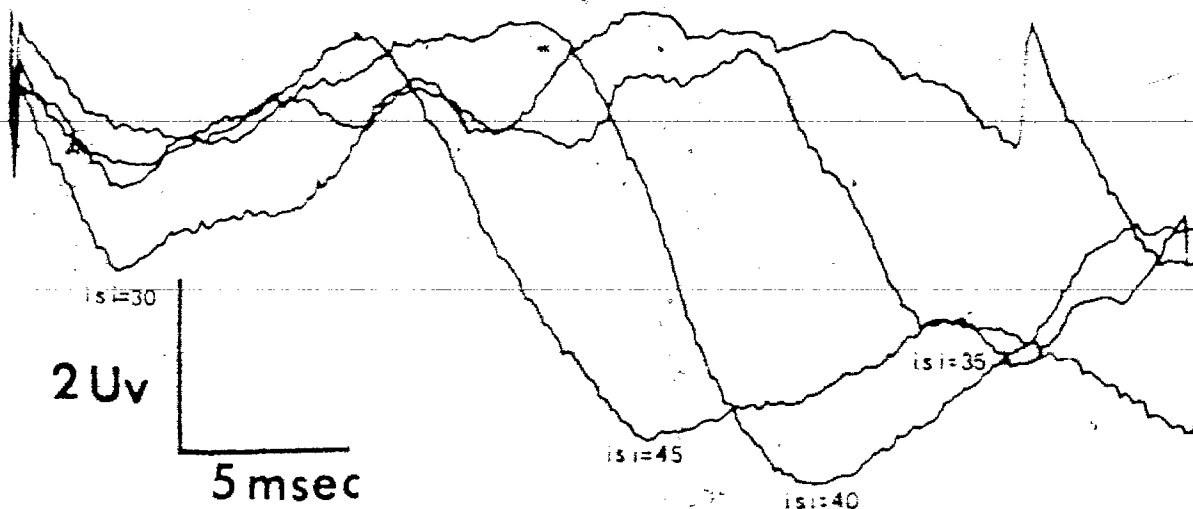
Figure 6

Steady state VEP recorded over identical experimental conditions. Lower trace recorded 45 minutes after pupils were immobilized by mydriatic agent (1% Cyclogyl).

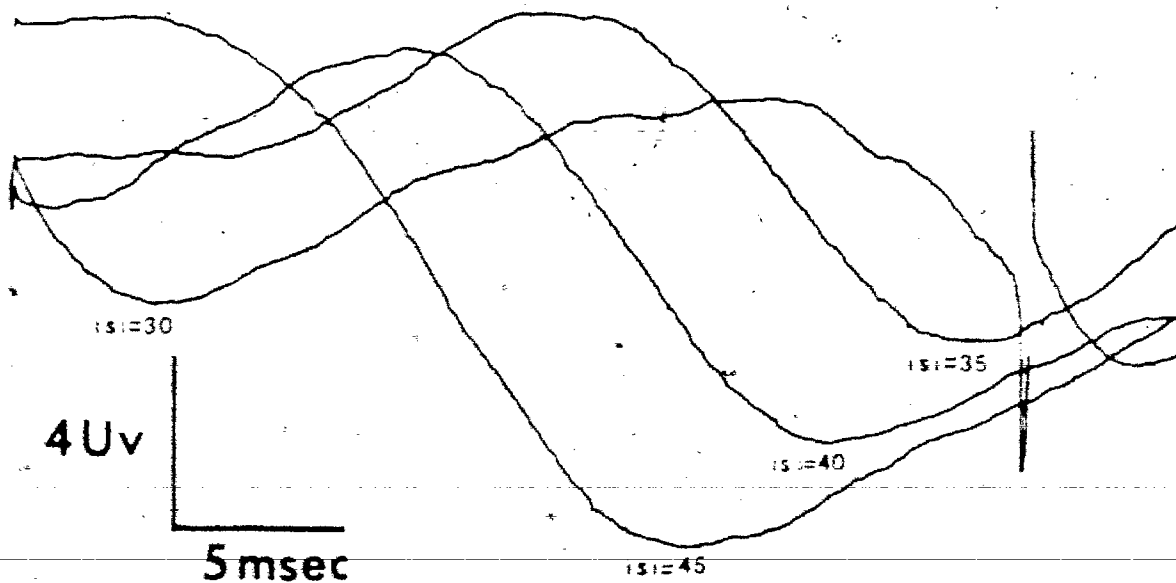
AQ

512 reps

natural pupil



fixed pupil



pupillary following at low flicker frequencies was eliminated (Armington, 1974).

After electrode application the S was seated in a sound attenuated and electrically shielded booth with the head positioned with appropriate chin and forehead restraint to position the stimulus field, in Newtonian view, directly on the pupillary axis of the right eye. The S's left eye was occluded for the duration of the experiment. No artificial pupil was employed. Sometimes subjects were required to instill local anesthetic (1 % Ophthacaine or 1/2 % Pontocaine) into the right eye as necessary to reduce blinking during the course of the experiment.

Subjects were always dark adapted for 5-15 minutes, followed by 3-5 minutes of light adaptation to a background luminance. After the subject was light adapted a standard stimulation-adaptation cycle was initiated and maintained throughout the experiment.

The stimulation period consisted of 60 seconds of flickering light stimulation, followed by 102 seconds of light adaptation to the background or surround luminance. The 102 second light adaptation period had been empirically determined to be sufficient to ensure that subsequent EP measures were not

affected by the preceding EP measures. No signal averaging occurred during the first 20 seconds of flicker stimulation to allow the S sufficient time to orient towards the stimulus field and to allow VEP stationarity to become established.

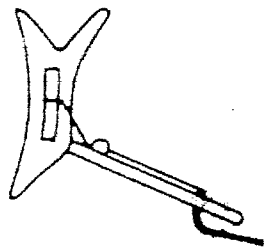
STUDIES 1 AND 2: E.E.G. ELECTRODE RECORDING CONFIGURATION

These two studies concern a preliminary investigation of various ERG electrode configurations with the objective of selecting an appropriate electroretinographic recording electrode for use in subsequent studies. The kinds and configurations of ERG electrodes are numerous and have been well reviewed by Arrington (1974) and Koopowitz (1974). At the 2nd ISCERG symposium the topic of recording methodology was intensively reviewed by Karpe (1961) and Jacobson (1961). Jacobson (1961) described desirable ERG electrode characteristics in terms of patient comfort, recording stability, and experimenter convenience. It was with these three selection criteria in mind that the experimenter conducted the first two studies to determine the most suitable electroretinographic recording configuration.

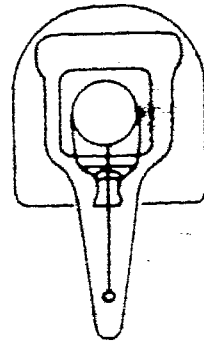
By far the most frequently used ERG electrode in clinical research is the Burian-Allen contact lens electrode (see Fig.

Figure 7

Burian-Allen contact lens electrode.



SIDE VIEW



FRONT VIEW

7), which makes use of a smaller corneal lens which fits the eye closely, silver wire around the circumference of the smaller lens makes the actual contact with the cornea. A speculum, attached to the assembly holds the eyelids apart and although uncomfortable with practice the assembly can be worn for periods of several hours (Burian, 1953; Burian & Allen, 1954). Some of the disadvantages of this lens include its mass and bulky dimensions (Figure 7), conjunctival abrasion and irritation produced by movements of the lens assembly. Additionally, the Burian-Allen contact lens assembly causes both subsequent drying of the conjunctiva produced by prolonged eyelid retraction and finally, uncontrolled optical absorption and scatter by the smaller corneal lens can be problematic if precise retinal imaging is required.

More recently, Schoessler & Jones (1975) have described a soft hydrophilic contact lens electrode with excellent recording characteristics. This electrode is formed by a fine gold or platinum wire sandwiched between two soft contact lenses. Schoessler & Jones claim that their recording electrode is more comfortable and stable than a Riggs hard contact lens electrode and provides a minimum obstruction to vision.

Under some circumstances it is possible to record an ✓
electroretinal response with noncorneal electrode placements

(Tepas & Arrington, 1962; Stephens et al., 1971). Tepas & Arrington (1962) using bipolar nasal and temporal canthi placements reported that averaged-ERGs could be reliably recorded to a wide range of stimuli conditions. Stephens et al. (1971) using nasal and temporal canthi placements with subsequent head rotation to displace the cornea towards the active electrode reported larger averaged-ERG's when the cornea was displaced towards the nasal canthus.

The present two studies were designed to investigate the recording characteristics of these three electrode configurations with the objective of selecting a method which would be most convenient for subsequent experimentation.

Study 1: A Comparison of Two Corneal Electroretinographic Recording Assemblies

In the first study one subject (A.Q.) had ERG's successively recorded with two corneal electrode placements - a hard contact lens (Burian Allen P629 Hansen Ophthalmic Laboratory) and a soft hydrophilic contact lenses electrode. Electrodes and recording configurations: a standard Burian-Allen (P629-adultsize) monopolar electrode assembly referenced to the right earlobe was provided. The soft lens electrode was constructed by the experimenter from a 25mm gold wire sandwiched between a pair of

Figure 8a

Averaged-ERG recorded from standard Burian-Allen
contact lens electrode over experimental time

T(min) 0-60.

AQ

ISI = 150 msec
16 reps

Time (min)

T₀

T₆₀

10 LV

40 msec



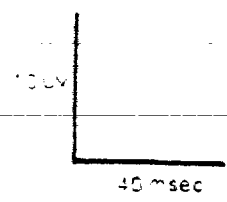
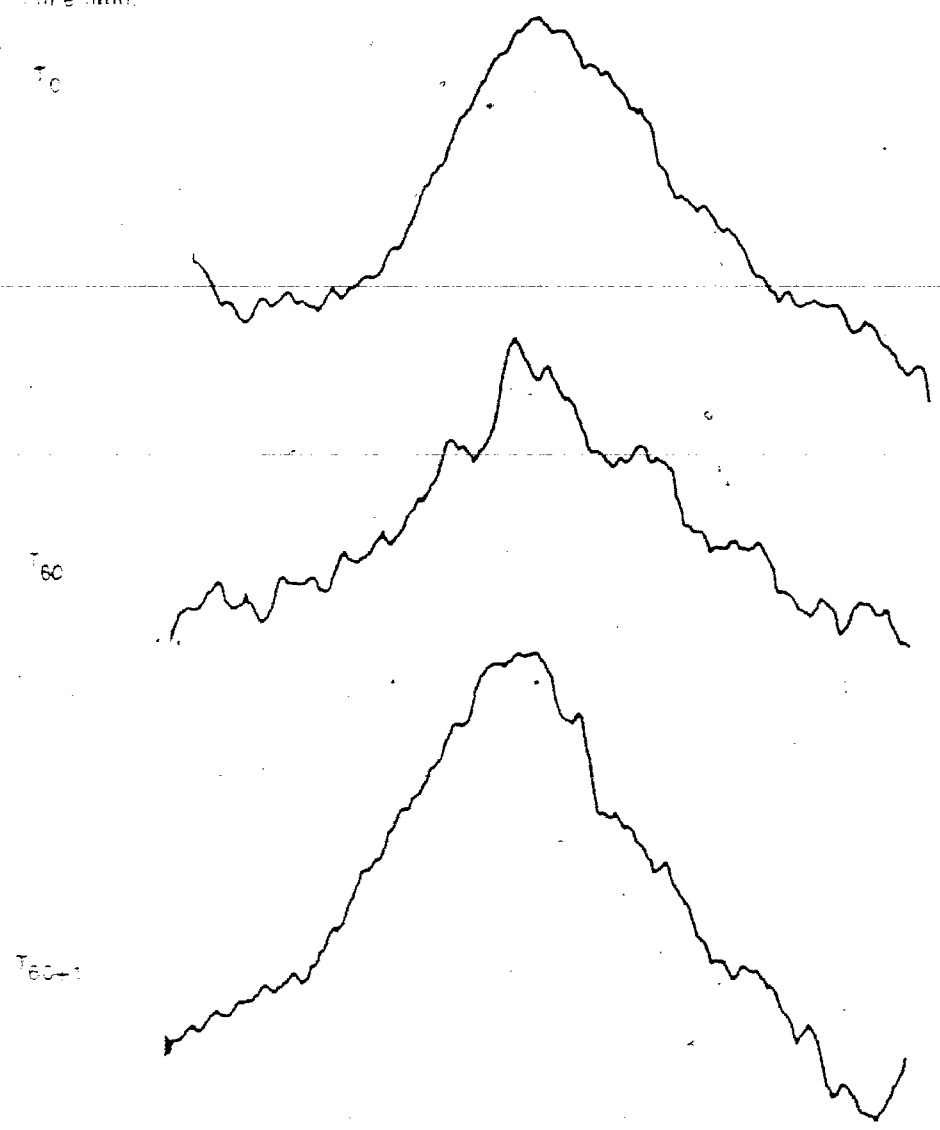
Figure 8b

Averaged-ERG recorded from hydrophilic (soft lens) recording electrode at various experimental times T(min). High frequency noise with lens dessication (T60) temporarily reduced by rehydration with 0.9% saline (T60+1):

AQ

Time (min):

ISI = 190 msec
16 reps



soft hydrogel lenses (Bausch & Lomb C-series polymacon hydrophilic lenses) in the manner described by Schoessler & Jones (1975) also referenced to the right earlobe. Both the hard and soft lenses were refract corrected for subject (A.Q.). The hydrophilic lenses were hydrated with 0.9 % saline to provide an electrolytic conducting medium, while normal saline and 1 % Isoptotears provided the electrolyte for the Burian-Allen system.

Procedure: The following modifications to the standard ERG recording procedure were made: in both recording trials the right pupil was immobilized by 1 % cyclogyl. Topical anesthetic (1 % Ophthcaine) was also used in both recording trials. An average of 256 samples of ERG were recorded at a number of repetition frequencies and stimulus intensities over several recording sessions lasting 2-3 hours.

Results: Figures 8a,b illustrate the averaged flicker-ERG recorded for subject, A.Q., in two sessions recorded several hours apart using the Burian-Allen and soft lens recording configurations. While amplitude of the b-wave is comparable from each corneal recording placement at the beginning of both sessions it is apparent that the soft lens recording system appears to be less stable over recording sessions lasting several hours. This lack of recording stability is evidenced by the increasing high frequency noise superimposed over the ERG

waveform. After rehydrating the soft lenses with 0.9 % saline the high frequency noise was temporarily reduced (Figure 8b). While the soft lenses were more comfortable to wear, they required frequent rehydrating since the outer soft lens was not in contact with the moistened conjunctiva and would rapidly dehydrate. As the outer lens desiccates it begins to deform allowing air to enter the interlenticular space producing an increasingly noisy ERG recording (Figure 8b). Unlike Schoessler & Jones (1975) the experimenter found the soft lens electrode less stable and centered on the cornea than the more cumbersome Burian-Allen assembly. Another problem although not directly related to recording efficacy per se was the tendency of the outer hydrophilic lens to tear around the gold wire's 50mm exit hole. Although extreme care was taken in handling these lenses over several weeks 2 outer lenses were damaged through tearing. The writer concluded the hydrogel lens sandwich too delicate (and too expensive - \$120/pr) to be used in subsequent experimental research.

Study 2: A comparison of corneal and noncorneal electroretinographic recording sites

In the second study three subjects (A.Q., M.T., W.R.) had averaged-ERGs successively recorded with a Burian-Allen (P629-adultsize) contact lens electrode or a noncorneal electrode

situated over the right infraorbital ridge over several 2 hour recording sessions.

Procedure: Using the standard stimulation-adaptation cycle previously described for subjects A.Q. and M.T., separate ERG recordings were taken with the Burian-Allen monopolar electrode referenced to the right earlobe or with a Beckman Ag-AgCl EEG electrode secured with a skin collar over the right infraorbital ridge referred to right earlobe. In subject W.R. simultaneous corneal and noncorneal ERG recordings were obtained to a 12 degree field of 0.8 mL at various flicker frequencies. In this study no cycloplegic was employed for observer W.R. but topical anesthetic (1 % Opthcaine or 1/2 % Pontocaine) was used for the Burian-Allen recording placement.

Results: For subjects M.T. and A.Q. the noncorneal flicker-ERG was greatly diminished in amplitude but still appeared to have the same waveform as the corneal ERG recordings. Simultaneously recorded corneal and infraorbital ERG for W.R. are presented in Figure 9. In both records the b-wave is clearly visible having a peak latency of 40 msec. Although infraorbital ERG peak to peak amplitude is about 1/8 of that obtained with a corneal electrode placement, there is a good correspondence in waveform.

Figure 9

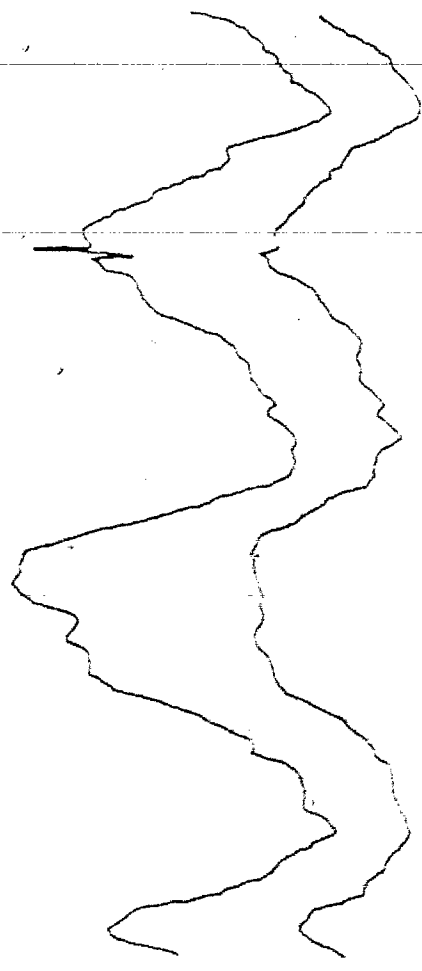
Simultaneously recorded ERG from corneal and infraorbital placements for W.R. Although good correspondence in waveform is demonstrated an eightfold attenuation in peak to peak amplitude is present in the ERGs recorded from the infraorbital site.

WR

ISI = 70 msec
64 reps

corneal ERG

intraorbital ERG



4 UV
10 msec

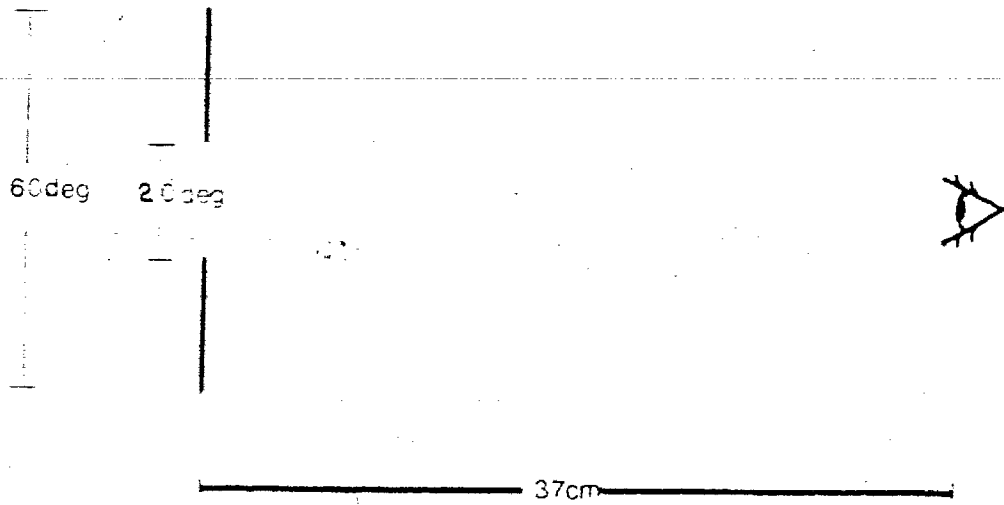
1 UV
10 msec

STUDY 3: SELECTION OF TEST AND SURROUND FIELD LUMINANCES

The aim of the third pilot study was the selection of suitable luminance parameters for both the test and surround fields. There are several methodological advantages in using an illuminated surround in sensory research. Firstly, the surround field of moderate luminance provides a method for obtaining electroretinograms which are relatively free of stray light effects. Fry & Bartley (1935) and Boynton (1953) have demonstrated that the scotopic b-wave component of the human electroretinogram resulting from small area (1 to 12 degree) stimulation arises almost entirely from stray light which weakly illuminates large peripheral rod-predominant areas. Crampton & Armington (1955) suggested that stray light effects could be reduced by using small area low luminance stimuli, however, the resulting electroretinal response was extremely small. It was not until the introduction of signal averaging into electroretinography by Armington et al. (1961) that it became possible to detect photopic b-wave components in averaged-ERG's of less than 2uV evoked by orange stimuli flickering at 20 hz. The second advantage of using an illuminated surround is for the control of retinal light adaptation level between successive flicker trials. If subjects were allowed to dark adapt between trials the extent of the inter-trial interval becomes critical, by providing a large illuminated surround a constant light

Figure 10

Stimulus viewing configuration



adaptation level can be maintained. The third rationale for using a moderately illuminated surround is to increase the relative contribution of photopic mechanisms in the ERG (Armington, 1953).

Procedure: Simultaneous ERG's and VER's were recorded from two subjects (MT and DH). During the experiment, the observers were dark adapted for 15 minutes followed by a 5 minute light adaptation period in which they viewed the surround wearing a pair of well-fitted goggles equipped with several neutral density filters (Kodak Wratten Filters No. 96) over the right eyepiece (the left eyepiece was occluded). Subjects viewed (with a fixed pupil) a fixation point located in the center of the surround (see Figure 10). The 20 degree central test field was made to flicker for 60 seconds over an interstimulus range of 75-175 msec by incremental test flashes whose time average luminance when flickering at 25 hz is 0.7 mL. Simultaneous averaged electroretinal and visual evoked responses were recorded to this incrementally flickering stimulus. After the measurements the subject then unscrewed the goggle lens caps and removed one neutral density filter while the experimental chamber was completely darkened for 45 seconds. The surround was illuminated once more and the observer light-adapted for 5 minutes before the next stimulation cycle. The modulation depth of the test field was independently manipulated by inserting Wratten filters in

front of the photostimulator tube which was located outside of the experimental chamber.

In any psychophysical or electrophysiological investigation involving the manipulation of stimulus intensity and/or light adaptation level, trial length, trial order and intertrial interval become critical, possibly confounding, variables which must be strenuously controlled. When presenting flickering stimuli it is necessary to allow the eye sufficient time to adjust to the stimulus before signal averaging is initiated (Arrington, 1964). Early control trials indicated that a 15-20 second flicker period was sufficient to allow the steady state response to stabilize in amplitude and latency. Arrington (1964) reports that for the flicker-electroretinogram the first response in a photic train has the largest b-wave component; the second response is greatly attenuated and recovery effects produce subsequent responses of intermediate size. By the fifth flash of the series the b-wave amplitude tends to stabilize but complete long term flicker-adaptation can take several minutes to reach completion (Arrington, 1964). Regan (1966) recording the steady state synchronous component in the EEG reported that stationarity is established approximately 20 seconds after stimulus onset. Intertrial interval was also empirically determined such that successive steady-state response measures were not contaminated by adaptation effects arising from the previous stimulation

cycles. A 5 minute light adaptation period was found to be sufficient for this study to remove the adaptation effects of previous stimulation trials of the same incremental intensity. While in most experimental research it is desirable to randomize trial order whenever possible it is an unwise procedure in any experimentation affecting visual sensitivity. Upon continued exposure to a bright flickering stimulus the visual system light adapts to the time average luminance of the stimulus. It then takes a considerable time for recovery of visual sensitivity after cessation of stimulation. Since it was impractical to allow observers more than 5 minutes adaptation time between trials the experimenter always ordered intensity and adaptation trial conditions from lowest to highest luminance, thus reducing the possibility of uncontrolled adaptation effects.

Results: The data for subject M.T. are illustrated in Figures 11a,b. The flicker-electroretinogram and visual evoked potentials both show similar changes in amplitude and latency. In the ERG at any adapting luminance (L_a) the effect of increasing incremental flicker luminance (dL) is a decrease in peak latency and an increase in peak to peak amplitude until saturation occurs at log relative luminance of 1.2. The steady state VEP changes are less straightforward in appearance but still appeared consistent across trials (Figure 11a). With adapting luminance (L_a) held constant the effect of increasing

Figure 11a

Steady state ERG and VEP recordings as a function of increasing incremental flicker luminance (δL) at various levels of constant adapting luminance (L_a).

MT

ISI=140 msec
64x2=128 reps

VEP

log rel. $L_a=0.6$

ERG

log rel. dL

0.2

0.4

0.6

0.8

log rel. $L_a=1.0$

dL

0.2

0.4

0.6

0.8

log rel. $L_a=1.2$

dL

0.2

0.4

0.6

0.8

2.0Uv 50ms

2.0Uv 50ms

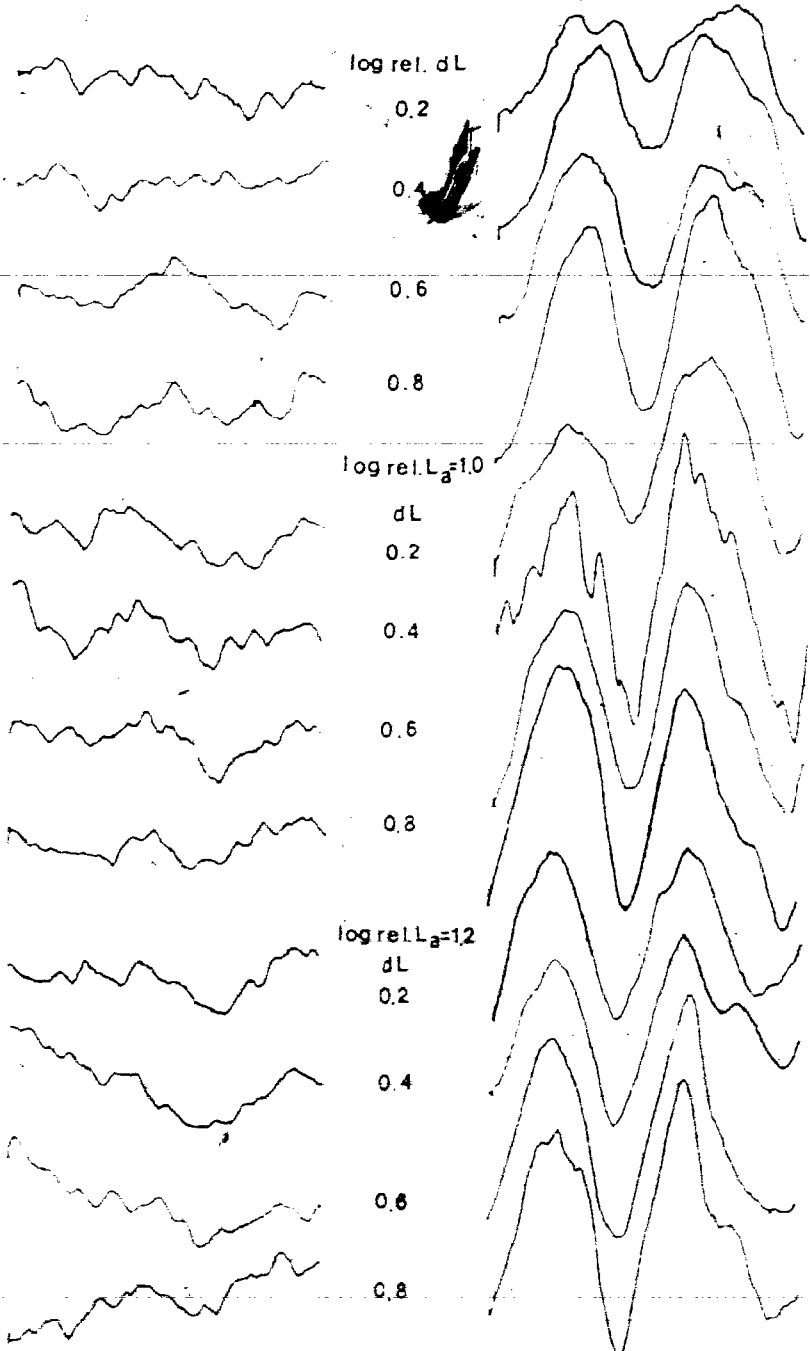


Figure 11b

Steady state ERG and VEP recordings to constant
incremental flicker luminance (dL) as a function
of increasing adapting luminance (L_a).

MT

isi=140 msec

64 x 2=128 repr

VEP

ERG

log rel dL=0.2

log rel L_a

0.6

1.0

1.2

log rel dL=0.4

L_a

0.6

1.0

1.2

log rel dL=0.6

L_a

0.6

1.0

1.2

log rel dL=0.8

L_a

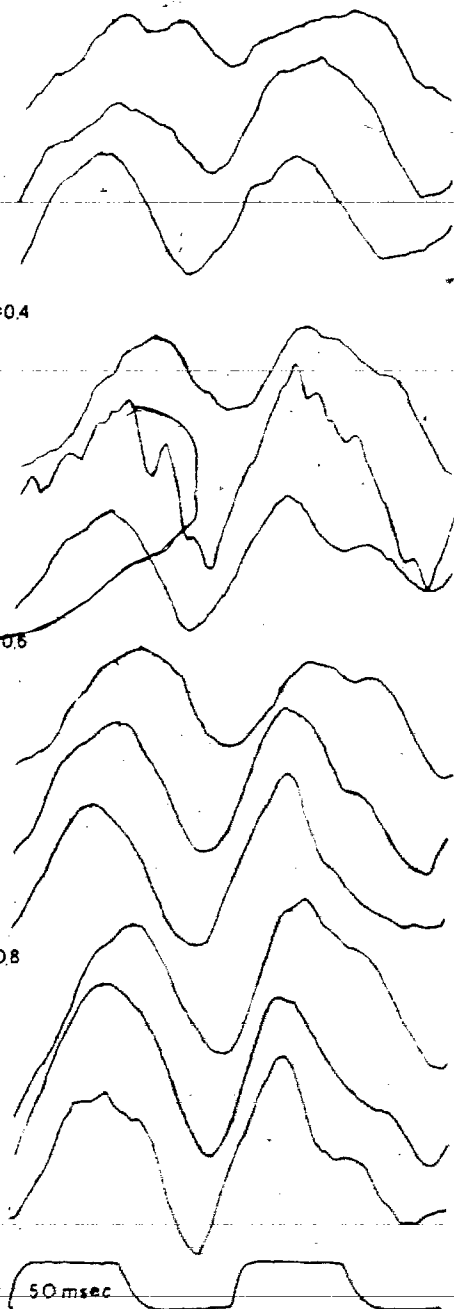
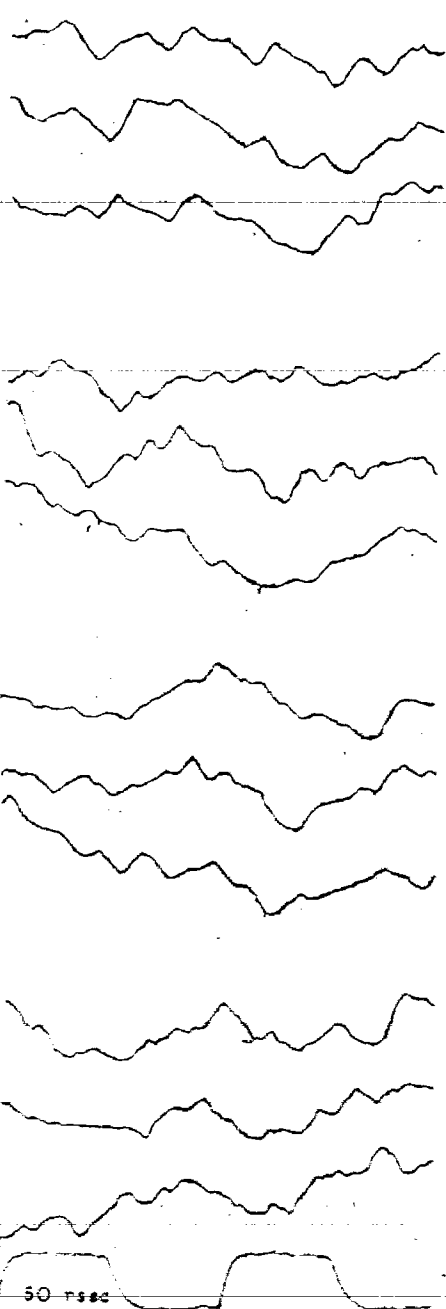
0.6

1.0

1.2

20 50 msec

20 Uv 50 msec



J

incremental flicker luminance (dL) appears to decrease the latency of the late negative component (N120-150). However, the peak to peak amplitude of the diphasic component (P100 - N150) appeared to be largely unaffected by the range of incremental flicker luminances used. Subject D.H. showed similar results but generally the electroretinal peak to peak amplitude was about one-third the size of M.T.'s. For any single incremental flicker luminance (dL) the effect of increasing adapting luminance (La) can also be seen clearly in Figure 11b. For the flicker-ERG's increasing adaptation level appeared to cause the b-wave component latency to decrease as the peak to peak amplitude increased. It was apparent that at lower incremental luminances the steady state electroretinal amplitude appeared to reach saturation. The steady state VEP appeared to progressively decrease the latency of N150 with increasing adapting luminance. From these and other data the luminances of the test and adaptation (surround) fields to be used in the parametric flicker response study were selected. Following is a description of the experimental method used for the study of electroretinal and central visual flicker response.

Parametric Flicker Response Study

Subjects: Simultaneous ERG and VEPs to brief squarewave flickering light were recorded from five (three male, two female) graduate students in the Psychology department at Simon Fraser

University. All individuals were students in electrophysiology, familiar with the evoked potential recording situation with sophistication in the demand characteristics of psychophysiological experimentation. Subjects were paid a \$4.00 /hr. honorarium.

Stimulus and Recording System: The stimulus was provided by a Xenon strobe (Grass PS2) positioned behind a white translucent diffusing screen. The flash duration, as specified by the manufacturer, was 10 microseconds. The interflash or interstimulus interval (ISI) was controlled by a solid state quartz crystal Stimulus Control Unit (SCU) designed and constructed by H. P. Gabert. The flickering circular test field, 20 degrees in visual angle, is surrounded by a 60 x 60 degree field of 1.5 μ L luminance. Test field time average luminance varied between 1.5 μ L during the 102 second adaptation cycle and 2.2 μ L with the stimulus flickering at 25 Hz. All photometric measures were calibrated with a Pritchard Spot Photometer.

Both VER and ERG were recorded with Beckman skin electrodes, filled with Hewlett-Packard REDUX paste, which formed the electrode-dermal bridge. Electrodes were applied after the skin had been cleansed with 95% isopropyl alcohol and had been digitally abraded with REDUX. Interelectrode impedance was

equalized and maintained below 3 Kohms as measured by Grass Model EZH impedance meter.

The visual evoked potential (VEP) was recorded with Beckman Ag-AgCl electrode secured by collodian impregnated gauze using a monopolar derivation from a position 2 cm. above theinion on the midline occiput and referred to the right earlobe. The electroretinogram (ERG) was recorded either from a corneal placement at O.D. using standard Burian-Allen contact lens electrode (Hansen ophthalmic lab P964), or from a noncorneal placement over the right infraorbital ridge using a small Beckman skin electrode secured by adhesive skin collar. A Grass silver disk electrode applied to the left earlobe served to ground the subject.

Preparation of O.D. for corneal placement consisted of flushing the orbit with sterile normal saline, followed by instillation of 0.5 % Pontocaine (or 1 % Opthcaine) to induce corneal anesthesia. After anesthesia was established the orbit was again flushed by normal saline followed by instillation of 2-3 drops of 1 % Isoptotears to provide sufficient lubrication during the recording session. At this point the Burian-Allen electrode assembly was gently inserted under the eyelids which were brought over the electrode to contact the speculum ridge which served to hold the eyelids apart while the electrode was in

place. A 2 milliamperere instrumentation fuse was placed between the corneal lens electrode and the amplifiers to ensure the safety of the observer's eye in accordance to ISCERG recommendations (Karpe, 1962).

Observers were positioned in the experimental chamber and dark adapted for a 15 minute period. The veiling luminance was then increased to 1.5 mL and the subject fixated the 60 by 60 degree adaptation surround field for 5 minutes. After light adaptation had been established the standard stimulation-adaptation cycle was initiated, consisting of 60 seconds of incremental flicker of the 20 deg. central test field. The test field luminance when flickering at 25 hz was 2.1 mL. After the stimulation cycle was complete the test field luminance remained at 1.5 mL for 102 seconds (adaptation cycle).

During the 60 second stimulation period the ISI was set at one of 22 ISI values ranging from 40 to 210 msec.; and 128 samples of EEG and VER activity were recorded and averaged at each ISI value. ISI values were presented with a 5 second verbal warning ("five seconds") prior to stimulus presentation. After completion of the 22 measurement trials a 1 microvolt, 50 msec. duration calibration pulse, provided by a Bioelectric CA5 calibrator was amplified, signal averaged, and stored along with the S's data. The raw flicker-evoked responses were amplified by

Elema-Schonander EEG EMT-12B differential a.c. amplifiers whose filter time constants provided 3 dB signal attenuation at turnover frequencies of 5 Hz and 700 Hz. The amplified signals were then routed to a direct airpen writer (Mingograf model 800) and simultaneously input to a signal averaging computer (Nicolet series 1070). Second stage filter cascading was provided at the input to the signal averager resulting in an effective bandwidth of 5-250 Hz. The penwriter provided an ongoing record which was scrutinized for artifacts during recording trials. Most artifacts originate from the subject and are extracerebral in origin (Armington, 1974). The most frequent artifacts were due to eyeblinks, eyelid flutter, or twitching of the lateral rectus muscle during photic stimulation. These artifacts were clearly detected in the raw EOG and EEG records and were more pronounced during trials where low flicker frequencies (< 7 Hz) were used. It was found that cotton wool padding applied against the occluded eyelid was somewhat beneficial in blink reduction; but that instillation of a local anesthetic (1% Pontocaine) was most effective in reduction of photic reflex. If any obvious artifacts occurred during a recording trial it was discarded and re-recorded. Through the use of attentive and sophisticated subjects the artifact discard rate was maintained at about 5%.

The signal averaging computer, a Nicolet Fabritek Series 1072, samples, digitizes and summarizes the ongoing activity at

regular intervals to achieve signal to noise enhancement. The Fabritek 1072 system consists of three modules: the data accumulator, a signal digitizer (SD-72/4A), and a sweep control unit (SW-71A). The sweep control unit, when triggered by a spike impulse originating from the stimulus control unit (SCU), initiates 256 signal sampling commands over a 200 msec. period in each recording channel. The signal voltage is digitized at 255 points, with one memory address reserved for sweep counting purposes. Fabritek address advancing was externally controlled by a Marconi TP2103 oscillator which produced a square wave pulse which advanced the address register 255 times during the 200 msec. sweep duration. Once the 256 (255 + 1) data points have been sampled the signal averaging system halts until another trigger pulse is received from the SCU. At each sweep the 255 digitized values are summed to the previous address contents until 128 sweeps have been summed. These 255 totals are normalized by the number of sweeps (128) which had been recorded in the last memory address of the 256 word record. The resultant waveform represents the averaged evoked activity (ERG or VER) to 128 samples of 200 msec. duration. These averaged-ERGs and VERs were displayed on a Tetrax (5031) oscilloscope and transferred as 1024 bit words to disk storage on a HP-2116B, using a data transfer program, FASO, written by H.P. Gabert.

Once digitized, the averages were plotted on a Omnigraphic Complot X-Y plotter (Houston Instruments) and dumped on magnetic tape and transferred to disk storage on IBM 370/155 for further analysis. Time-domain analysis of the resultant stimulus-locked activity was conducted by two methods: each single waveform was visually inspected by the experimenter and a peak identification algorithm (see Appendix U) was applied to detect peak reference points within the 200 msec sample. Positive and negative peak reference points were graphically plotted for the two ISI ranges studied, 40 - 75 msec and 80 - 210 msec, with ISI on the ordinate and sweep duration on the abscissa. Time-difference calculation of steady state latency (t) by least-squares regression determined the abscissa intercept for each of the lines.

The second technique was a modified time-difference calculation based upon a recently developed perspective feature detection technique (Coupland et al., 1978). This technique utilized computer graphic representation of the averaged evoked activity as a family of waveforms forming an apparent three dimensional terrain. The analytic utility of this surface perspective technique will now be discussed.

OVERVIEW OF PERSPECTIVE LATENCY CALCULATION

There currently exists an increasing interest in graphic (pictorial) display of electrophysiological information, paralleled by the development of computer system technology. Teicholz's (1975) survey of computer graphic applications in medicine and health care sciences provides an interesting review of the history of this infant field. Computer graphic techniques, for the representation of geographical surfaces, have been used by cartographers since the 1960's. Peuker's (1972) excellent review of 25 major cartographic programs includes seven capable of plotting perspective views of regular grid matrix data, in addition to other programs which plot flow patterns, contour mapping or perform geographic cosmetic routines such as analytic hill-shading.

Typically, cartographic programs would accept x , y , and z -values for input variables. The program would perform the necessary interpolation and other mathematical operations necessary to produce a continuous two-dimensional line drawing of the three-dimensional surface, in which the illusion of height is achieved by techniques an artist might use such as shading, texture, suppression of hidden features and perspective. The user can specify to the program various parameters to define the viewpoint from which the surface is to be seen, its' distance,

angle of view and magnification. The significance of the existence of such programs is that they may be used to depict not only physical surfaces but more generally the relation between any variable and any two other variables. Coupland, Taylor & Koopman (1978) reported the use of a three dimensional computer mapping program for the display of EEG data.

The writer used an interactive computer graphics system, THE PICTURE SYSTEM, produced by Evans & Sutherland. THE PICTURE SYSTEM is a general purpose, stand alone interactive computer graphics system which can display smoothly moving pictures of two- or three-dimensional objects including such features as perspective, rotation and zooming in depth. Basically the Picture System components include: a DEC PDP-11/34; hardware processing units for performing such functions as rotation, zooming and perspective; an 8192-point Picture Refresh Buffer, a Picture generator and a 21" CRT display and software support. Appendix C illustrates the standard configuration of THE PICTURE SYSTEM.

Picture Presentation and Preparation

Averaged-electroretinal and visual evoked potentials were transferred from IBM-370 disc partitioned data sets to the PDP-11/34 as grid matrices of 8x256 and 14x256 points comprising

a family of averaged-EEG waveforms each evoked by eight (40-75 msec) or fourteen (80-210 msec) interstimulus intervals. Each of the resultant 2048 or 3584 points in the database is defined in terms of its corresponding x, y and z-value. The display file is prepared through a series of linear transformations on the database matrix. Simple and compound linear transformations such as rotations, perspective, windowing and scissoring, translations and scalings can be described by a stack transformation matrix which is then sequentially multiplied by the original database by the matrix arithmetic processor. The resulting processed display frame is loaded into the refresh buffer. For each frame refresh the terminal control reads the data in the Refresh Buffer and passes the data to the Picture Generator, where the data is converted to analog signals to drive the electron beam positioning in the Picture Display. Picture refreshing occurs at the rate of 30 times a second.

A specific multichannel time-series graphics display program for the experimenter's data, MA2 (see Appendix D) provided the user capability to manipulate the data through 16 separate function switches under program control. The experimenter could define the data matrix x, y and z-scaling, the elevation of view, azimuth, distance, as well as the resolution and direction of linear interpolation (across rows or columns). In addition, moving x-scale background and foreground markers were utilized for the visual sighting of peak reference events.

PROCEDURE FOR PERSPECTIVE LATENCY CALCULATION

Each grid matrix of averaged-electroretinal or visual evoked potential datapoints was viewed from an 80 degree elevation, 360 degree azimuth at a distance of twice the row length. Linear interpolation across rows produced the appearance of 8 (or 14) 256 point averaged-ERG or VER waveforms viewed in perspective (looking due north). Trial flicker rate, expressed as interstimulus interval, systematically decreased from foreground to background. The amplitude of the evoked activity was expressed as surface elevation. In order to provide a view of all of the data, hidden-line suppression was not utilized. Axis labelling and the legend describing program options in use, parameters being displayed and marker values were deleted from the display during dynamic visual inspection of the surface.

Three observers (A.Q., M.T., D.B.) visually inspected static and dynamic perspective displays for surface feature regularities such as peaks, pits, ridges, ravines. After becoming familiar with three dimensional display manipulation each observer then psychophysically determined the visual best-fitting line through perspective reference features. This was done by moving background and foreground markers to respective X-scale values; a line was "drawn" between the tips of the two markers. The

foreground and background markers were positioned by the observers so that the connecting straight line (eg., A-A, B-B, etc. in Figures 12a,b; 13a,b) represented the best psychophysical estimation of the relation between averaged-ERG reference features and the interstimulus interval. Observers were required to psychophysically curve-fit both positive (ridges) and negative (ravines) polarity events in each of the ERG and EEG landscapes. When the best "line of sight" had been determined for a set of positive (or negative) sloping features the slope estimate of this interconnecting line was used to predict the corresponding X-intercept values by the method of least squares. The corresponding average X-scale intercept value of these quasi-regression lines in tridimensional space determined the steady-state electroretinal or VEP latency for each ISI range (80-210 or 40-75 msec). This psychophysically approximated quasi-regression solution assumed a constant following latency (of the ERG or VEP), which could be empirically tested by deleting matrix rows and recalculating the steady-state latency on the smaller ISI range sub-matrix.

Figure 12a

Average-ERG family composed of eight 256 point waveforms each evoked by a different flicker rate. ERG amplitude expressed as surface elevation. This planometric projection is viewed from 80 degree elevation and 345 degree azimuth. Peak reference points lie directly under the lines joining the letter pairs A-F.

GR

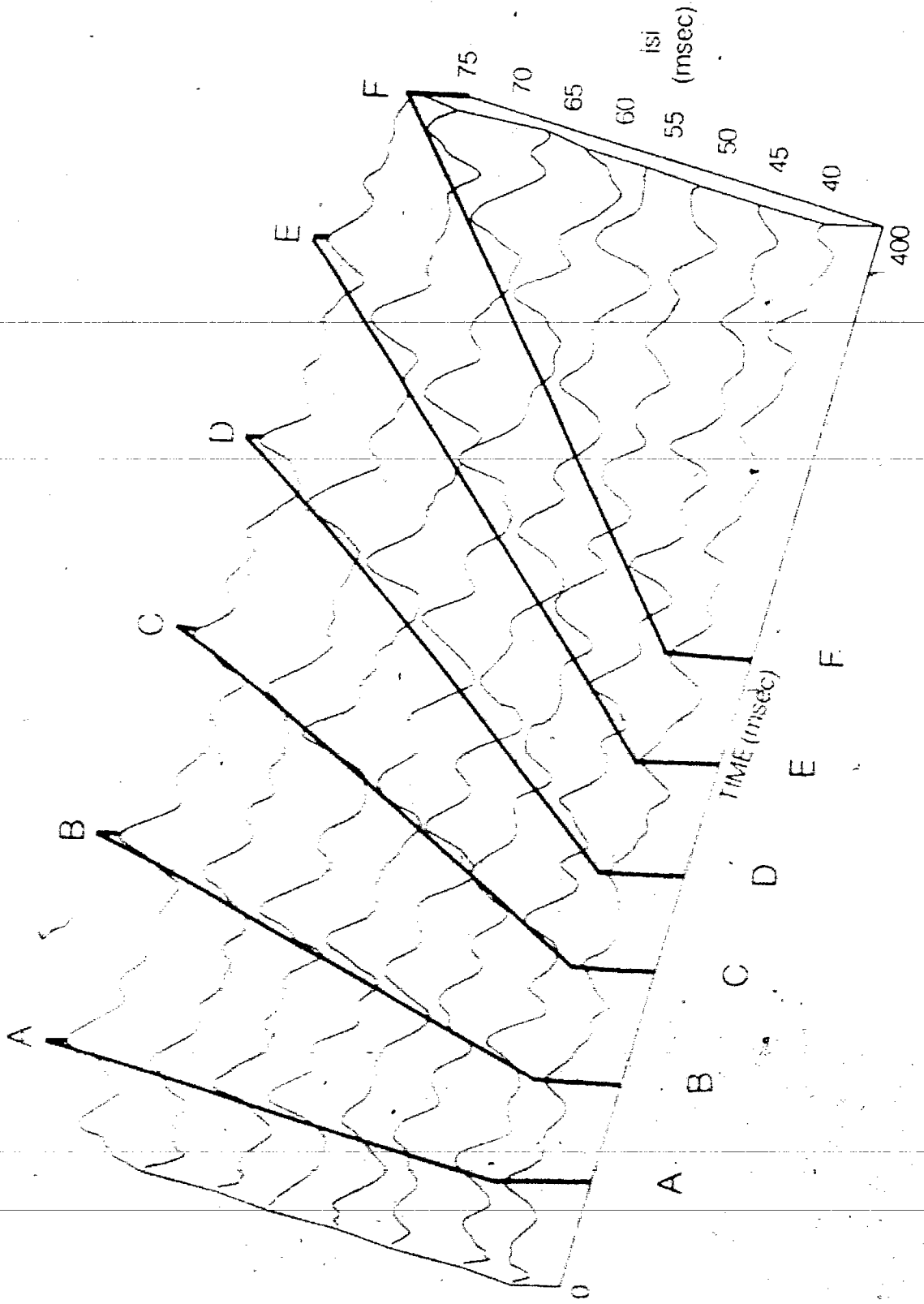


Figure 12b

The same view as Figure 12a, but with linear interpolation across diagonal matrix elements and with the horizontal intersecting lines A-F deleted. Diagonal lines increase surface texture and promote visibility of relevant features.

CR

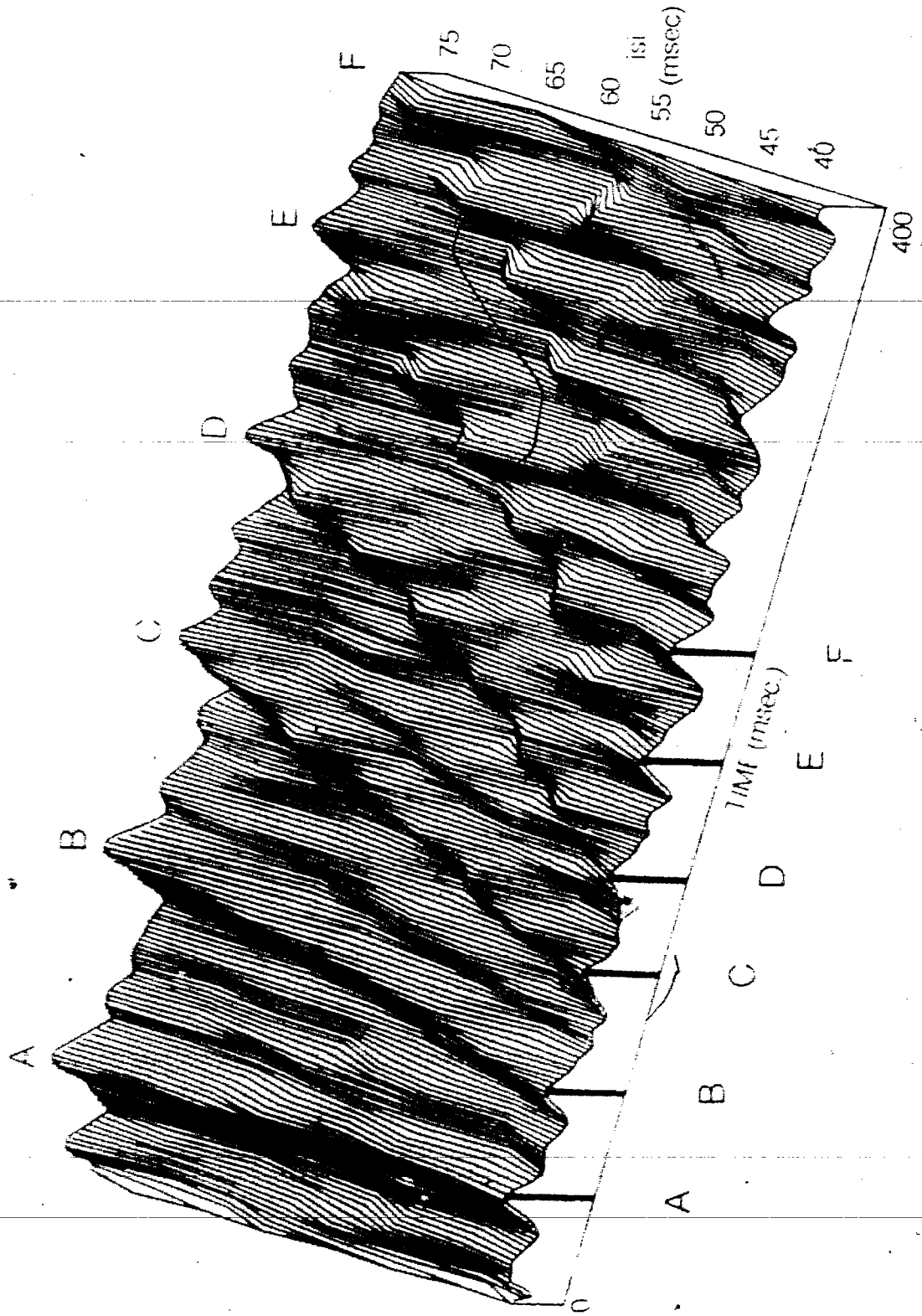
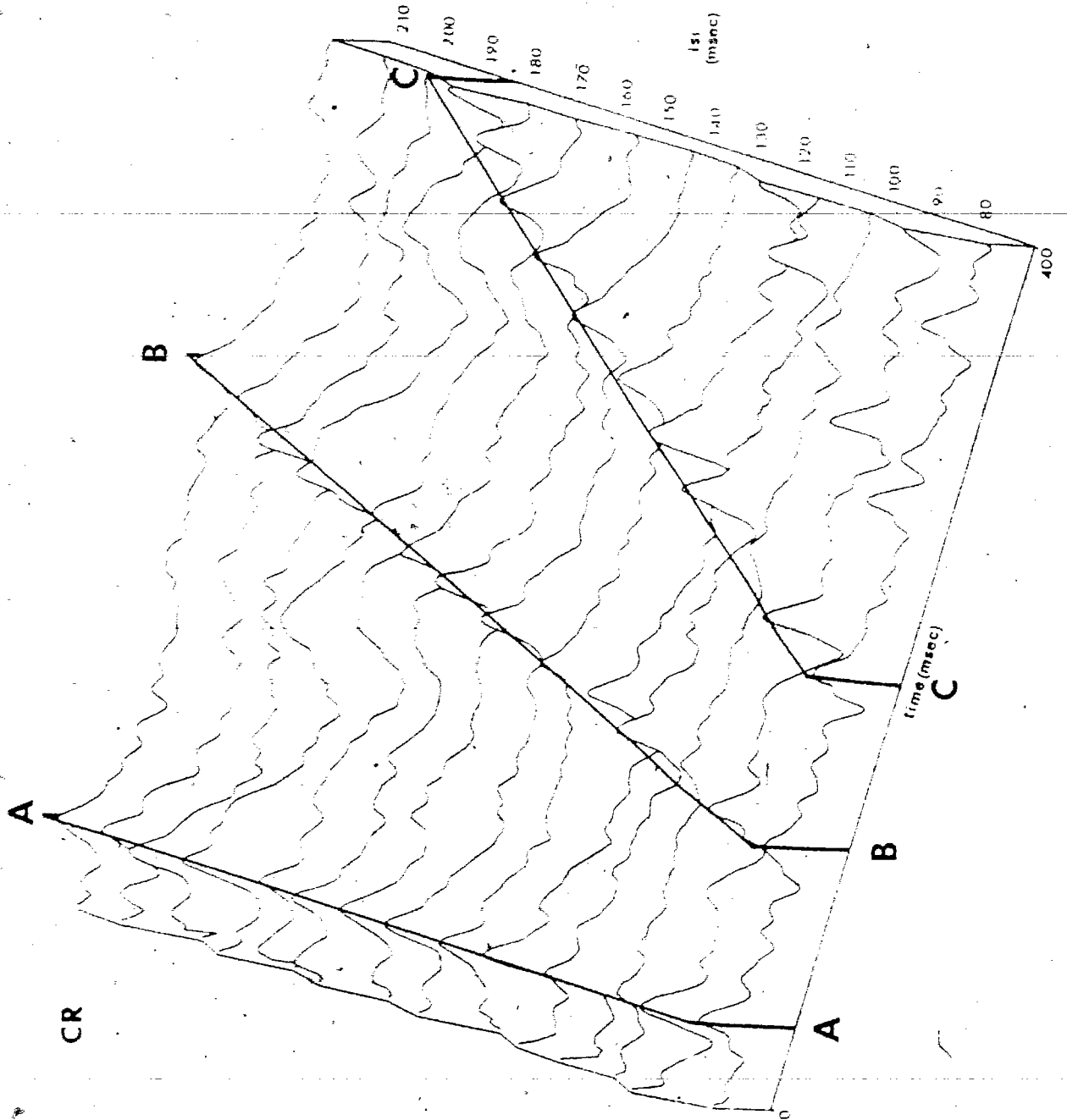


Figure 13a

Averaged-ERG family of fourteen 256 point waveforms each evoked by different flicker rate. This planometric projection is viewed from 80 degree elevation and 345 degree azimuth. ERG amplitude is expressed as surface elevation. Peak reference points lie directly under the lines joining the letter pairs A-C.



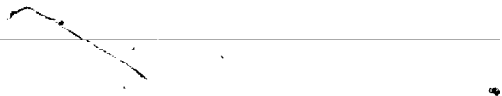
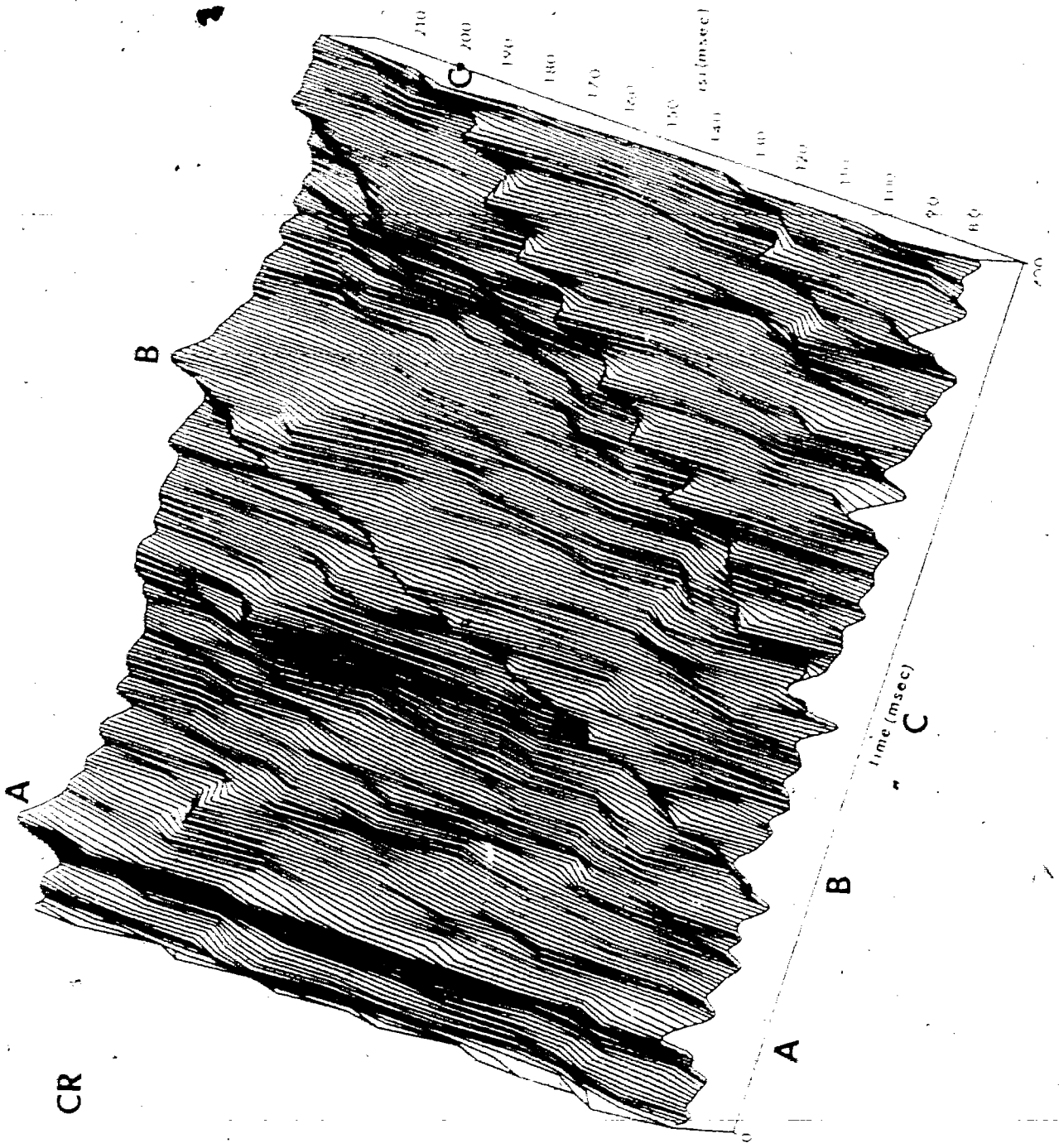


Figure 13b

The same view as Figure 13a, but with linear interpolation across diagonal matrix elements and with horizontal lines A-C deleted. ~~Diagonal lines increase surface texture and~~ promote visibility of relevant features.



CR

CHAPTER 3

RESULTS

TIME DIFFERENCE CALCULATION

After several years experience visually inspecting averaged electroretinal and evoked potential recordings a reasonably working peak detection algorithm for deriving the peak latencies of EP minima and maxima events was developed (see Appendix U). Peak latency was determined as a function of signal amplitude and temporal features of the EP waveform. This two-dimensional peak latency calculation (2-D LC) was used in handscoring of the 220 flicker frequency trials by S.C. To assess the consistency of the 2-D LC procedure, three other naive raters (D.H., P.B., M.T.) were given 25 randomly selected averaged ERG and VEP waveforms to hand score. Each 200 msec unlabelled VEP or ERG record was accompanied by a calibration signal. Observers were also given an accompanying example of an EP record on which positive and negative peak latencies had been indicated. From S.C.'s 2-D LC scoring of the corresponding EP records 128 peak reference features were selected and the standard error of rater estimates of peak latencies were calculated for all 128 selected features. Frequency histograms of the sample standard deviations (E) and variances (EE) are presented in Appendix A. For the four psychophysical observers (SC, MT, DH, PB) using the 2-D LC peak

detection algorithm the mean standard deviation in estimation of peak latency was 1.6 msec (s.d.=1.2 msec). These results indicate a high inter-rater agreement on the peak latency of single-trial averaged ERG and VEP features using the handscoring 2-D LC peak detection procedure.

The Effect of Flicker Rate upon Steady State Latency of ERG and VEP: Two-dimensional Latency Calculation (2-D LC)

Having gained some confidence that other electrophysiologists can "see" the same EP events, for each subject the experimenter plotted graphs of the ERG and VEP latencies of positive and negative peak reference points in the two ISI-ranges (40-75 and 80-210 msec) with ISI on the ordinate and sweep duration on the abscissa. Figure 14a illustrates the plotted peak (positive and negative) reference points for subject C.B., for averaged-VEP's recorded for 400 msec sweep duration in an ISI range of 80-210 msec. Positive peak latency reference points are indicated as '+' and negative points are designated as open squares. Least-squares regression lines have been drawn through each set of positively (1P, 3P, 4P) and negatively sloping (1N, 3N, 4N) peak reference points and can be seen converging towards the (sweep duration) X-axis. Graphic presentations of peak latency points were produced on a PDP-12 using LINDSYX, a Lap 6-W graphic plotting routine. Curve fit

Table I: Steady state latency (t) derived from the average X-intercept of regression lines tabulated in Appendix I.

Time-difference calculated steady-state latency from positive (Tpos) and negative (Tneg) peak reference points changes as a function of ISI range.

	VER					
	Tpos			Tneg		
	slow flicker series	fast flicker series	Δ Tpos	slow flicker series	fast flicker series	Δ Tneg
CR	109.45	95.00	14.45	140.43	77.38	63.05
DH	107.49	74.39	34.10	73.05	67.37	5.68
AQ	105.05	116.70	-11.65	137.94	93.86	44.08
PB	112.24	112.25	-0.01	139.88	111.97	27.91
MT	108.48	89.35	19.13	123.46	76.65	46.81
Mean	108.54	97.54	11.00	122.95	85.46	37.49

Table I continued

ERG

	tpos			tneg		
	slow flicker series	fast flicker series	Δ tpos	slow flicker series	fast flicker series	Δ tneg
CR	34.13	34.79	-0.66	14.12	17.32	-3.20
DH	43.04	36.95	6.09	26.07	25.46	0.61
AQ	34.67	31.79	2.88	15.50	15.94	-0.44
PB	38.82	37.33	1.49	22.14	17.39	4.75
HT	32.55	32.21	0.34	18.27	18.73	-0.53
Mean	36.64	34.61	2.03	19.22	18.97	0.25

values of slope, X-intercept and standard error (SE) for each regression solution are presented in Appendix I. The average X-intercepts of VEP and ERG regression lines are presented in Table I where it can be seen that for C.R. the average X-intercept value for positive (Tpos) VEP peaks is 109.5 msec, while negative peak latency regression lines appear to be converging toward an average X-intercept (Tneg) value of 140.4 msec. These average intercept values identify the true steady state latency (Diamond, 1977b) for the ISI range of 80-210 msec. It should be noted that such a straight line regression calculation assumes a constant EP latency over the ISI range studied.

Figures 14b and 14c illustrate the averaged-ERG waveform over the same ISI range (80-210 msec) for subject C.R. Here the positive and negative peak reference events are indicated by '+' and open squares respectively. Linear regression lines calculated by least squares have been fitted through each set of positive or negative peak reference points. Slope and X-intercept curve fit values for each set of peak reference features for all five subjects are summarized in Appendix I. Steady state electroretinal (tpos and tneg) and visual evoked potential (Tpos and Tneg) latencies are summarized in Table I. Figures 14d - 14g represent the ISI range (40 - 75 msec.) for subject C.R. and the associated 2-D LC plot of peak positive and

Figure 14a

Positive (+) and negative (open squares) VEP peak latencies
for C.P. over an ISI range of 80 - 210 msec..

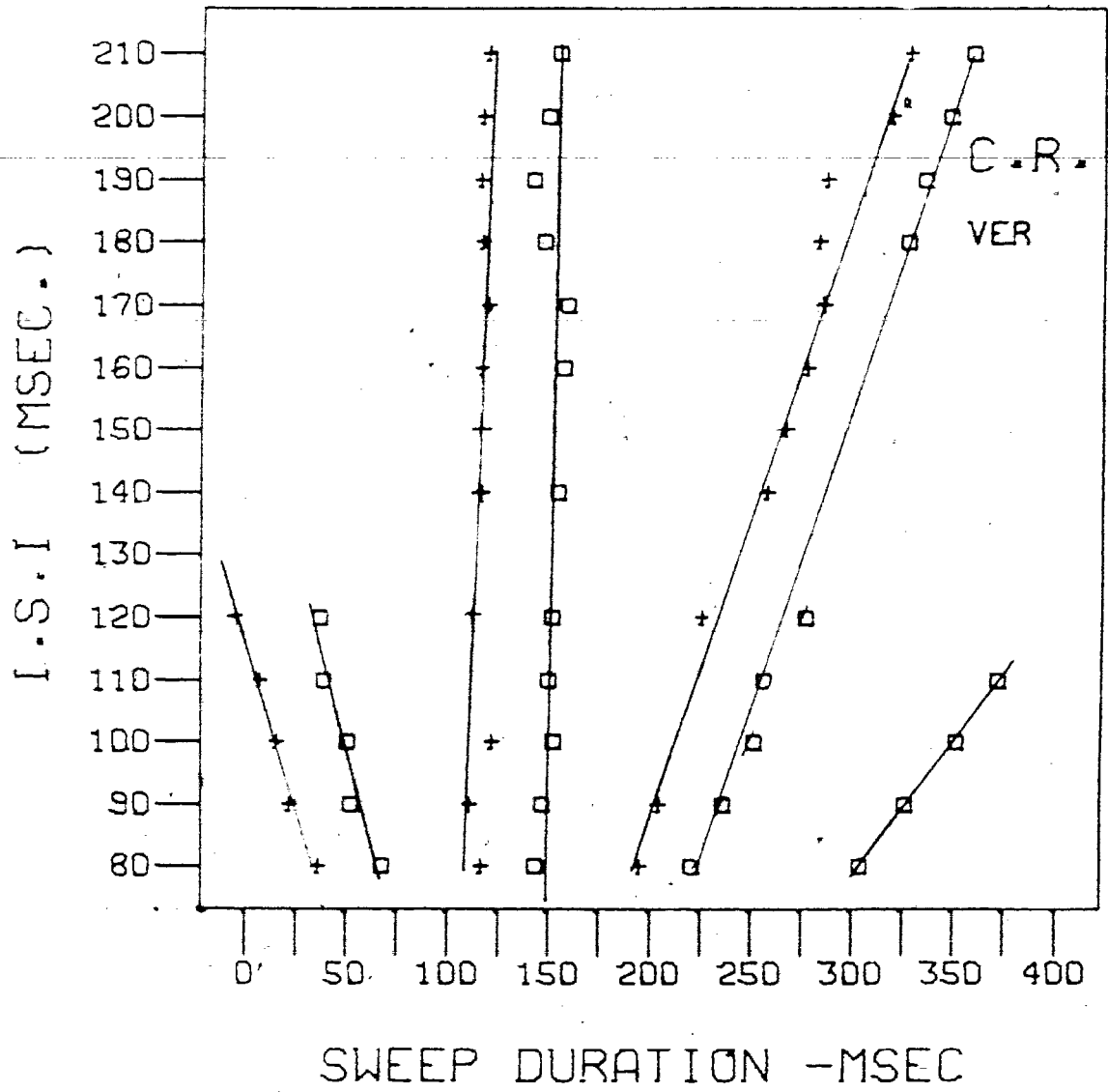


Figure 14b

ERG positive peak reference points for C.R. over an ISI range
= 80 - 210 msec. (slow flicker series).

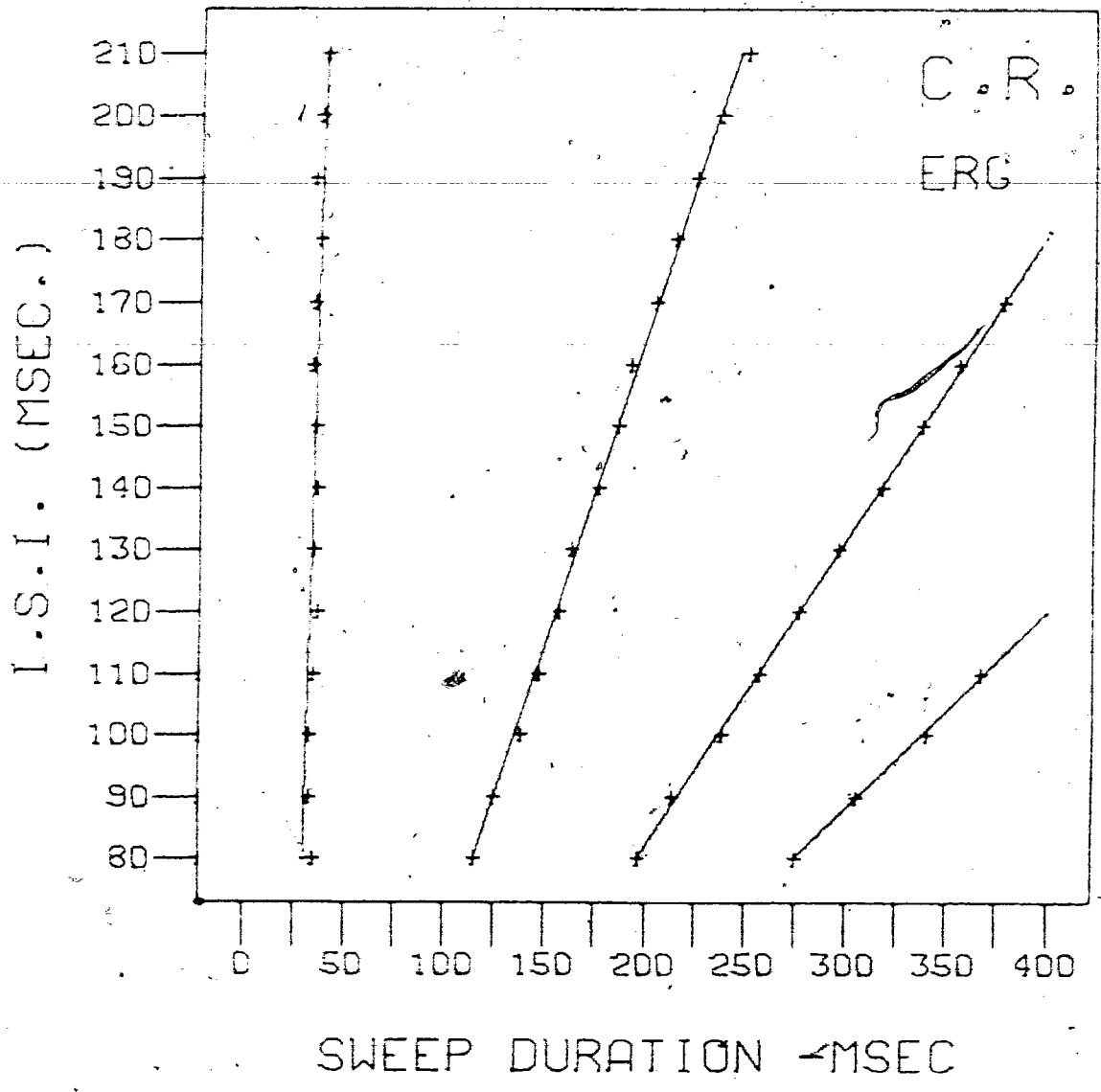


Figure 14c

ERG negative peak latency reference points for C.R. over an
ISI range = 80 - 210 msec. (slow flicker series).

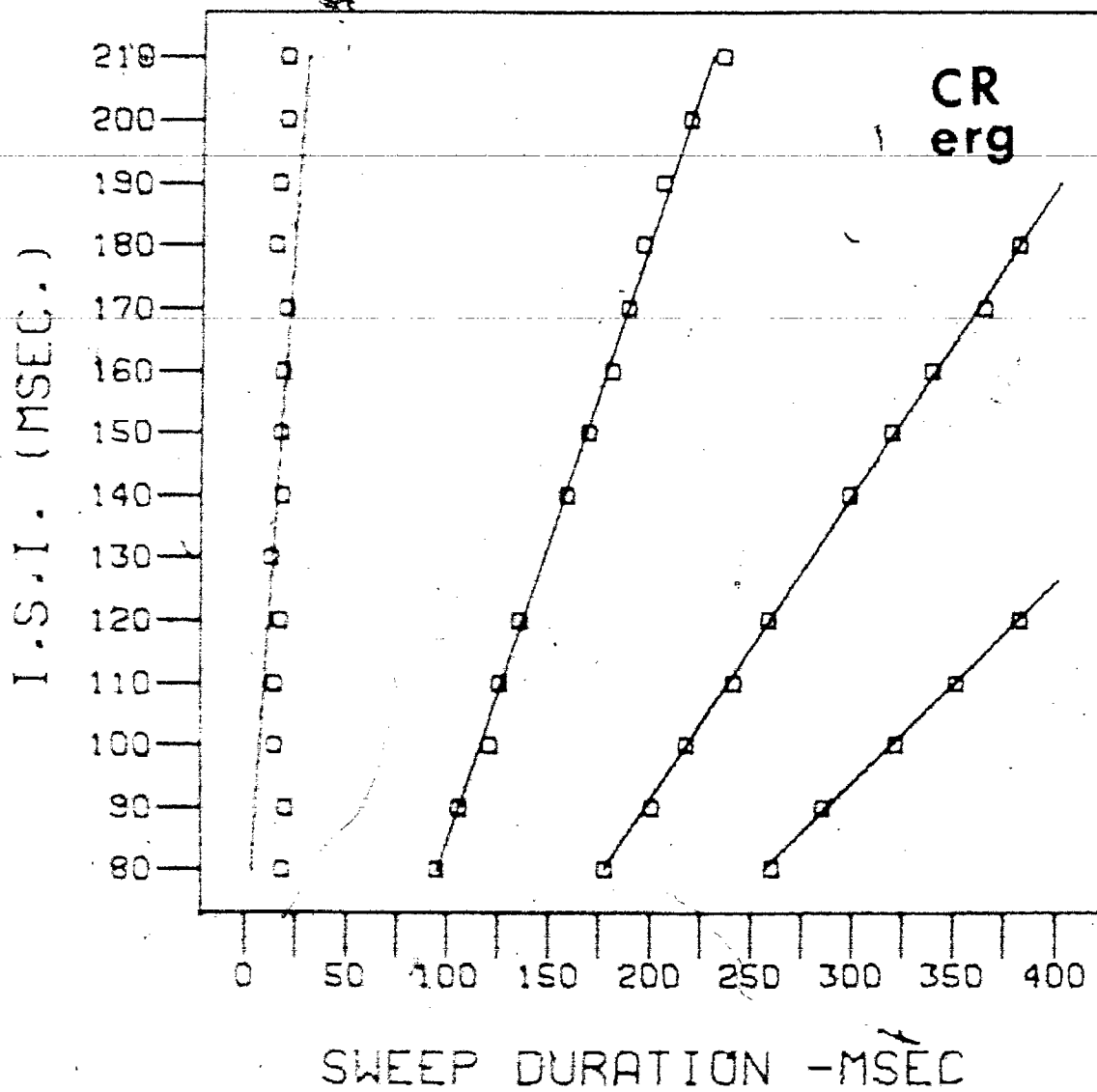


Figure 14d

VER positive peak reference points for C.R. over an ISI

range = 40 - 75 msec. (fast flicker series).

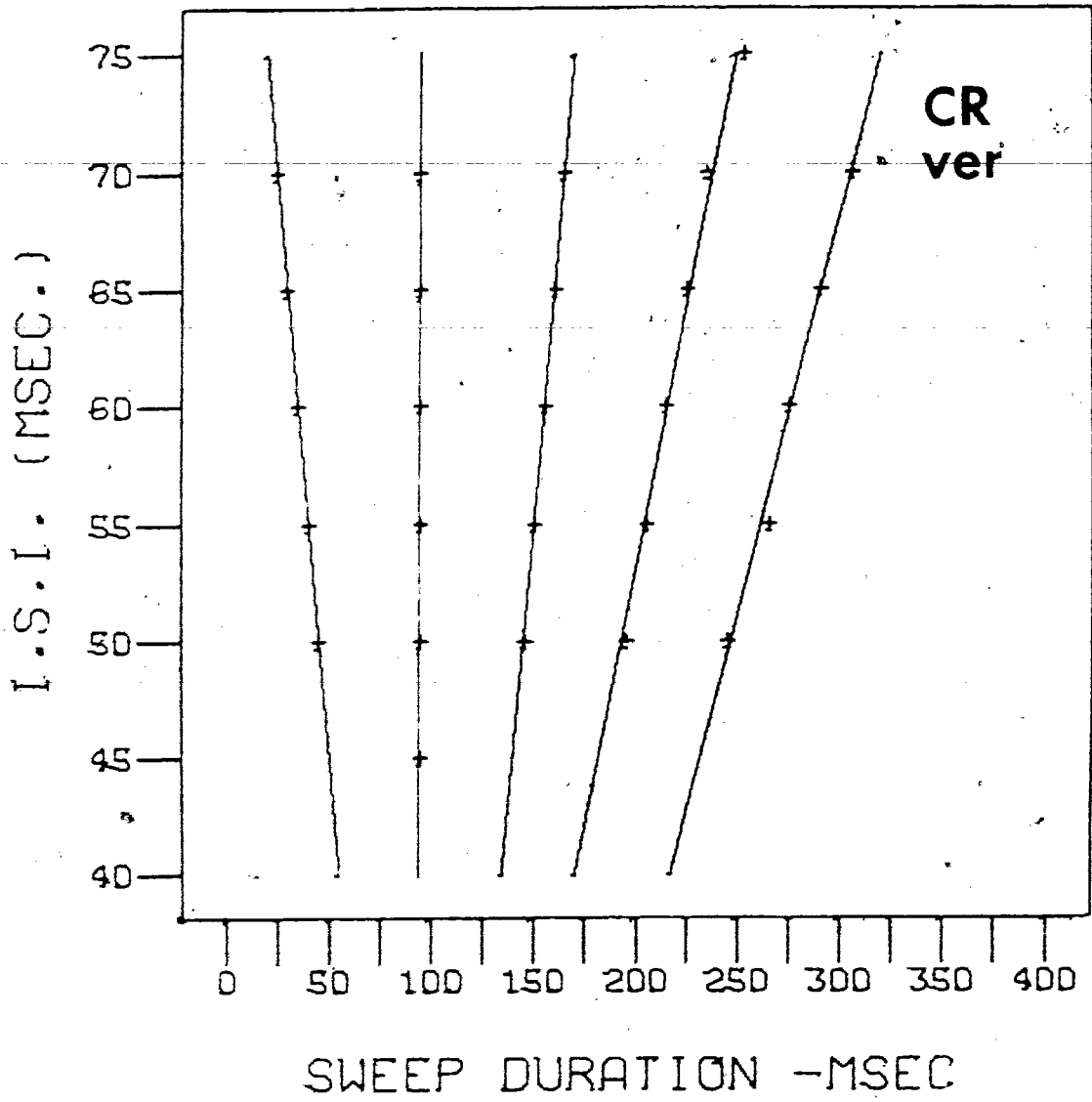


Figure 14e

VER negative peak reference points for C.R. over an ISI range
= 40 - 75 msec. (fast flicker series).

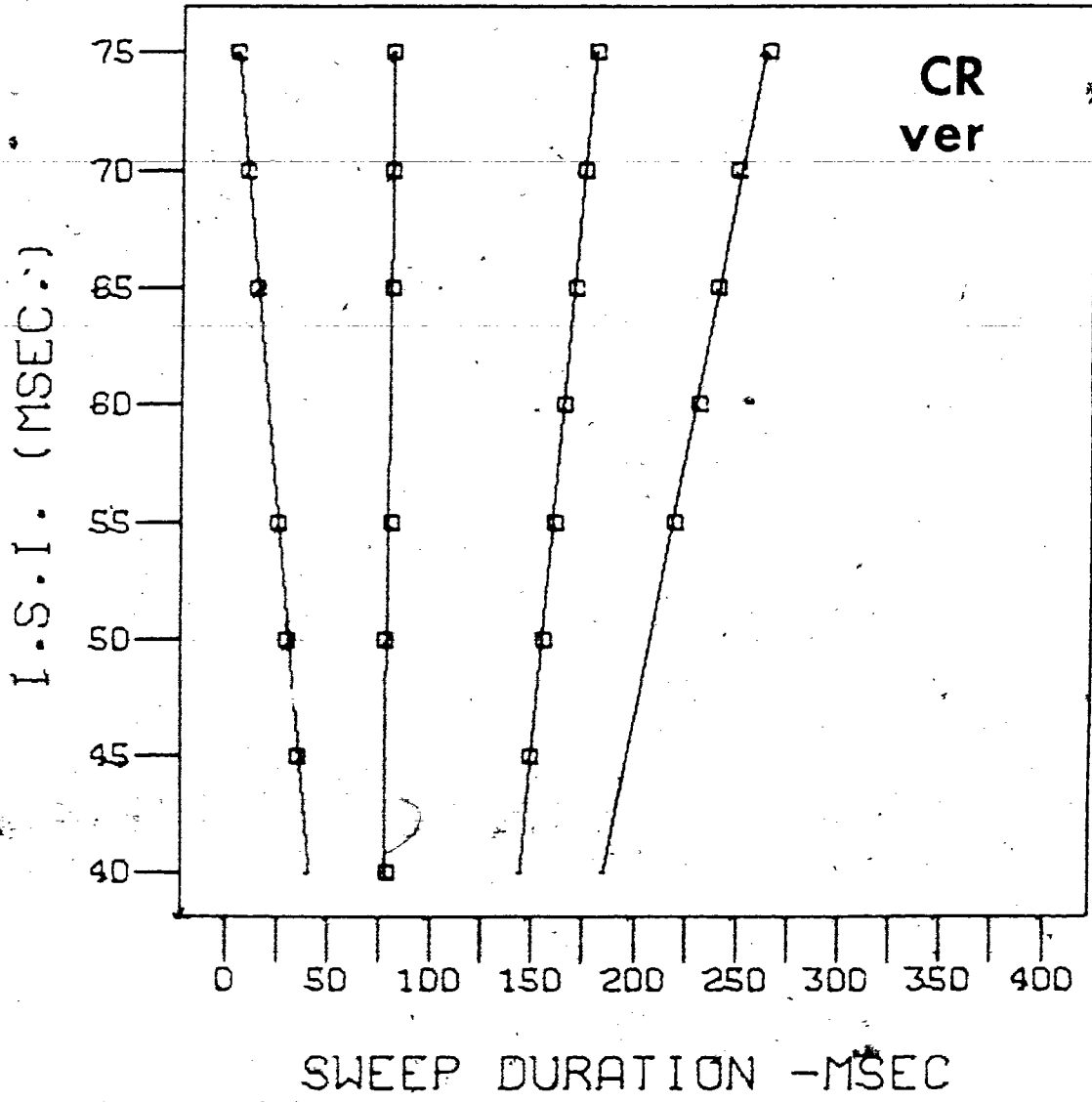


Figure 14f

ERG positive peak reference points for C.R. over an ISI range

=40 - 75 msec. (fast flicker series).

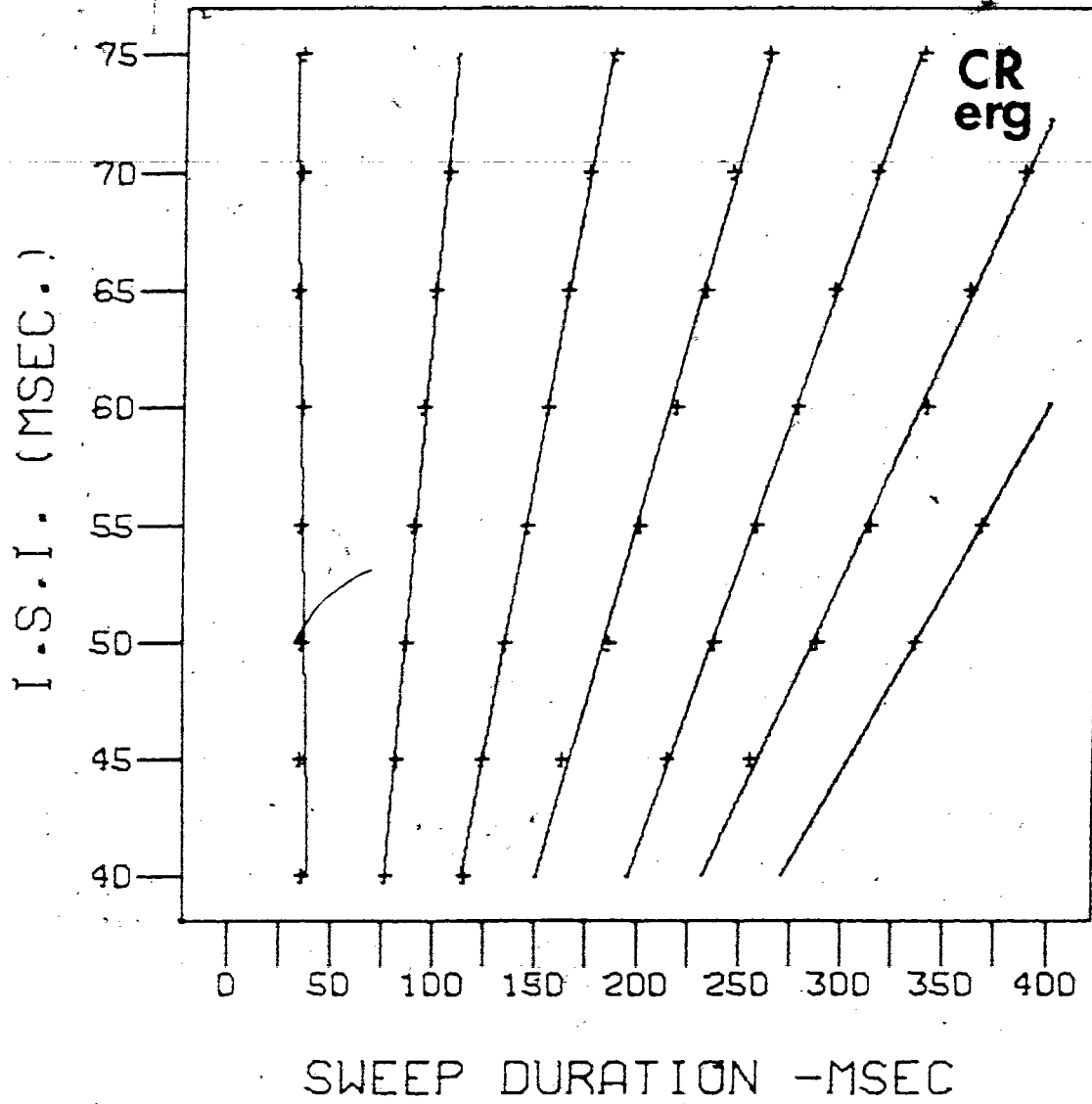
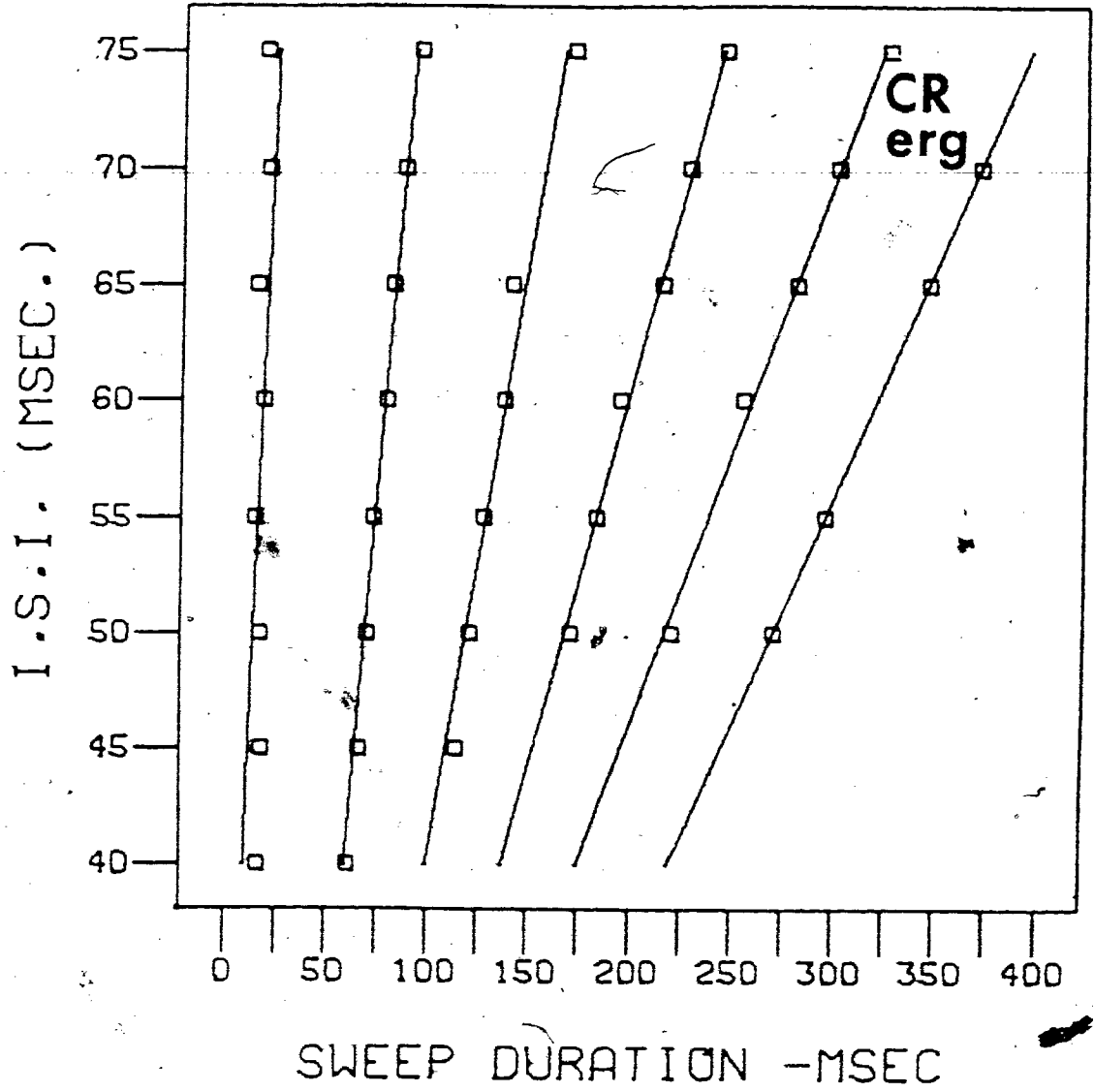


Figure 14g

ERG negative peak reference points for C.R. over an ISI
range = 40 - 75 msec. (fast flicker series).



peak negative features are presented.

Inspection of Table I indicates that for the steady state VEP the mean Tpos latency for the slow flicker series (ISI=80-210 msec) was 108.54 msec where the corresponding fast flicker series (ISI=40-75 msec) mean Tpos was 97.54 msec, indicating an average Tpos latency decrease of 11.0 msec. The steady-state VEP latency (Tneg) determined from negative peak reference points showed a corresponding frequency-dependent latency shift, decreasing from a mean value of 122.95 msec (for the slow flicker series) to 85.46 msec (for the fast flicker series), a 37.49 msec shift.

It is apparent from inspection of Table I that electroretinal steady-state latency is relatively independent of flicker rate. Mean positive electroretinal steady-state latency (tpos) for the slow flicker series was 36.64 msec, while the fast flicker series produced a tpos of 34.61 msec, a decrease of 2.0 msec. Steady state negative ERG components also demonstrate no apparent latency shifting as flicker rate increases. Mean negative electroretinal latency (tneg) decreases only 0.25 msec from 19.22 to 18.97 msec as ISI is systematically reduced from 210 msec to 40 msec.

Figures 15a and 15b illustrate the scalp-recorded steady

Figure 15a

Plot of steady-state VEP latency shift of positive component
(T_{pos}) as a function of ISI range.

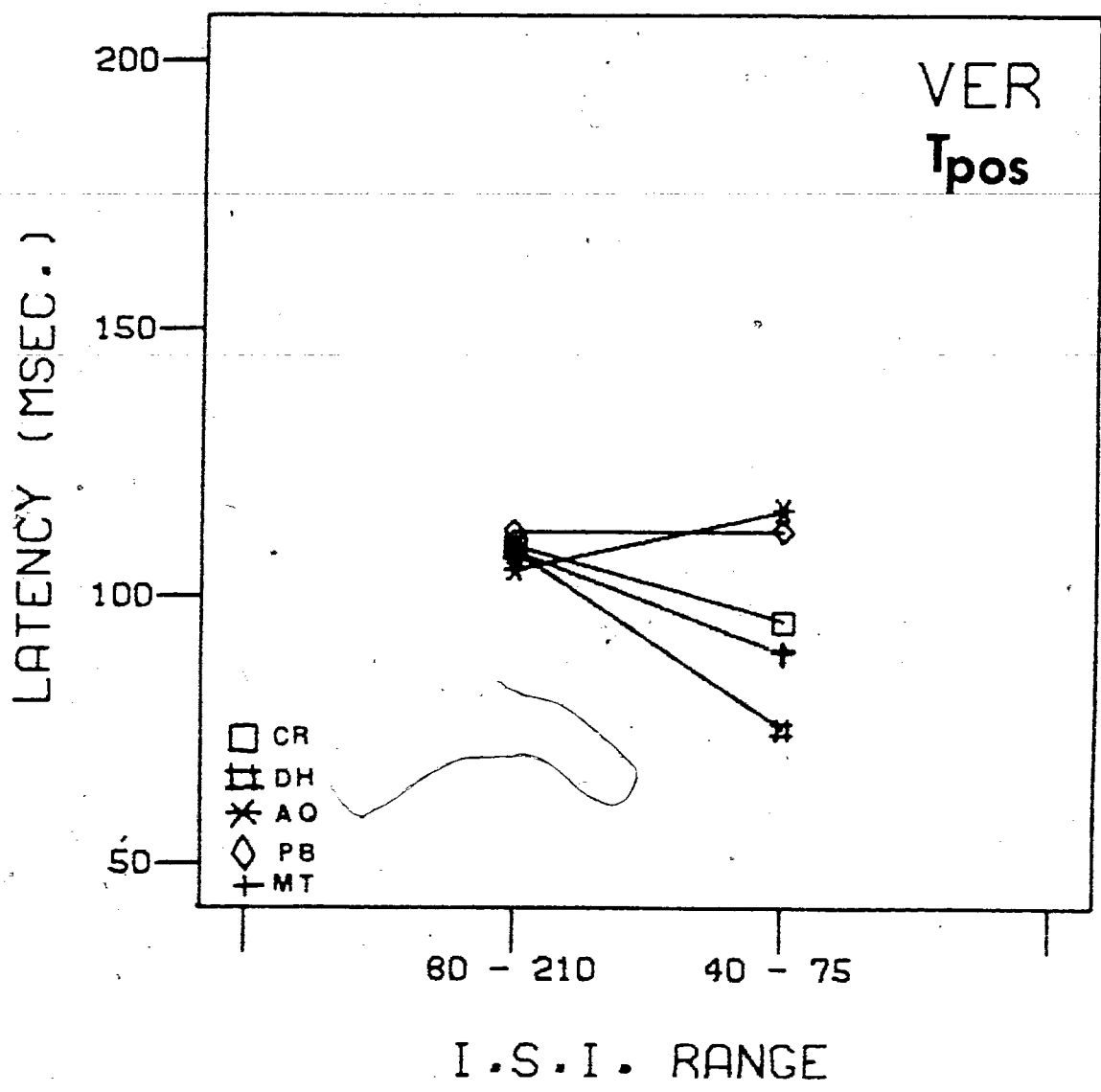


Figure 15b

Plot of steady-state VEP latency shift of negative component
(T_{neg}) as a function of ISI range.

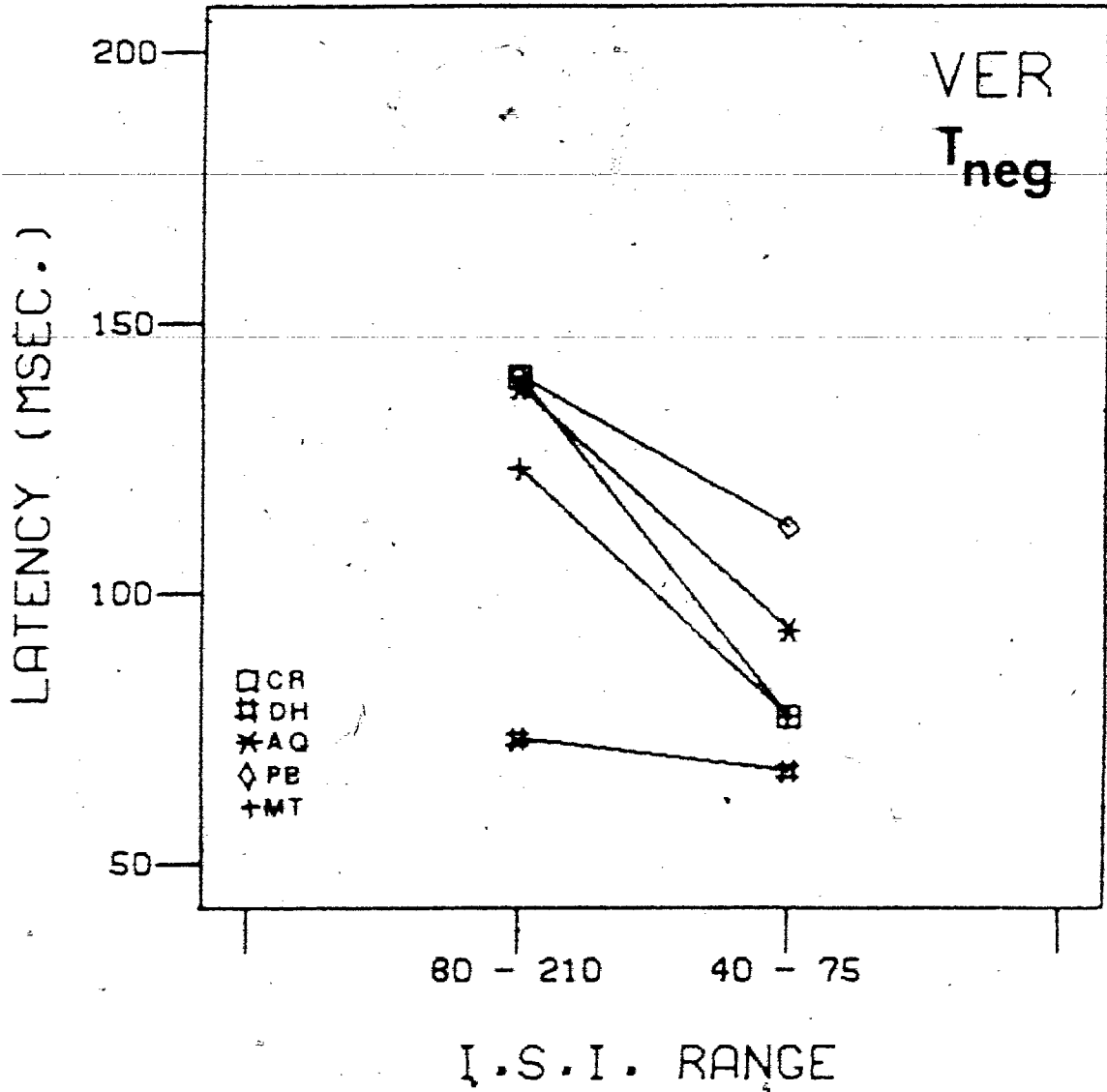


Figure 16a

Plot of steady-state ERG latency shift of positive (tpos)
component as a function of ISI range.

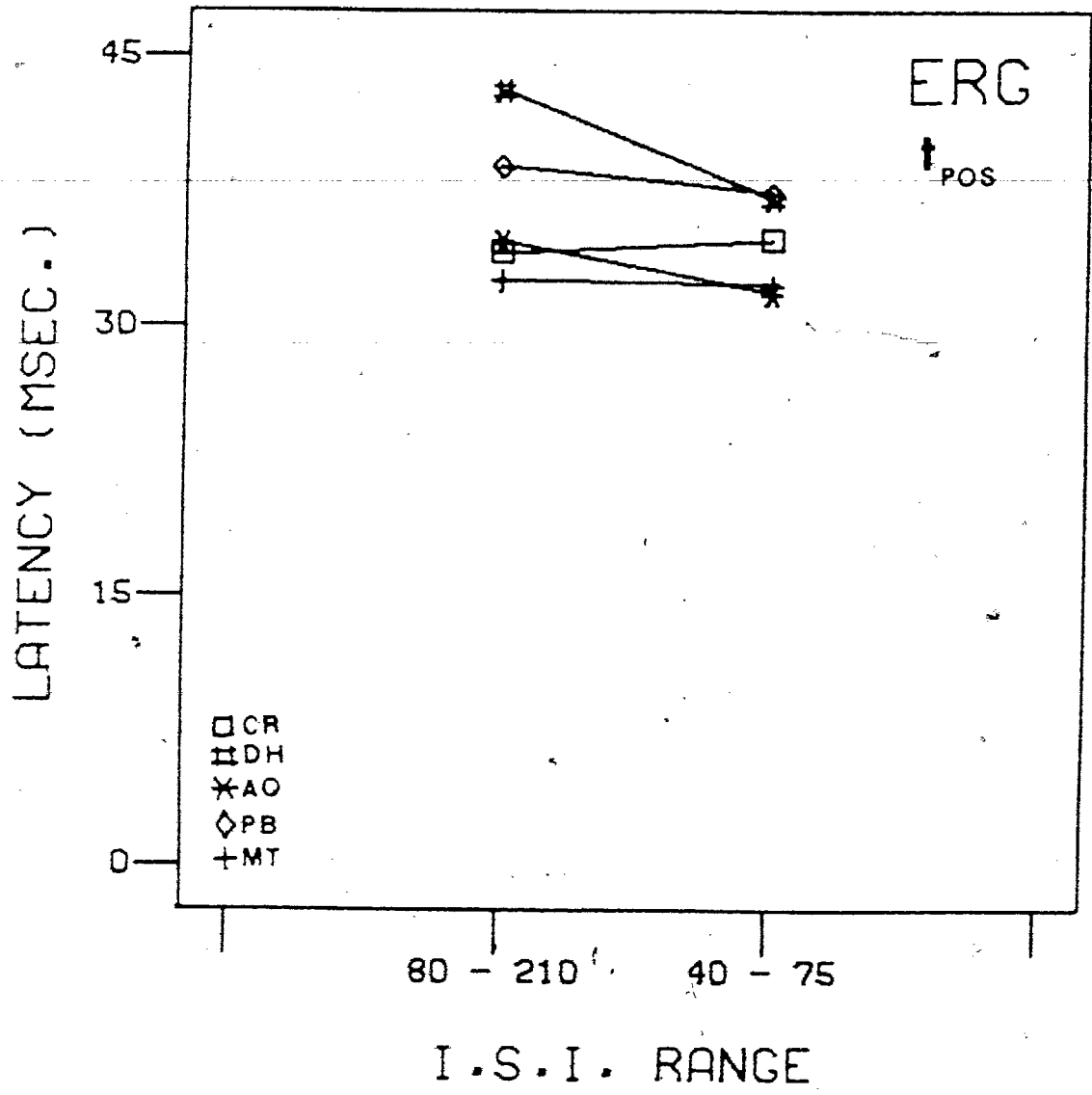
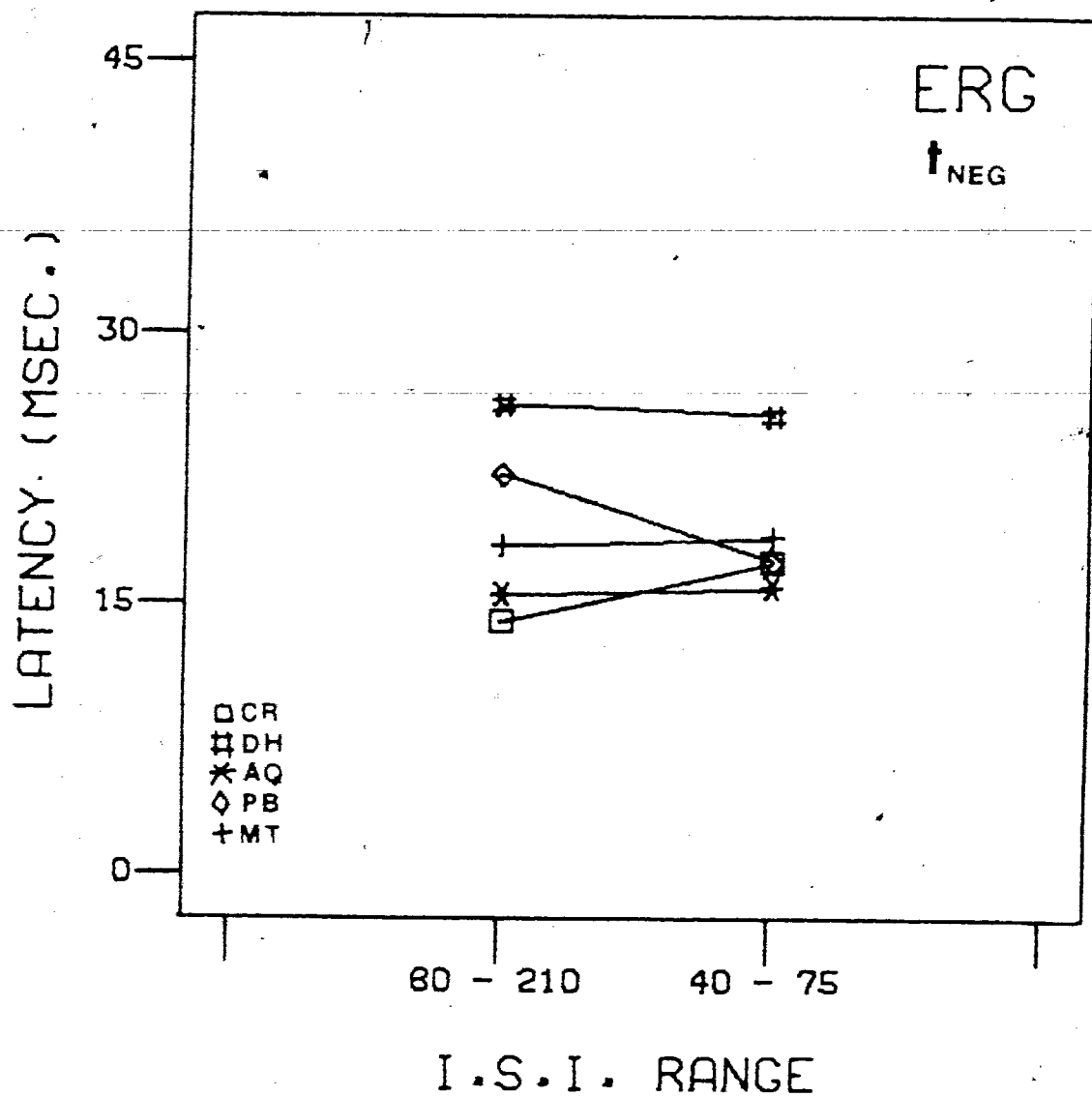


Figure 16b

Plot of steady-state ERG latency shift of negative (tneg)
component as a function of ISI range.



state VEP latency shift for all 5 subjects for calculated T_{pos} and T_{neg} values for Table I. Corresponding steady-state ERG t_{pos} and t_{neg} values are presented in Figures 16a and 16b. While there appears to be a slight discrepancy in the direction of A.Q.'s VEP flicker induced latency shift the overall agreement is quite good.

The Effect of Flicker Rate upon Steady State Latency of VEP and ERG: Three Dimensional Latency Calculation (3-D LC)

The procedure for three dimensional latency calculation (3-D LC) already outlined was utilized by 3 psychophysical observers (S.C., D.H., M.T.) in the determination of steady state electroretinal and VEP latency for each subject's slow flicker and fast flicker perspective display. Appendix K contains the averaged-ERG and VER slow and fast flicker series for subject C.R. with psychophysically-estimated quasi-regression lines fitted to the positive peak reference features. The amount of variability among X-intercept values used in determining true steady state latency was assessed by the standard error of estimate. Table II illustrates the mean standard errors (E) and variances (EE) averaged across all raters. The mean standard error for true steady state latency determined by a single perspective sighting of positive (or negative) peak reference features was 6.2 msec. (or 5.5 msec.) respectively.

Table II: Mean standard error (E) and
variance (EE) of true steady-state
latency derived by 3-D LC procedure.

Table II: Mean standard error (E) and variance (EE) of true steady state latency derived by 3-D LC procedure.

3-D LC derived from positive pks. (n=60)	3-D LC derived from negative pks. (n=60)	3-D LC derived from both peaks (n=120)
E= 6.2 msec.	E= 5.5 msec.	E= 5.9 msec.
EE= 38.6 msec.	EE= 30.1 msec.	EE= 34.8 msec.

Graphic 3-D LC plots of the interobserver agreement in their ability to visually discriminate the same peak reference features are presented in Appendix K. The lines connecting points are quasi-regression lines whose slopes are used in the determination of the X-intercept and corresponding steady state latency (t'_{pos} or t'_{neg}).

ANOVA OF THE 3-D LC DETERMINED STEADY-STATE LATENCIES

Two separate fourway ANOVAs (rater x subject x ISI range x recording site) were conducted on the positive and negative perspective-determined steady-state latencies reported in Table IV. Inspection of the ANOVA summary tables presented in Table III indicated a significant ISI range by recording locus interaction (I x L) for steady-state latency determined by both positive and negative peak reference features ($p < .05$ and $p < .001$ respectively).

Statistically nonsignificant effects were found for raters (R), rater by ISI range (RI), rater by recording locus (RL), and rater by ISI range by recording locus (RIL) interactions. In contrast, subject main effect (S), subjects by ISI range (SI), subjects by recording locus (SL), and subjects by ISI range by locus (SIL) interaction effects were statistically significant

Table III: ANOVA summary tables for 3-D LC positive and
negative determinations. Raters (R) by
subjects (S) by ISI range (I)
by recording locus (L).

ANOVA SUMMARY FOR 3-DLC POS. PEAK LATENCY DETERMINATION

SOURCE	ERROR TERM	F		DEG. OF FREEDOM	MEAN SQUARE	
1	MEAN			1	319740.0	
2	R	RS	1.5438	ns (p >.25)	2	25.55045
3	S	RS	18.6482**		4	308.6248
4	I	SI	1.4469	ns (p >.25)	1	470.3999
5	L	SL	202.87**		1	71691.25
6	RS				8	16.54984
7	RI	RSI	1.3471	ns (p >.25)	2	17.15002
8	SI	RSI	25.5359**		4	325.1079
9	RL	RSL	0.1301	ns (p >.25)	2	2.281250
10	SL	RSL	20.1513**		4	353.3750
11	IL	RIL+SIL-RSIL	5.624*		1	374.9375
12	RSI				8	12.73141
13	RSL				8	17.53610
14	RIL	RSIL	0.3112	ns (p >.25)	2	3.662476
15	SIL	RSIL	21.6716**		4	255.0326
16	RSIL				8	11.76804

** p <.001

* p <.05

ANOVA SUMMARY FOR 3-DLC NEG. PEAK LATENCY DETERMINATION

SOURCE	ERROR TERM	F.		DEG. OF FREEDOM	MEAN SQUARE
1	MEAN			1	257677.1
2	R	RS	1.5055 ns (p >.10)	2	38.21689
3	S	RS	37.6060**	4	954.6079
4	I	SI	7.573 ns (p >.05)	1	4437.598
5	L	SL	75.9**	1	117926.6
6	RS			8	25.38446
7	RI	RSI	2.6634 ns (p >.10)	2	51.45117
8	SI	RSI	30.3328**	4	585.9746
9	RL	RSL	1.0384 ns (p >.25)	2	30.46875
10	SL	RSL	52.8864**	4	1551.781
11	IL	IL+SIL-RSIL	25.219**	1	5301.563
12	RSI			8	19.31818
13	RSL			8	29.34180
14	RIL	RSIL	0.7930 ns (p >.25)	2	12.98633
15	SIL	RSIL	46.5298**	4	762.0254
16	RSIL			8	16.37714

** p<.001

($p < .001$).

Table IV summarizes the mean perspective-determined steady state latencies for all subjects across the two ISI ranges. Table IV indicates that the positive component of the steady state VEP decreases in mean latency (T'_{pos}) from 114.5 msec to 99.6 msec as flicker rate is increased, a mean overall decrease of 14.9 msec. As in the two dimensional latency calculation (2-D LC) the 3-D LC of negative steady-state VEP latency (T'_{neg}) appears to decrease by 37.2 msec, from 127.6 msec (for the slow flicker series) to 90.4 msec (for the fast flicker series).

Examination of the 3-D LC of positive and negative flicker-ERG components confirms the findings of the two-dimensional time-difference calculated steady-state latency. For both positive and negative steady-state ERG components there appears to be no systematic frequency related latency shift. Since changes in latency of steady-state electroretinal response (t'_{pos} and t'_{neg}) noted in Table IV are all less than the standard error of estimate they were considered to be nonsignificant, hence the ERG component steady-state latency did not change as a function of increasing flicker rate. The significance of these experimental observations will be discussed.

Table IV: Three-dimensional time-difference
calculated steady-state latency (t)
for five subjects over two ISI ranges.

Table IV: Three-dimensional time-difference calculated steady-state latency (t) for five subjects over two ISI ranges.

	VER					
	T'pos (msec)			T'neg (msec)		
	slow flicker series	fast flicker series	$\Delta T'_{pos}$	slow flicker series	fast flicker series	$\Delta T'_{neg}$
CB	119.9	78.25	41.65	150.50	73.50	77.00
DH	106.6	96.1	10.50	79.10	74.61	4.49
AQ	115.20	120.05	-4.85	142.10	98.90	43.20
PB	114.61	112.86	2.15	137.52	120.43	17.09
MT	116.30	90.83	25.47	128.80	84.75	44.05
Mean	114.52	99.62	14.90	127.60	90.44	37.16

Table IV continued

	ERG					
	t'pos (msec)			t'neg (msec)		
	slow flicker series	fast flicker series	$\Delta t'_{pos}$	slow flicker series	fast flicker series	$\Delta t'_{neg}$
CR	35.60	30.40	5.2	21.45	24.44	-2.99
DH	44.20	41.11	3.19	25.71	24.70	1.01
AQ	35.00	34.50	0.50	16.30	16.80	-0.50
PB	40.30	39.00	1.30	19.76	16.86	2.90
HT	35.32	37.13	-1.81	18.70	19.60	-0.90
Mean	38.08	36.43	1.65	20.38	20.48	-0.10

CHAPTER 4

DISCUSSION

The organization of this chapter will deal with the following issues: the consistency between the two time-difference latency estimates (2-D LC and 3-D LC) of steady state electroretinal and visual evoked potentials. The writer will then discuss the theoretical significance of the general experimental findings in terms of the level of signal processing of flicker evoked events, including speculation about their possible physiological origin.

CONSISTENCY BETWEEN THE TWO TIME-DIFFERENCE LATENCY
CALCULATIONS (2-D LC AND 3-D LC)

Examination of Table I and Table IV suggests the overall agreement between the two time-difference methods in estimation of steady state ERG and VEP latency is extremely high. Inspection of the mean T_{pos} and T_{neg} values in Table I and Table IV indicates that both 2-D LC and 3-D LC methods are tracking the same set of electroretinal and EP reference features. Single subject examination of 3-D LC and 2-D LC results in the ERG reveals that the greatest difference between the two procedures for latency calculation occurs for C.R.'s t_{neg} estimates. The difference between the two methods' calculated latencies for the

ERG a-wave ($t_{\text{neg}} - t'_{\text{neg}}$) for the slow flicker series was 7.3 msec. For all other subjects the agreement between the two methods for estimation of electroretinal latency was typically within ± 2 msec. It should be noted however, that the discrepancy in C.R.'s data was due in fact to the increased sweep duration in these recordings (400 msec.). Doubling the sweep duration produces twice the number of peak reference features, which would at first appear to increase reliability in mean latency calculation. However, it should be noted that as the total number of peak reference features increases likewise there is a resultant increase in the number of regression slope estimates. Examination of the tables in Appendix I reveals that as regression slope diverges from zero the standard error of error increases systematically. This relationship of increasing standard error size with increasing regression slope magnitude is reflected in every subject's data; but is more apparent for C.R. since there were at least two peak reference slope estimates. Simply stated, in such cases where there are more peak reference slope estimates (e.g. P-4 and P-5 for subject C.R.) then the least squares fitted regression line of latency on ISI is being estimated on fewer datapoints. Subsequent variability in the latency of each individual peak reference feature has a greater effect on the regression slope as the total number of peak reference features decreases.

Ideally the magnitude of this slope-related standard error could be reduced in the average X-intercept values in tables in Appendix I by some weighting function based in part upon the number of data points in each regression estimate. This would have the effect of reducing the contribution of those regression lines whose slope diverges from zero. Such a weighting function was not utilized in this study, instead the X-intercept values of all peak slope estimates were equally weighted. After visual inspection of the tabulated data in Appendix I, it was concluded that the overall agreement between individual peak reference X-intercepts were acceptable for the purpose of calculation.

A Pearson-r correlation was performed between the 2-D and 3-D LC calculated steady-state latencies in Tables I and IV, revealing a highly positive relationship ($r = .9915$) between these two time-difference latency estimation techniques. In summary, it appears that both 2-D LC and 3-D LC procedures have derived a sufficiently equivalent quantification of a steady-state ERG and VEP event.

DISCUSSION OF RESULTS FROM 3-D LC ANALYSIS OF VARIANCE

From inspection of the two ANOVA summary tables (see Table III) several conclusions can be reached: firstly, the statistically nonsignificant R, RI and RL effects indicate that

raters are essentially parallel or unchanging in their visual discrimination of salient surface feature regularities in the electrophysiological landscapes. That is, raters are selecting the same sets of features in each of the 20 perspective displays. The second conclusion concerns the large F ratios for all subject main and interaction effects. The statistically significant SI and SI interactions ($p < .001$) indicate that subjects are significantly different from each other in their true steady state latency both as a function of recording site and ISI range. This finding is further supported by inspection of Tables I and IV which reveal obvious intersubject differences in true steady state latency. Likewise, the significant SIL interaction ($p < .001$) indicates subjects significantly differ in the amount of site-dependent latency shift, that is some subjects are showing significantly different latency shifts at each recording site. Inspection of the individual subject's ISI-dependent latency shifts in Figures 15a,b and 16a,b confirm this finding. Finally, the previously discussed significant ISI range by recording locus (I x L) interaction indicates that magnitude of steady-state latency shift varies as a function of the recording site.

THEORETICAL SIGNIFICANCE OF EXPERIMENTAL RESULTS

The results of the parametric flicker study outlined in this dissertation clearly indicate that the mean latency of the steady

state visual evoked potential appears to decrease in quantal step fashion as a function of increasing flicker rate. The magnitude of the resulting frequency-dependent VEP latency shift is seen to be a function of the EP-component polarity. Table IV indicates mean latency shift to be in the order of 14.93 msec for the positive component reference points and 37.16 msec for negative component reference points. At this point the neurogenesis and physiological significance of steady-state EP time-components is still a matter for speculation (Spekreijse et al., 1977). However, frequency-domain analysis of steady state EP's to homogeneous field stimulation has identified three frequency component subsystems with different cortical origins in the human visual system. Spekreijse et al., (1977) described a high frequency signal system which apparently underlies the primary response arising in the striate cortex. This signal dominates in the 40-60 Hz frequency range (Regan, 1968) and appears to have an apparent latency of about 80 msec. A medium-frequency signal subsystem dominating the 14-20 Hz range, probably arising from striate projection area 18 (and possibly 19), was isolated by van der Tweel (1964) and later by Regan (1966), having an apparent latency range of 100-120 msec. The slow-frequency signal subsystem predominates around the spontaneous alpha rhythm (9-12 Hz) and has an estimated latency of 120-200 msec. Spekreijse et al., (1977) and others (Regan, 1972; van der Tweel, 1964) have developed electronic-analogue models for the human evoked

response system to account for the responses obtained with sinusoidal Gaussian-modulated homogeneous fields. Unfortunately, these models do not apply when incremental flicker or flash stimuli are used, since these models have been derived using the small signal approach in an attempt to linearize the visual response. Intense flash stimuli introduce various nonlinearities that make frequency-domain analysis of doubtful value. However, it does suggest that the VEP time-components reported in this study may likewise be characteristic of these same steady-state frequency-specific signal subsystems, since there appears to be discrete incremental shift in the VEP steady-state latency as flicker frequency increases from the slow (4.76 - 12 Hz) to the fast (13 - 25 Hz) flicker range. Therefore, one can conclude that frequency domain models alone do not offer a unique description of the human evoked response system to flicker.

Time-difference methods of calculating steady-state latency make possible the analysis of specific time components of the steady-state EP (Diamond, 1977b). In the present study the steady state b-wave (t_{pos}) and a-wave (t_{neg}) were clearly identified in the averaged-ERG and were found to shift less than ± 2 msec. across the flicker range (4.76 - 25 Hz), while the positive and negative components of the steady-state VEP shifted in the order of 14.9 and 37.2 msec respectively (Table I and IV). The theoretical significance of this finding in terms of a

time-domain model of visual flicker signal processing lies chiefly in the indication that frequency-dependent latency shift is of cortical origin in the human visual system.

Another finding that positive and negative steady state components are differentially affected (in terms of latency shift) suggests that the component polarity itself might reflect different signal subsystems. It appears that the positive component P115 is the most consistent feature for all subjects in the slow flicker range. De Voe et al., (1968) examining the evoked occipital response in a study of foveal function concluded that the VEP latency of P110 provided a response characteristic that was in excellent agreement with psychophysical determined photopic sensitivity functions. De Voe et al. (1968) concluded that the scalp recorded VEP was indeed of foveal (cone process) origin. Whether the steady-state VEP positive component reported in this study also reflects cone system functioning cannot presently be clarified. However, appropriate psychophysical manipulation of chromatic flicker adaptation could possibly tease out concomitant rod-cone contributions in the steady-state ERG and VEP.

Inspection of individual subject's steady-state VEP and ERG latency shifts (Table I) indicates that for two subjects (A.Q., P.B.) these same VEP positive component latency does not appear

to shift significantly with increasing flicker rate. However, both P.B. and A.Q. do have moderately large frequency dependent negative component latency decrements. Further inspection of the "raw" averaged-EP records revealed the cortical following response to be amplitude attenuated and sinusoidal in waveform with associated response doubling at low ISI range for A.Q. The writer suggests that for A.Q. this apparent lack of frequency-dependent latency decrement could be due to the loss of peak feature uniqueness associated with EP amplitude attenuation and sinusoidal entrainment. As EP amplitude diminishes the waveform loses characteristic reference features becoming less distinct as it takes on a sinusoidal appearance. This loss of peak identification information is confounded by EP frequency-doubling, which makes estimation of peak latency difficult for the 2-D LC or 3-D LC procedures. Generally, in all subjects the VEP following at low ISI's (<50 msec) made peak latency determination increasingly inferential for reasons already discussed, and it appears that both 2-D LC and 3-D LC time-difference procedures are less suited to situations where the EP waveform loses characteristic reference features.

CONCLUSIONS

In conclusion the findings of this parametric investigation of electroretinal and VEP flicker response by time-difference

techniques can be summarized as follows: firstly, time-difference analysis indicated a flicker frequency-dependent latency shift for the steady-state VEP, but with no corresponding electroretinal latency shift. Secondly, these experimental findings were interpreted and discussed as indicating that the ISI-dependent latency shift originates at some central (possibly cortical) loci in the human visual system, with no apparent contribution of peripheral (retinal) mechanisms. This observed relationship between electroretinal and cortical evoked potential events was predicted by two time-difference latency calculation procedures--a classic two-dimensional time-difference method (Diamond, 1977a,b) and a recently described three-dimensional perspective viewing technique (Coupland et al., 1978). The role of time-difference methodology for the investigation of the human visual flicker response appears to lie in their ability to provide complementary information about visual signal processing not readily accessible to phase-difference analytic methods, because of the methodological and theoretical constraints of these frequency-domain techniques.

APPENDIX Q

SUBJECT CONSENT TO EXPERIMENT AND
MEDICAL RELEASE FORMS

CONSENT TO EXPERIMENT

THIS EXPERIMENTAL PROCEDURE HAS BEEN REQUESTED BY
STUART G. COUPLAND

THE GENERAL NATURE OF THIS EXPERIMENT INCLUDES:

1. ERGS AND VERS RECORDED FROM SKIN ELECTRODES
PLACED ON SCALP AND SKIN AREAS.
2. EPS WILL BE RECORDED TO FLICKERING STROBE
FLASHING IN FREQUENCY RANGE FROM 4 - 25 HZ.
3. EXPERIMENTAL PROCEDURE LASTS APPROXIMATELY
TWO HOURS.

I HAVE BEEN INFORMED OF THE PROCEDURES TO BE USED AND
UNDERSTAND THEM. I ALSO UNDERSTAND THAT AT ANY TIME
THE EXPERIMENT WILL BE TERMINATED UPON MY REQUEST.

MY SIGNATURE BELOW CERTIFIES THAT I DO CONSENT TO
THE EXPERIMENTAL PROCEDURES DESCRIBED ABOVE AND
WHICH ARE TO BE CONDUCTED.

SIGNATURE

DATE

MEDICAL RELEASE

I understand that although this procedure of pupillary dilation is clinically routine, it does involve some degree of personal risk on my part.

Dr. Laughton has performed an ophthalmological examination and has informed me of the possibility of individual hypersensitivity to either of the two medications. If, for any reason, I wish to have this experiment terminated at any time, I may do so.

My signature below indicates that I am giving my informed consent to this procedure of pupillary dilation and do so realizing the degree of personal risk involved.

signature

date

APPENDIX U

PEAK IDENTIFICATION ALGORITHM

FOR 2-D LC

PEAK IDENTIFICATION

GENERAL INFORMATION

All records are 200 msec. in duration and with each VER/ERG waveform is a calibration pulse from which to derive amplitude measurements.

Delete the first and last 5 msec. intervals in the record (i.e. score only from 5 - 195 msec. interval).

In the single VER or ERG waveform the peak to peak amplitude is first measured (Y_{max} on Fig. 1).

Baselines defining the total amplitude range are drawn as labelled B_p and B_n in Fig. 1.

PEAK EVENTS

Peak events are maximum positive deflections (upwards from B_p) that are $> .40 Y_{max}$ and are bounded for ± 5 msec. by no data points of greater positivity (or negativity in defining neg. pks).

PEAK LATENCY DETERMINATION

Peak latency determination proceeds from left to right on the VER/ERG waveform.

Indicate on the plot the point where each positive (and negative) peak latency occurs (see Fig. 1).

If two positive maxima occur within .20 Xisi and Ydiff is LESS than .75 microvolts, then the peak latency is calculated as the midpoint between these two maxima.

If two positive maxima occur within .20 Xisi and Ydiff is GREATER than .75 microvolts, then the peak latency of the larger amplitude event is noted and the latency of the smaller amplitude maxima is disregarded.

In cases where three or more positive maxima occur within .20 Xisi disregard latency determination.

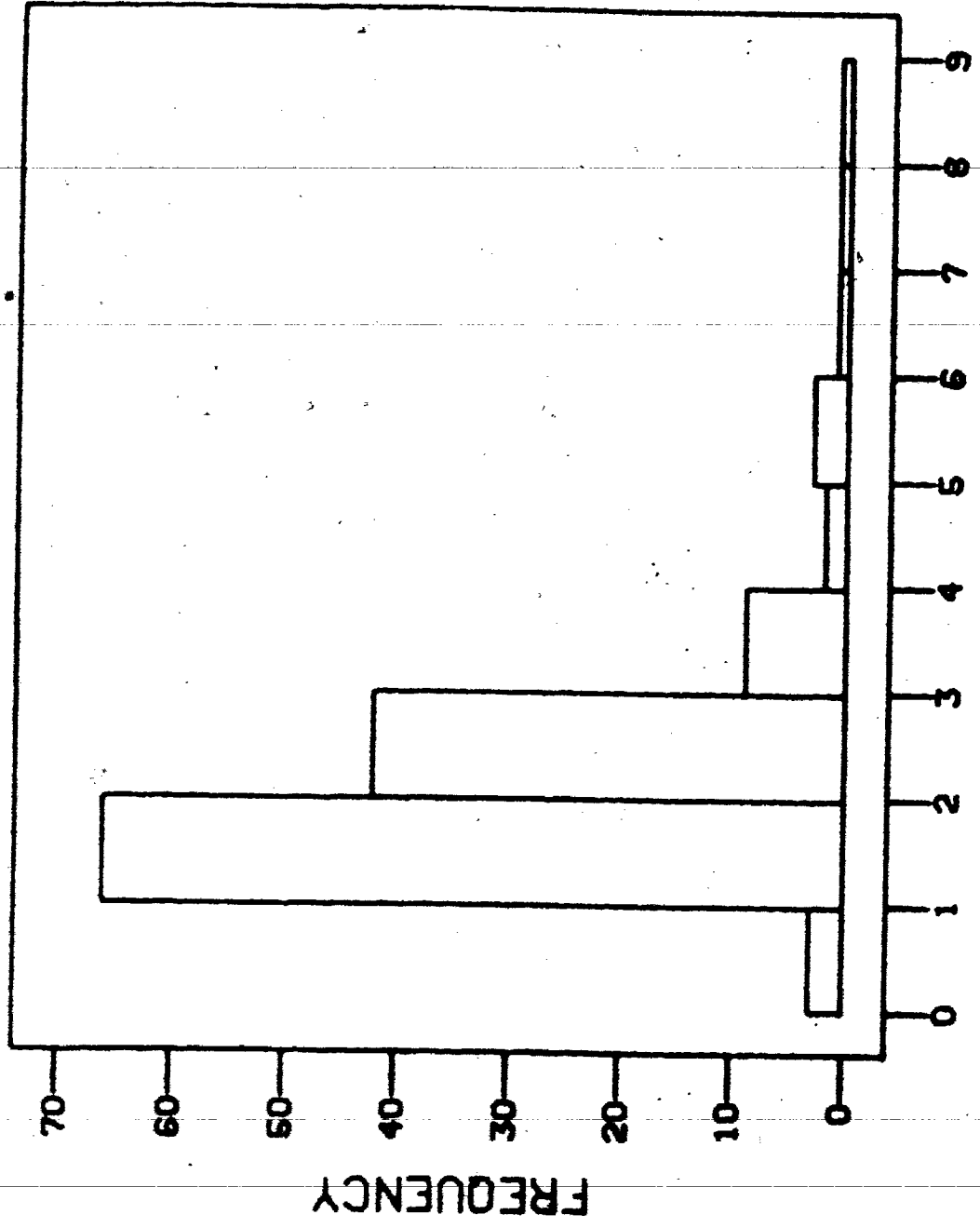
After positive peak latencies have been determined, negative peak latencies are likewise determined by applying the these same rules to negative maxima measured downwards from Bn (see Fig. 1).

APPENDIX A

Summary tables and frequency histograms of the sample standard deviations (E) and variance (EE) components for 2-D LC procedure on 128 peak reference events.

SUMMARY STATISTICS ON THE DISTRIBUTION OF SAMPLE STANDARD
DEVIATIONS (E) FOR 128 PEAK OBSERVATIONS BY 4 RATERS USING THE
2-D LC PROCEDURE

MEAN	1.629	STD ERR	0.109
MODE	0.500	STD DEV	1.230
KURTOSIS	8.911	SKEWNESS	2.480
MEDIAN	1.412	VARIANCE	1.513

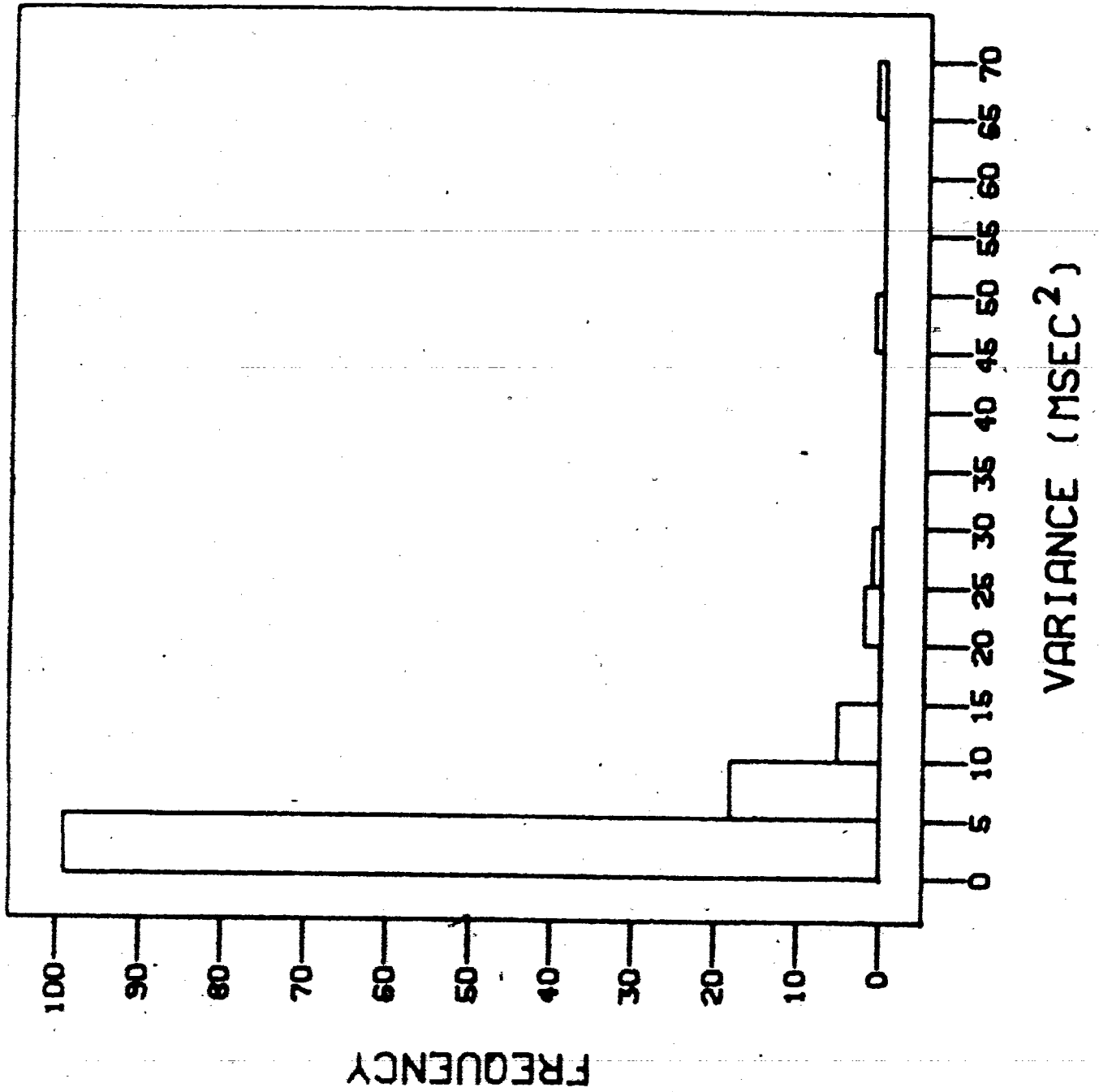


STANDARD DEV. (MSEC)

FREQUENCY

SUMMARY STATISTICS ON THE DISTRIBUTION OF SAMPLE VARIANCE
COMPONENTS (EE) FOR 128 PEAK OBSERVATIONS BY 4 RATERS USING THE
2-D LC PROCEDURE

MEAN	4.154	STD ERR	0.737
MODE	0.250	STD DEV	8.341
KURTOSIS	32.493	SKEWNESS	5.203
MEDIAN	1.990	VARIANCE	69.577



APPENDIX P

EVANS AND SUTHERLAND PICTURE SYSTEM
USER'S MANUAL FOR 3-D PICTURE PRESENTATION

User Manual

Please follow the following steps in order to get on the Picture System to run your program:

- (1) Sign on the PDP11 AND THE Evan & Sutherland
 - 1/. Power on the disk drive (ie. PERTEC)
 - 2/. Wait for the 'SAFE' light on the disk pannel to light.
 - 3/. Open the disk drive door. Remove any disk that is already there and slide in the CMPT 451 disk gently.
 - 4/. Close the disk drive door, and press the button RUN/STOP. Wait until the 'READY' lighth is on before you proceed with other parts of the sign on procedure.
 - 5/. This is IMPORTANT. To avoid damage to the display CRT, turn VEDEO GAIN on its right front to the minumum (ie. anticlockwise).
 - 6/. If you plan to use the display soon, turn it on now. If not, leave it off until you want to use it.
 - 7/. Open the Picture System cabinet (big black box) door on the right hand side, and turn on the power switch. Close the door.
 - 8/. Turn the power switch on the PDP11 console to DC ON.
note: the 'console' is to your left. it is not the keyboard.

- 9/. On the PDP11 console, scunch up your fingers and type
CNTRL HLT/SS. This stops any program running in the PDP11,
just in case there is a program in there which is smart
enough to keep going after you turned the power back on.
- 10/. Press CNTRL BOOT on the PDP12 console. This should result
in four unfriendly looking numbers being typed on the console
terminal, followed by a \$ on the next line.
- 11/. Make sure the key 'LOCK' is pressed down before you type
anything.
- 12/. Type DK1 and then hit the RETURN key
- 13/. There will be a noticeable delay while the PDP11 makes sure
it is all there and bootstraps in the RT11 operating system.
RT11 will then announce itself.
- 15/. Enter the date according to the following format:
'DATE day-month-year', for example 'DATE 10-MAY-78'. Then
hit the RETURN key.
- 16/. Assign all user files to the disk on the upper drive with the
command 'ASSIGN RK1:DK'.
- 17/. When you have a program ready which should produce a display,
turn VIDEO GAIN up until you can see the display clearly.
Please DO NOT turn it up too high.

Note: Do not leave a display on the screen for a long periods
of time because it will cause permanent damage to the
phosphor.

- (2) Switch on the modem (the blue box on the table)
- (3) Type the following command in order to get on WYLBUR TALKER:
R WYLBUR and then hit RETURN key.

- (4) Type your terminal, initial, account and keyword.
- (5) After you signon Wylbur exec the program #EXEVER1 by the following command: EXE FROM #EXEVER1 USE ZYA

The EXEVER1 program is used to send and convert the ASPEX Dataset to the Wylbur file, and will instruct the user to ship a dataset to the PDP11 disk.

- (6) Hit CTRL C in order to get back to PDP11 command mode.
- (7) The type the following command: R ASPEX

This command will run the program, and the program will send the data in the Wylbur file into the PDP11 disk and begin the display.

After typing the above command the system will ask the user for the data file name. Then the user should type in the file name as the same dataset name used before. Each time only one dataset will be send to the PDP11 disk. Therefore, if the user want to see another display of another data set he has to run the ASPEX program again.

The following are the functions of the knobs of the ASPeX program:

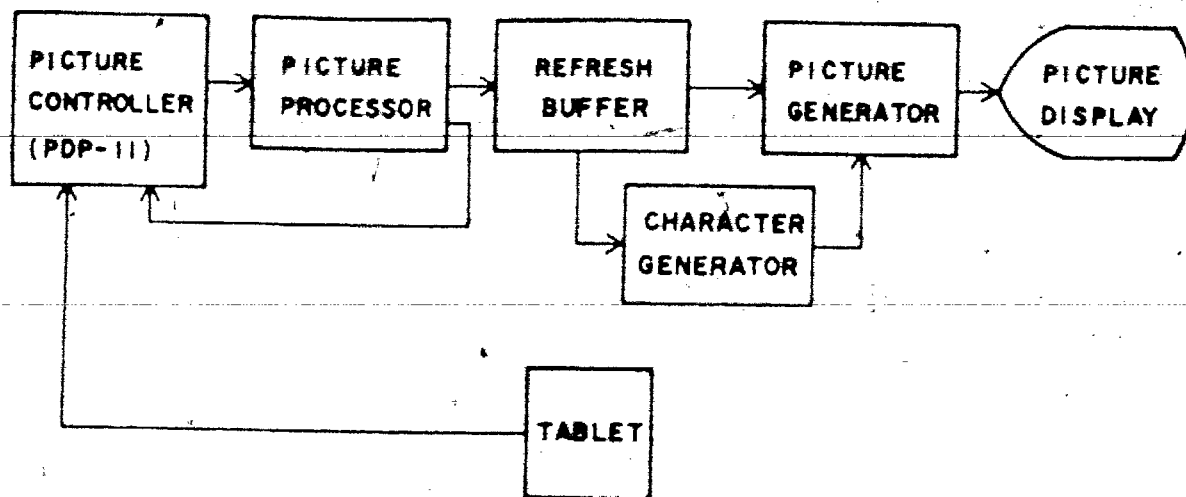
Knob.	Function
****	*****
9	Row A (select the specific row for add, delete or interchange rows operation)
10	Row B (select the specific row for interchange rows operation) note: row B does not change when row A is 0.
11	Col (The current value of of this knob is used to indicate the number of segments skip between segments when displaying.)
12	Time value
13	(the green button) when pressing it row A & B will be interchange
14	(the blue button) add/delete row A specified
15	(the red button) display continuous/hold display constant even the knob values is changing
16	(the yellow button) delete/add the message on the screen
17	rotate the object about the X axis
18	rotate the object about the Y axis
19	rotate the object about the Z axis
20	scale the object larger/smaller
21	elongate the portion of the X axis
22	expand the space between the rows
24	cross or diagonally flag
25	rotate the rod about the X axis
26	rotate the rod about the Y axis
27	rotate the rod about the Z axis
28	scale the rod larger/smaller

- 29 translate the rod along the X axis
- 30 translate the rod along the Y axis
- 31 translate the rod along the Z axis
- 32 Marker is used for align the peaks of the rows

(8) If the user have finish with the display, hit CTRL C in order to get back to PDP11 command mode.

(9) If the user want to signoff the PDP11 and the Picture System please follow the following instructions:

- 1/. Turn VIDEO GAIN on the front of the display CRT to its — minimum (anticlockwise). This will avoid possible damage when you turn off the CRT.
- 2/. Turn off the display CRT.
- 3/. Press CNTRL HLT/SS on the PDP11 console to stop whatever program may be running.
- 4/. Press RUN/OFF on the disks to stop the disks. It will take about 15 seconds to stop. DO NOT power off the drive yet.
- 5/. Turn off the PDP11 by truning the large dial switch from DC ON to OFF.
- 6/. Open the door on the right hand side of the Picture System cabinet (big black box), and power off the Picture System. Close the door.
- 7/. Wait for the SAFE light on the disk drive pannel to light. Then remove the disk and put it back to the shelf.
- 8/. Make sure the 'SAFE' light is still on. If so, power off the the disk drive.
- 9/. Before you left the room make sure you lock the door.



The Standard Configuration of THE PICTURE SYSTEM

APPENDIX I

TWO-DIMENSIONAL TIME-DIFFERENCE STEADY STATE LATENCY
ESTIMATES FOR POSITIVE AND NEGATIVE PEAK REFERENCE
FEATURES FOR ALL FIVE SUBJECTS, OVER THE TWO ISI
RANGES; SLOW FLICKER SERIES ISI RANGE = 80-210 MSEC,
FAST FLICKER SERIES ISI RANGE = 40-75 MSEC.

TABLES CONTAIN THE LEAST-SQUARES ESTIMATED SLOPE AND
X-INTERCEPT CURVE FIT VALUES.

Subject = C.R.

VER

VEP feature	slow flicker			fast flicker		
	slope	X-intercept	S.E.	slope	X-intercept	S.E.
P-1	-1.0	113.67	6.27	-1.0	95.00	3.53
P-2	0.02	111.17	0.63	0.01	95.02	0.20
P-3	1.06	103.51	1.63	1.0	95.00	3.53
P-4	2.08	115.61	4.82	2.22	82.04	8.57
P-5	--	--	--	3.48	68.80	13.58
N-1	-.834	129.16	5.40	-1.0	80.0	5.95
N-2	0.023	145.52	0.25	0.06	74.76	1.70
N-3	1.01	146.60	5.83	0.89	87.09	3.47
N-4	2.15	131.00	8.98	1.99	79.33	6.02

ERG

ERG feature	slow flicker			fast flicker		
	slope	X-intercept	S.E.	slope	X-intercept	S.E.
p-1	0.032	31.16	1.91	-0.046	37.86	0.37
p-2	1.01	34.46	0.51	1.02	34.76	4.30
p-3	2.00	36.78	9.59	2.06	31.76	8.25
p-4	3.11	26.30	20.09	3.14	33.90	14.10
n-1	0.031	13.06	0.55	0.097	11.09	0.79
n-2	1.026	13.59	1.93	0.963	20.57	3.70
n-3	2.02	16.07	11.55	1.95	20.30	11.05
n-4	3.09	18.10	19.41	3.04	15.48	11.06

Subject = P.B.

VER

VEP feature	slow flicker			fast flicker		
	slope	X-intercept	S.E.	slope	X-intercept	S.E.
P-1	-0.94	108.8	6.07	-1.00	112.0	3.67
P-2	-0.014	115.68	0.57	0.05	108.75	0.72
P-3	--	--		0.95	116.75	5.10
N-1	-0.499	132.49	5.27	-0.95	80.25	3.41
N-2	-0.021	147.27	0.84	-0.054	87.09	0.71

ERG

ERG feature	slow flicker			fast flicker		
	slope	X-intercept	S.E.	slope	X-intercept	S.E.
p-1	-0.001	38.35	0.24	-0.018	38.51	0.48
p-2	1.01	39.29	8.74	1.03	36.29	3.97
p-3	--	--	--	2.04	37.20	7.70
n-1	-0.009	20.34	0.42	0.07	13.35	0.53
n-2	0.973	23.93	9.38	0.98	20.74	3.17
n-3	--	--	--	2.03	18.08	8.78

Subject = A.Q.

VER

VER feature	slow flicker			fast flicker		
	slope	X-intercept	S.E.	slope	X-intercept	S.E.
P-1	-0.784	98.77	4.56	-1.45	135.2	6.96
P-2	0.00	110.71	0.84	0.047	106.12	1.03
P-3	0.65	105.75	4.14	0.94	108.3	3.21
N-1	-0.90	134.53	7.78	-1.22	99.71	5.90
N-2	0.048	141.35	0.97	-0.124	91.99	5.01
N-3	--	--	--	0.961	89.88	5.50

ERG

ERG feature	slow flicker			fast flicker		
	slope	X-intercept	S.E.	slope	X-intercept	S.E.
p-1	-0.001	35.56	0.21	0.014	32.02	0.42
p-2	1.01	33.78	2.94	1.08	28.36	4.75
p-3	--	--	--	2.00	35.00	7.63
n-1	0.00	15.61	0.16	0.059	11.58	0.74
n-2	1.01	15.39	4.67	0.928	20.12	4.63
n-3	--	--	--	2.02	16.13	8.81

Subject = D.H.

VER

VER feature	slow flicker			fast flicker		
	slope	X-intercept	S.E.	slope	X-intercept	S.E.
P-1	0.017	107.49	0.87	-0.65	74.75	2.37
P-2	--	--	--	-0.24	77.43	1.07
P-3	--	--	--	0.84	71.00	2.36
N-1	-0.293	78.14	2.11	-1.1	91.33	4.21
N-2	0.04	67.95	1.12	-0.142	93.37	0.93

ERG

ERG feature	slow flicker			fast flicker		
	slope	X-intercept	S.E.	slope	X-intercept	S.E.
p-1	-0.02	44.98	0.42	0.03	37.98	0.76
p-2	1.03	41.13	8.39	1.08	35.91	3.70
n-1	-0.02	25.35	0.35	0.0	22.5	0.00
n-2	0.98	26.79	7.52	1.97	28.41	2.61

Subject = M.T.

VER

VER feature	slow flicker			fast flicker		
	slope	X-intercept	S.E.	slope	X-intercept	S.E.
P-1	0.012	108.48	0.76	-0.99	91.08	4.88
P-2	--	--	--	0.0	91.22	1.37
P-3	--	--	--	1.12	85.76	4.90
N-1	-0.76	116.0	5.80	-0.25	75.7	4.20
N-2	0.10	130.93	1.45	0.79	77.6	1.71

ERG

ERG feature	slow flicker			fast flicker		
	slope	X-intercept	S.E.	slope	X-intercept	S.E.
p-1	0.016	32.87	0.41	0.066	29.87	1.10
p-2	1.03	32.23	3.45	1.01	35.0	2.81
p-3	--	--	--	2.02	31.75	4.31
n-1	0.042	9.95	0.85	-0.08	24.02	0.57
n-2	0.90	26.60	6.70	0.98	18.75	4.50
n-3	--	--	--	2.07	13.42	6.18

APPENDIX C

INTERSTIMULUS INTERVAL (ISI) VALUES AND CORRESPONDING
FLICKER FREQUENCY

Incremental Flicker Frequencies (Hz) and Corresponding
Interstimulus Intervals (msec.)

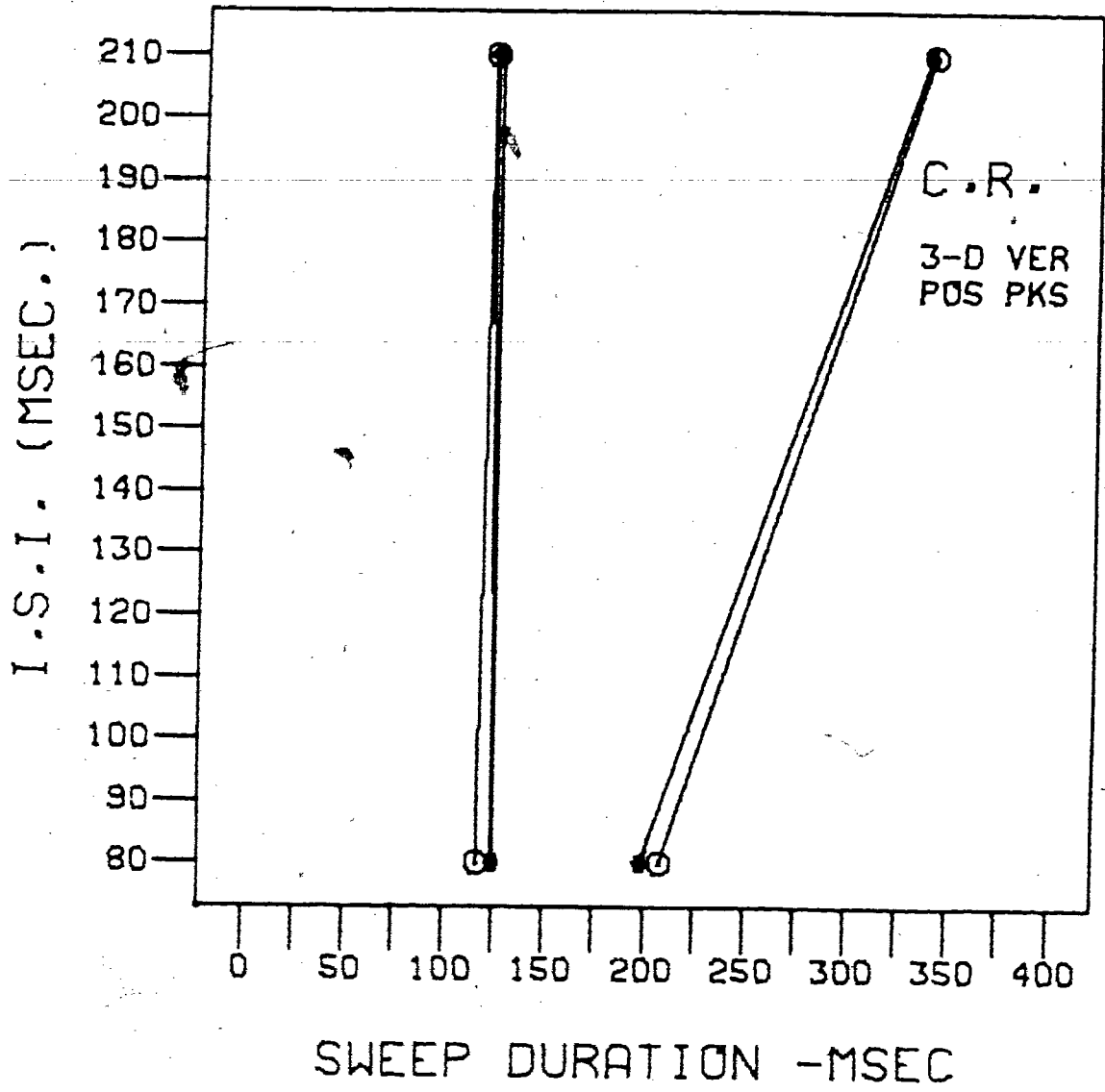
Flicker Frequency (F Hz.)		Interstimulus Interval (msec.)
4.76		210
5.00		200
5.25		190
5.56		180
5.88		170
6.25		160
6.67	SLOW FLICKER	150
7.14	RANGE	140
7.69		130
8.33		120
9.09		110
10.00		100
11.11		90
12.50		80
13.33		75
14.29		70
15.38		65
16.67		60
18.18	FAST FLICKER	55
20.00	RANGE	50
22.22		45
25.00		40

APPENDIX K

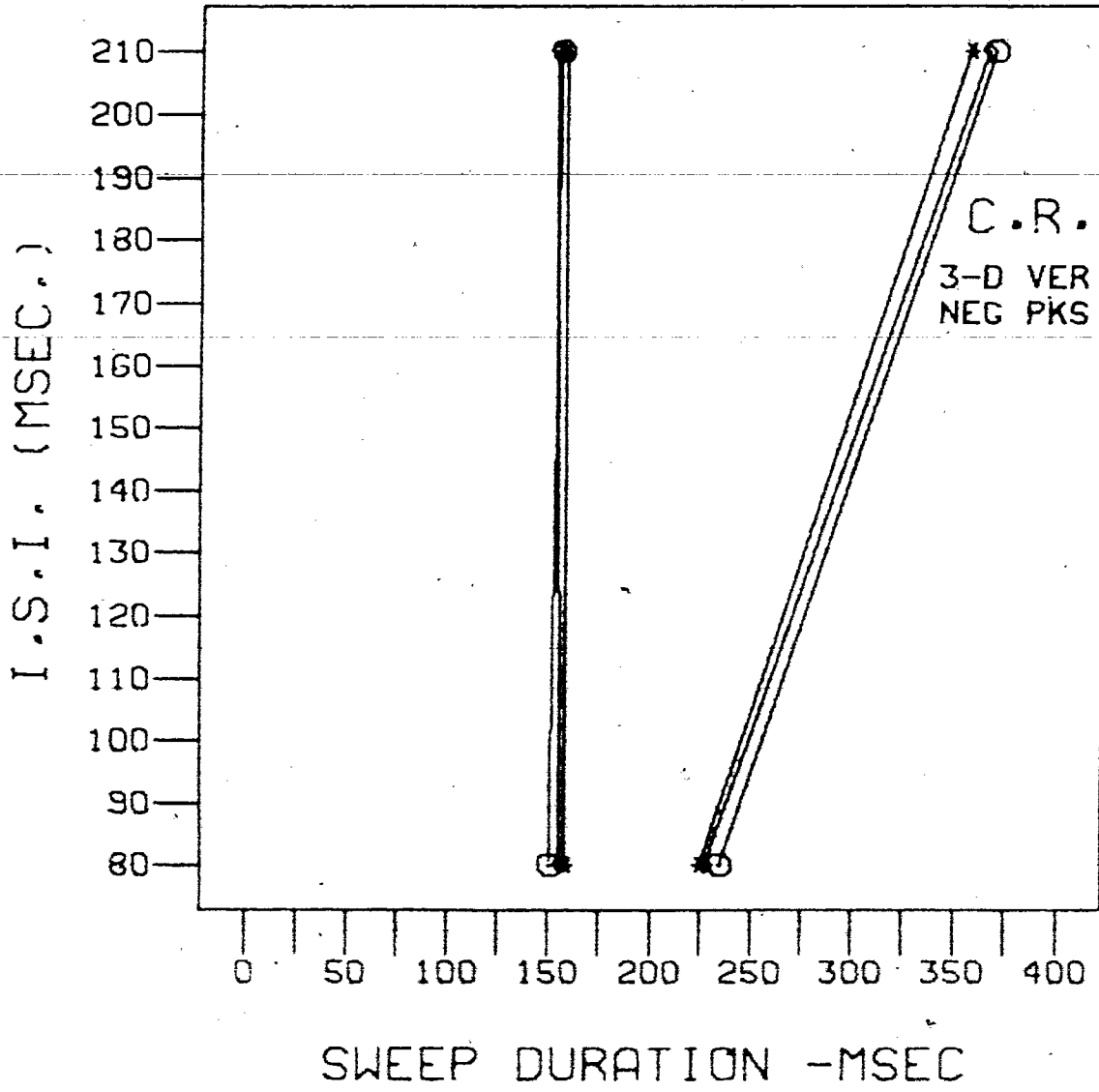
3-D LC INTEROBSERVER AGREEMENT FOR

C.R. DATA

VER positive peak latency for C.R. determined
through perspective (3-D) procedure by three
observers for ISI range = 80 - 210 msec.

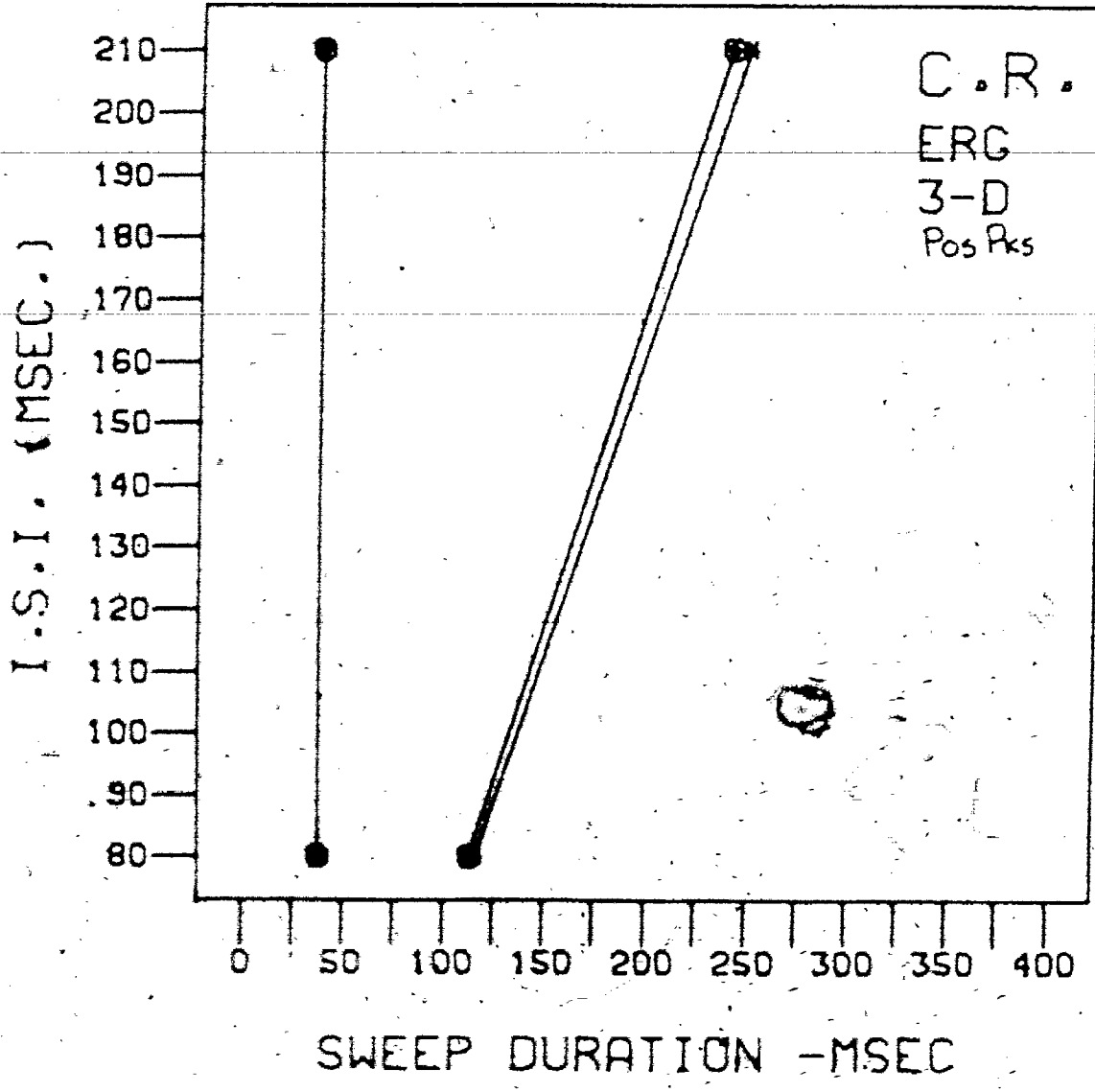


VER negative peak latency for C.R. determined
through perspective (3-D) procedure by three
observers for ISI range = 80-210 msec.

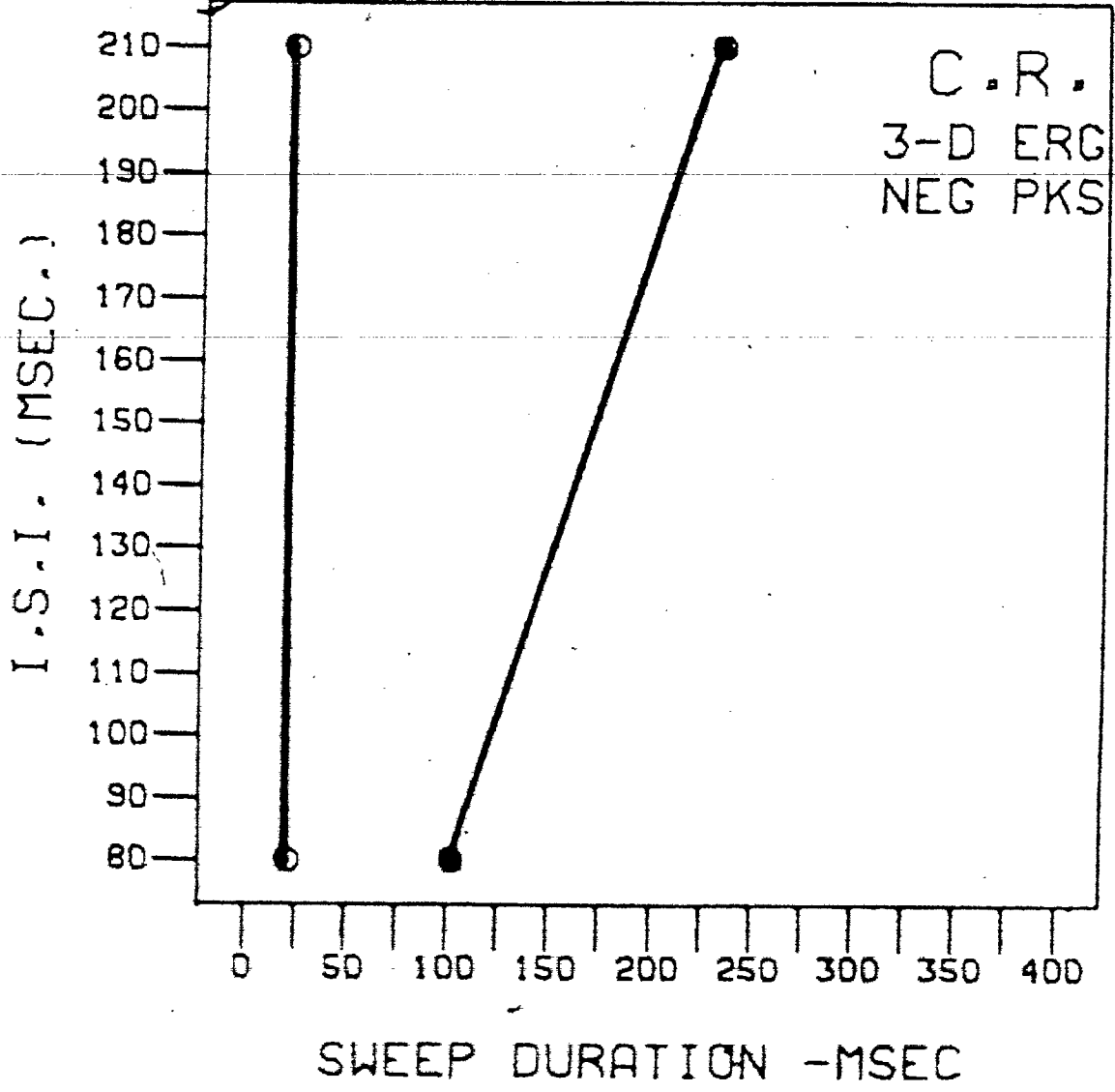


2

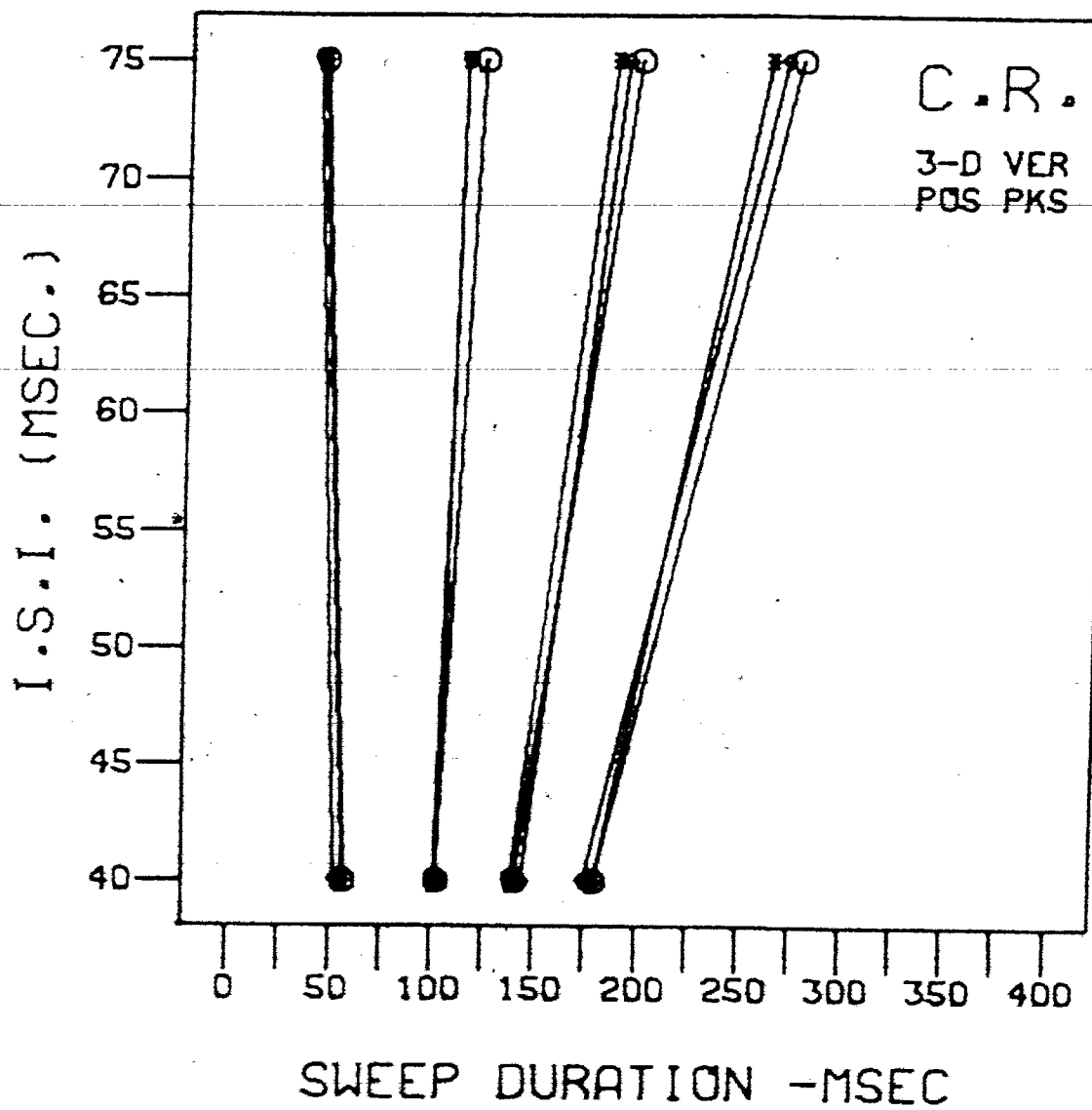
ERG positive peak latency for C.R. determined
through perspective (3-D) procedure by three
observers for ISI range = 80-210 msec.



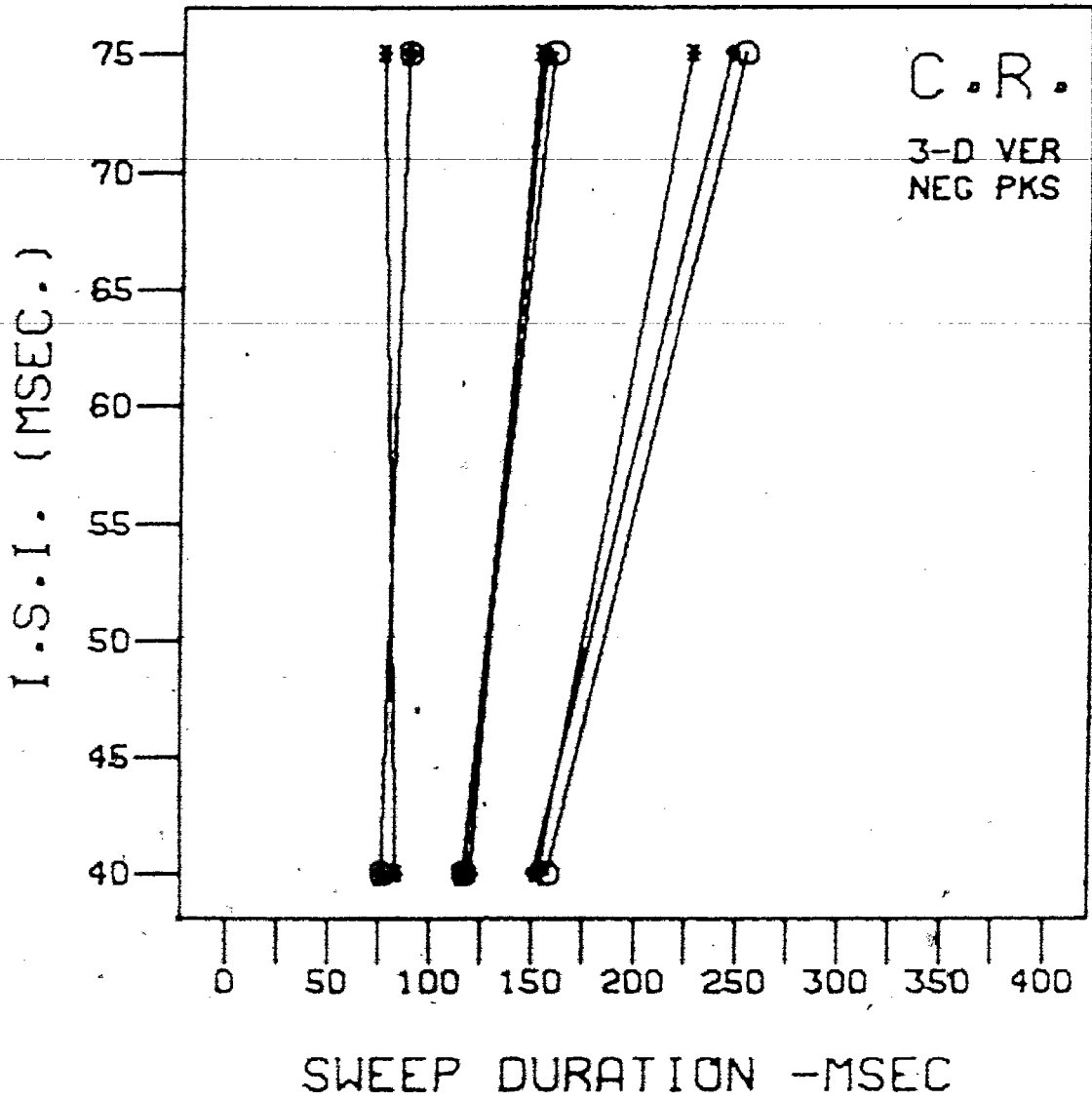
ERG negative peak latency for C.R. determined
through perspective (3-D) procedure by three
observers for ISI range = 80-210 msec.



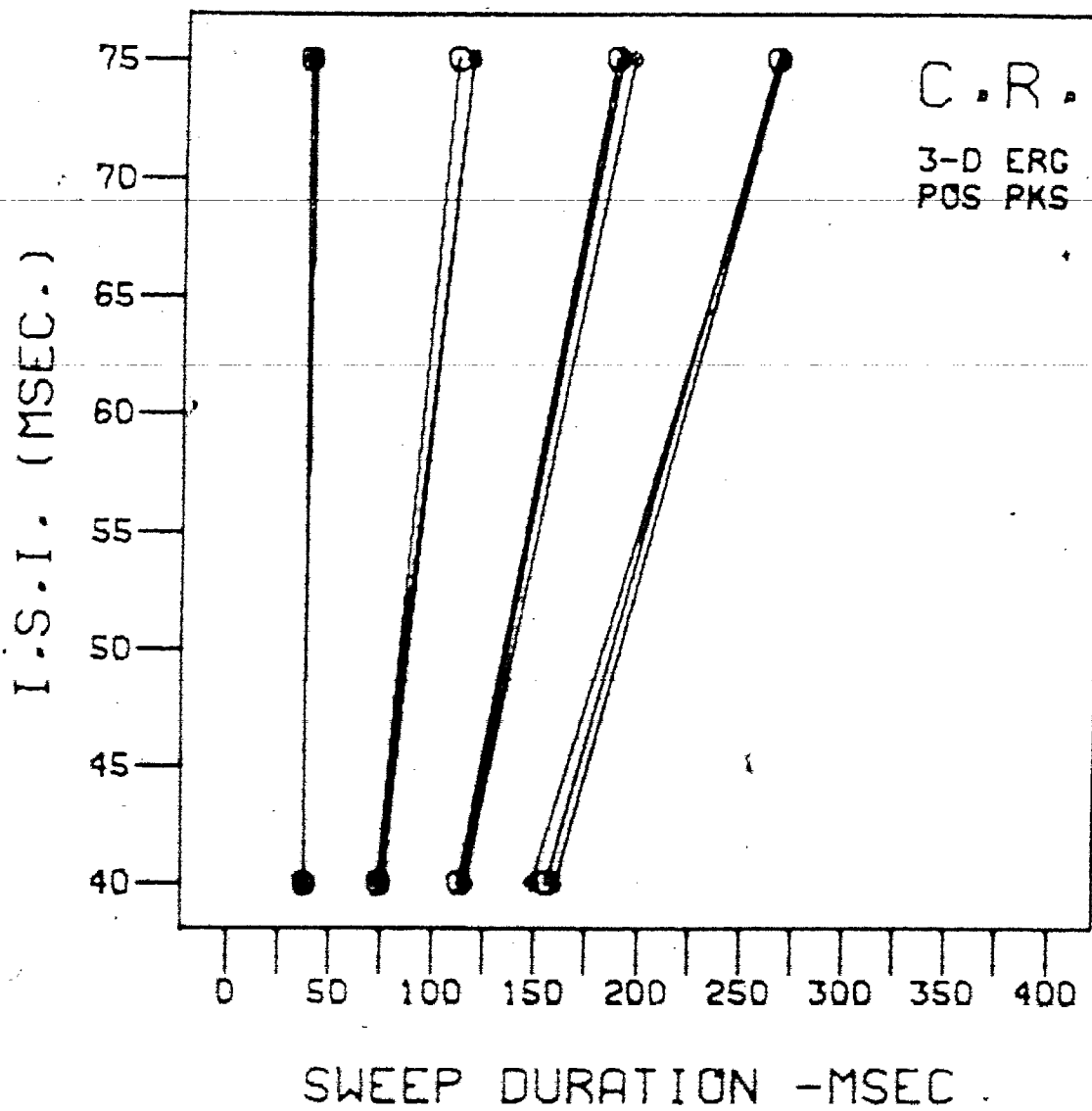
VER positive peak latency for C.R. determined
through perspective (3-D) procedure by three
observers for ISI range = 40-75 msec.



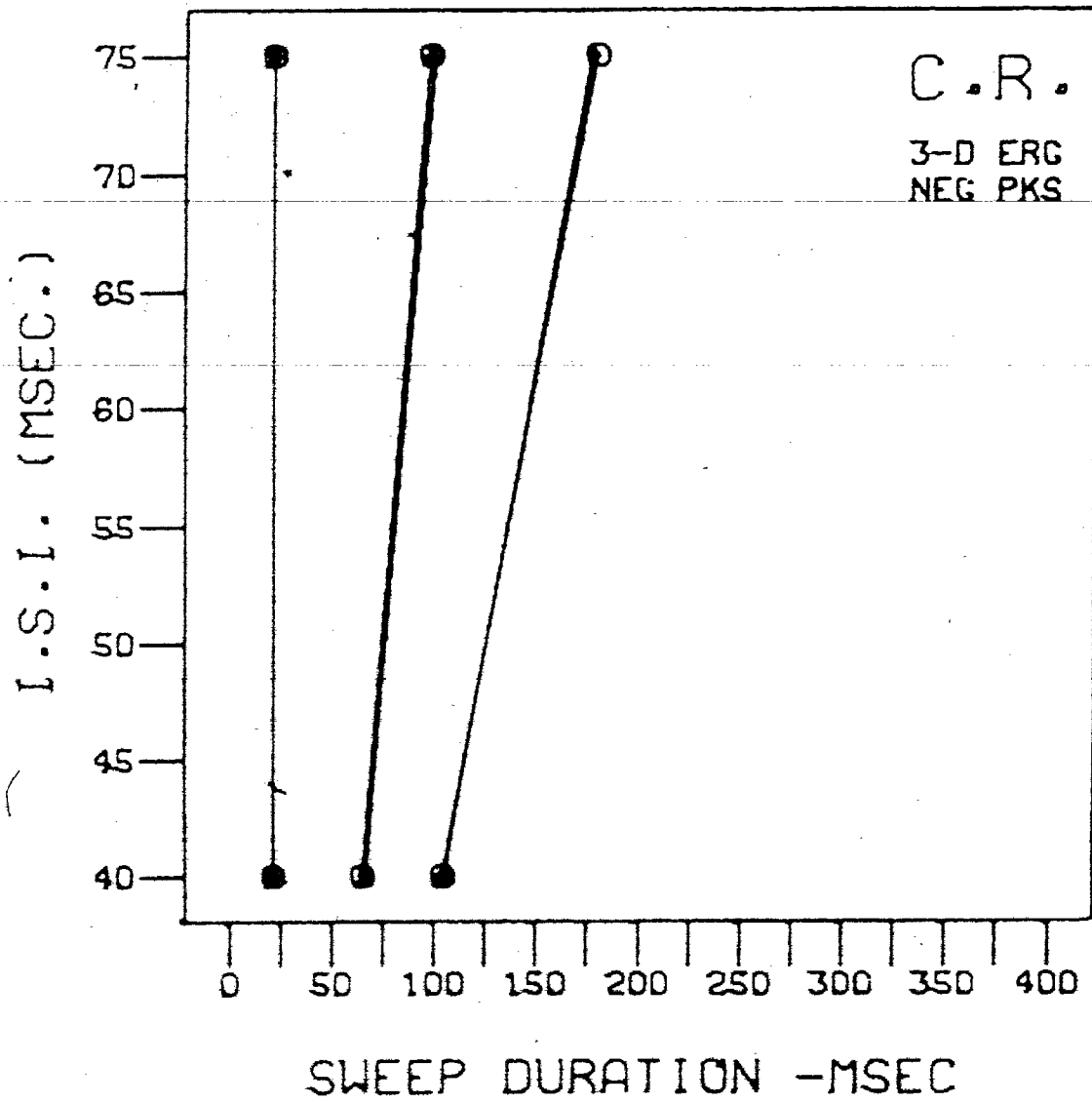
VER negative peak latency for C.R. determined
through perspective (3-D) procedure by three
observers for ISI range = 40-75 msec.



ERG positive peak latency for C.R. determined
through perspective (3-D) procedure by three
observers for ISI range = 40-75 msec.



ERG negative peak latency for C.R. determined
through perspective (3-D) procedure by three
observers for ISI range = 40-75 msec.



REFERENCES

- Adrian, E.D. The electrical response of the human eye. Journal of Physiology, 1945, 104, 84-104.
- d'Arcy. Sur la duree de la sensation de la vue. Mem. de l'Acad. roy. Sci., Paris, 1765, 439-451.
- Arden, G., Granit, R. & Ponte, F. Phase of suppression following each retinal b-wave in flicker. Jour. of Neurophysiol., 1960, 23, 305-314.
- Armington, J.C. Electrical responses of the light-adapted eye. Journal of Optical Society of America, 1953, 43, 450-456.
- Armington, J.C. Chromatic and short term dark adaptation of the human electroretinogram. Journal of the Optical Society of America, 1959, 49, 1169-1175.
- Armington, J.C. Adaptational changes in the human ERG and occipital response, Vision Research, 1964, 4, 179-192.
- Armington, J.C. The electroretinogram, the visual evoked potential and the area-luminance relation. Vision Research, 1968, 8, 263-276.
- Armington, J.C. The Electroretinogram. 1974, Academic Press, New York
- Armington, J.C. & Biersdorf, W.R. Flicker and color adaptation in the human electroretinogram. Journal of the Optical Society of America, 1956, 46, 6, 393-400.
- Armington, J.C., Tepas, D.I., Kropel, W.J. & Hengst, W.H. Summation of retinal potentials. Journal of the Optical Society of America, 1961, 8, 877-886.
- Auerbach, E., Beller, A.J., Henkes, H.E. & Goldhaber, G. Electric potentials of retina and cortex of cats evoked by monocular and binocular stimulation. Vision Research, 1960, 1, 166-182.
- Bernhard, C.G. Contributions to the neurophysiology of the optic pathway. Acta Physiologica Scandinavian, 1940, 1, (Suppl. 1), 1-94.

- Bornschein, H. & Schubert, G. Das photopische Flimmer-Elektroretinogramm des Menschen. Zeitschrift für Biologie, 1953, 106, 229-238.
- Boynton, R.M. Stray light and the human electroretinogram. Journal of the Optical Society of America, 1953, 43, 442-449.
- Brown, J.L. Flicker and intermittent stimulation. In: Graham, C.H. (Ed.) Vision and Visual Perception, 1965, John Wiley and Sons, Inc., New York, 251-320.
- Cartwright, R.P. & Regan, D. Semi-automatic, multi-channel Fourier analyser for evoked potential analysis. Electroencephalography & clinical Neurophysiology, 1974, 36, 547-550.
- Cobb, P.W. Some comments on the Ives theory of flicker. Jour. of the Optical Society of America, 1934a, 24, 91-98.
- Cobb, P.W. The dependence of flicker on the dark-light ratio of the stimulation cycle. Journal of the Optical Society of America, 1934b, 24, 107-113.
- Cooper, S., Creed, E.S. & Granit, R. A note on the retinal action potential of the human eye. Journal of Physiology, 1933, 79, 185-190.
- Coupland, S.G., Taylor, H.J. & Kocpmann, R.F. EEG landscapes: an application of computer cartography. Manuscript in preparation.
- De Lange, H. Experiments on flicker and some calculations on an electrical analogue of the foveal systems. Physica, 1952, 18, 935-950.
- de Lange, H. Relationship between critical flicker frequency and a set of low-frequency characteristics of the eye. Journal of the Optical Society of America, 1954, 44, 380-389.
- De Lange, H. Attenuation Characteristics and Phase-Shift Characteristics of the Human Fovea-Cortex Systems in Relation to Flicker-Fusion Phenomena. Doctoral Dissert., 1958, Technical University, Delft, Netherlands.
- de Lange, H. Eye's response at flicker fusion to square-wave modulation of a test field surrounded by a large steady field of equal mean luminance. Journal of the Optical Society of America, 1961, 51, 415-421.

- DeVoe, R.D. Linear relations between stimulus amplitudes and amplitudes of retinal action potentials from the eye of the wolf spider. Journal of General Physiology, 1963, 47, 13 - 23.
- DeVoe, R.D. Linear electrical flicker response from the eye of the wolf spider. Documenta Ophthalmologica, 1964, 18, 128 - 136.
- Dewar, J. The physiological action of light. I, II. Nature, 1877, 15, 433-435, 452-454.
- Dewar, J. & M'Kendrick, J.G. On the physiological action of light. Proceedings from the Royal Society of Edinburgh, 1873a, 100-104.
- Dewar, J. & M'Kendrick, J.G. On the physiological action of light. Proceedings from the Royal Society of Edinburgh, 1873b, 110-114.
- Dewar, J. & M'Kendrick, J.G. On the physiological action of light. Proceedings from the Royal Society of Edinburgh, 1873c, 179-182.
- Diamond, A.L. Latency of the steady state visual evoked potential. Electroencephalography & clinical Neurophysiology, 125-127.
- Diamond, A.L. Phase-versus-time analysis of the steady-state evoked potential latency. Journal of the Optical Society of America, 1977, 67, 841-842.
- Dodt, E. Cone electroretinography by flicker, Nature, 1951, 168, 738.
- Dodt, E. Beitrage zur Elektrophysiologie des Auges. Graefes Archiv fur Ophthalmologie. 1951b, 151, 672-692.
- Dodt, E. Elektretinographische Untersuchungen zur Analyse des Flimmerphanomens im menschlichen Auge. Zusammenkunft der Deutschen Ophthalmologischen Gesellschaft in Heidelberg, 1951c, 57, 242-245.
- Fishman, G.A. The electroretinogram and electro-oculogram in retinal and choroidal disease. American Academy of Ophthalmology and Otolaryngology, 1975.
- Fry, G.A. & Bartley, S.H. The relation of stray light in the eye to the retinal action potential. American Journal of Physiology, 1935, 111, 335-340.

- Ginsburg, N. Flicker fusion bibliography, 1953-1968.
Perceptual & Motor Skills, 1970, 30, 427-480.
- Granit, R. Sensory Mechanisms of the Retina. 1966, Hafner Publishing Company, New York.
- Henkes, H.E. & van der Tweel, L.H. (Eds.) Flicker. 1964, W. Junk Publishers, The Hague.
- Ives, H.E. Measurement of brightness-difference perception and hue-difference perception, by steady and intermittent vision Journal of the Franklin Institute, 1916, 182, 542.
- Ives, H.E. Visual diffusivity. Phil. Mag., 1917, 33, 18-33.
- Ives, H.E. Critical frequency relations in scotopic vision. Journal of the Optical Society of America, 1922a, 6, 254-268.
- Ives, H.E. A theory of intermittent vision. Journal of the Optical Society of America, 1922b, 6, 343-361.
- Jacobsen, J.H. & Berens, C. Clinical electroretinography: A review of the literature. Quarterly Review of Ophthalm., 1951, 7, 99-109.
- Karpe, G. Apparatus and method for clinical recording of the electroretinogram. Doc. Ophthalmology, 1948, 2, 268-276.
- Kelly, D.H. Flicker. In: Sensory Physiology, VII/4, 1974, 271-302.
- Koopowitz, H. The electroretinogram. In: Bioelectric Recording Techniques, Part C, 1974, Academic Press, New York, 63 - 85.
- Landis, C. An annotated bibliography of flicker fusion phenomena, covering the period of 1740-1952. Armed Forces National Research Council, June 1953.
- Peucker, T.K. Computer Cartography. Association of American Geographers, Resource Paper No. 17, 1972.
- Pieron, H. Vision in intermittent light. In: Contributions to Sensory Physiology, Vol. I, 1964, 180-264.
- Plateau, J. Sur la duree des sensations que les couleurs produisent dans l'oeil. Corres. Math. et Phys., 1827, 3, 27 - 31.

- Regan, D. Some characteristics of average steady-state and transient responses evoked by modulated light. Electroencephalography & clinical Neurophysiology, 1966, 20, 238-248.
- Regan, D. A high frequency mechanism which underlies visual evoked potentials. Electroencephalography & clinical Neurophysiology, 1968a, 25, 231-237.
- Regan, D. Evoked potentials and sensation. Perception & Psychophysics, 1968b, 4, 347-350.
- Regan, D. Evoked potential and psychophysical correlates of changes in stimulus colour and intensity. Vision Research, 1970, 10, 163-178.
- Regan, D. Evoked Potentials in Psychology, Sensory Physiology and Clinical Medicine. Chapman & Hall, London, 1972.
- Regan, D. Latencies of evoked potentials to flicker and to pattern speedily estimated by simultaneous stimulation method. Electroencephalography & clinical Neurophysiology, 1976, 40, 654-660.
- Regan, D. Fourier analysis of evoked potentials; some methods based on Fourier analysis. In: Visual Evoked Potentials in Man: New Developments, J.E. Desmedt (Ed.), 1977, Clarendon Press, Oxford, 110-117.
- Regan, D. & Cartwright, R.F. A method of measuring the potentials evoked by simultaneous stimulation of different retinal regions. Electroencephalography & clinical Neurophysiology, 1970, 28, 314-319.
- Riggs, L.A. Continuous and reproducible records of the electrical activity of the human retina. Proceedings of the Society of Experimental Biology of New York, 1941, 48, 204-207.
- Riggs, L.A., Johnson, E.P. & Vidale, E.B. A quantitative view of neuroelectric events in relation to sensory communication. In: Psychology: A Study of a Science. Koch, S. (ed) 1962, McGraw Hill; New York, 334-379.
- Sachs, E. Die Aktionsströme des menschlichen Auges, ihre Beziehung zu Reiz und Empfindung. Klin. Wschr., 1929, 8, 136-137.
- Schoessler, J.P. & Jones, R. A new corneal electrode for electroretinography. Vision Research, 1975, 15, 299-301.

- Shipley, T. & Hyson, M. Amplitude decrements in brain potentials in man evoked by repetitive auditory, visual, and intersensory stimulation. In: Sensory Processes, Vol. I, 1977, 338-353.
- Spekreijse, H. Analysis of EEG Responses in Man. 1966, Junk Publishers, The Hague, The Netherlands.
- Spekreijse, H. & van der Tweel, L.H. Flicker and noise. In: Clinical Electoretinography, Burian, Hermann & Jacobsen (Eds.), 1966, Pergamon Press, Oxford, 55-59.
- Spekreijse, H., Estevez, O. & Reits, D. Visual evoked potentials and the physiological analysis of visual processes in man. In: Visual Evoked Potentials in Man: New Developments, J.E. Desmedt (Ed.), 1977, Clarendon Press, Oxford, 16-89.
- Sperling, G. Linear theory and the psychophysics of flicker. In: Flicker. Henke, H.E. & van der Tweel, L.H. (Eds.), 1964, W.Junk Publishers, The Hague, 3-15.
- Stephens, G.M., Inomata, K., Cinotti, A., Kiebel, G. & Manev, I. Canthi skin electrode method with corneal displacement. Vision Research, 1971, 11, 1213.
- Teicholz, E. Computer graphics: a perspective. Biosciences Communications, 1975, 1, 262-278.
- Tepas, D.I. & Arrington, J.C. Properties of evoked visual Potentials. Vision Research, 1962, 2, #49-461.
- Tepas, D.I. & Arrington, J.C. Electroretinograms from noncorneal electrodes. Investigative Ophthalmology, 1962, 1, 784-786.
- Troelstra, A. & Garcia, C.A. The electrical response of the human eye to sinusoidal light stimulation. IEEE Transactions on Biomedical Engineering, Vol. BME-22, No. 5, 1975 369-378.
- Troelstra, A., & Schweitzer, M.H.J. On the relationship between the single flash ERG and the ERG elicited by more complex stimuli. Documenta Ophthalmologica, 1964, 18, 114-127.
- Uttal, W.R. Evoked brain potentials: Signs or codes? In: Sensory Coding: Selected Readings, Uttal, W.R. (Ed.), 1972, Little, Brown and Company, Boston, 119-131.

van der Tweel, L.H. Relation between psychophysics and electrophysiology of flicker. In: Flicker. Henke, H.E. & van der Tweel, L.H. (Eds.), 1964, W. Junk Publishers, The Hague, 287-304.

van der Tweel, L.H. & Verduyn Lunel, H.F.E. Human visual responses to sinusoidally modulated light. Electroencephalography and clinical Neurophysiology, 1965, 18, 587-598.